Ontario Hydro

RESEARCH DIVISION

91602
new 82-10

COMPLIMENTARY COPY
Please Credit Ontario Hydro Research if Reproduced in Whole or in Part

ontario hydro
research division

DESIGN AND EVALUATION OF A QUENCHER FOR A PLASMA REACTOR

Report No 86-182-K

M. Alvarez-Cuenca, Engineer-
Process Chemistry Section
and G.P. Kushla, M.A.Sc. Candidate
Chemical Research Department

ABSTRACT

Plasma, described as the fourth state of matter, is recognized as an ionized gas exhibiting unique behaviour. It counts among its many growing and largely unexplored applications, that of chemical processing.

In a chemical synthesis, following plasma generation and its mixing with reactants, the stream is quenched to preserve or enhance product yields. Previous investigators have discussed methods of quenching which fall into four broad categories: injection of a fluid into the quenching region, stream contact with a cooled surface, interaction with a fluidized bed, and passage through a De Laval nozzle.

This investigation evaluated the performances of quenchers incorporating the concepts of cool gas injection and cooled-surface contact. The quenchers were described as follows:

job	file	date	report no.
31-554-011	836.76	April 2, 1987	86-182-K

i) a gas injection ring with multiple, small diameter injection orifices,

ii) a water-cooled gas injection ring with dual, larger diameter injection orifices,

iii) a cooled-surface, constant-diameter flow passage attached to the outlet of the water-cooled gas injection ring,

iv) a cooled-surface, convergent flow passage attached to the outlet of the water-cooled gas injection ring.

The last configuration was conceived for this investigation.

By comparing axial temperature profiles of the effluent region, the water-cooled gas injection ring was judged to perform marginally better than the uncooled version. This ring was used to help study the effects of a constant-diameter or a convergent-diameter flow passage addition. The rate and degree of cooling, providing the basis for evaluation, required the calculation of average quenching rates and analysis of effluent region temperature contour plots, respectively. The gas injection ring plus convergent flow passage gave the highest average quenching rates while the ring and constant-diameter flow passage gave the highest degree of cooling.

Further work is recommended to design a cooled-surface module incorporating features found in both types of flow passage. Improvements to the existing experimental setup are suggested.

91602
new 82-10

ontario hydro
research division

EXECUTIVE SUMMARY

DESIGN AND EVALUATION OF A QUENCHER FOR A PLASMA REACTOR

M. Alvarez-Cuenca and G.P. Kushla
Process Chemistry Section
Chemical Research Department

Selectivity or yield in a plasma chemical synthesis is enhanced by quenching the intermediate reaction products. Thus, quenching is an essential operation in plasma chemistry.

This work has assessed the performance of four quenchers based on two heat transfer concepts: cool gas injection and cooled-surface contact. Two of the four quenchers, designed during this investigation, incorporates the two heat transfer concepts.

Based on two parameters, average quenching rate and degree of cooling, it was found that a gas injection ring assembled to either a convergent or a constant diameter nozzle gave the highest average quenching rate and highest degree of cooling, respectively. A cooled-surface module incorporating features found in both prototypes is suggested as a future program for optimizing the quenching system performance.

MAC
OK

job	file	date	report no.
31-554-011	836.76	April 2, 1987	86-182-K

TABLE OF CONTENTS

	Page
LIST OF FIGURES	vi
LIST OF TABLES	ix
1.0 INTRODUCTION	1
1.1 Plasmas in Chemical Processing	2
1.2 Plasma Reactors	3
1.2.1 The Plasma Generator	3
1.2.2 The Plasma Mixing and Reaction Zone	6
1.2.3 Product Stream Quenching	6
1.3 Quenching Study Objectives	9
1.4 Method of Investigation	9
2.0 PROMISING PLASMA-CHEMICAL PROCESSES	10
2.1 Fuels from Coal	10
2.2 Fuels from Municipal Refuse	12
2.3 Other Processes	13
3.0 LITERATURE REVIEW ON QUENCHING	14
3.1 Fluid Injection	16
3.2 Cooled Surface Contact	18
3.3 Fluidized Beds	23
3.4 De Laval Nozzles	26
4.0 THE QUENCHING EXPERIMENTS	33
4.1 The Experimental Apparatus	33
4.1.1 The Plasma Chemical Reactor	33
a) The Plasma Torch	33
b) The Diagnostic Chamber	36
c) The Power Supply	36
D) The Gas Supply System	36
e) The Cooling Water Network	38
f) The Data Acquisition and Control System	38
g) The Quenching Systems	39
4.1.2 Quench Experiment Diagnostics	44
4.2 Experimental Procedure	50
4.3 Analysis of Data	50
4.3.1 Examination of Effluent Region Temperatures	51
4.3.2 Calculation of Average Quenching Rates	51
4.3.3 Uncertainty Analysis	53

TABLE OF CONTENTS(Continued)

	Page
5.0 RESULTS AND DISCUSSION	53
6.0 CONCLUSIONS AND RECOMMENDATIONS	67
6.1 Conclusions	67
6.2 Recommendations	68
REFERENCES	71
NOMENCLATURE	78
APPENDIX A: INSTRUMENTAL CALIBRATIONS	80
APPENDIX B: EXPERIMENTAL DATA	88
APPENDIX C: SAMPLE CALCULATIONS AND UNCERTAINTY ANALYSES	91

LIST OF FIGURES

Figure		Page
1-1	An Arc and Radio-Frequency Plasma Generator	7
3-1	The Quenching Law for Nitrogen Oxides	15
3-2	The Water-Cooled Quenching Probe	20
3-3	A Fluidized Bed Quenching System	25
3-4	The De Laval Nozzle	28
3-5	A Proposed Plasma Process for Nitrogen Oxide Production Utilizing a Nozzle/Turbine Quencher	28
3-6	The Aerodynamic Quench Probe	31
3-7	Comparison of Quenching Process Under Typical Conditions	32
4-1	Schematic of the Plasma Chemical Reactor	34
4-2	The Plasma Torch	35
4-3	The Diagnostic Chamber	37
4-4	The Plasma Reactor Assembly for Gas Injection Ring #1	41
4-5	The Plasma Reactor Assembly for Gas Injection Ring #2	42
4-6	The Plasma Reactor Assembly for Gas Injection Ring #2 Plus the Cooled-Surface, Constant-Diameter Flow Passage	43
4-7	The Plasma Reactor Assembly for Gas Injection Ring #2 Plus the Cooled-Surface, Convergent Flow Passage (Nozzle)	45
4-8	The Calorimetric Probe	47
5-1	The Effect of Current on Temperatures in the Effluent Region	54

LIST OF FIGURES (Continued)

Figure Page

5-2 The Effect of Arc Gas Flowrate on Temperatures in the Effluent Region 56

5-3 The Effect of Quench Gas Flowrate on Temperatures in the Effluent Region 57

5-4 Effluent Region Axial Temperature Profiles for Gas Injection Rings 1 and 2 (current = 150 A, arc gas flowrate = 45 L/min @ 25°C, quench gas flowrate = 25 L/min @ 25°C) 58

5-5 Effluent Region Axial Temperature Profiles for Gas Injection Rings 1 and 2 (current = 250 A, arc gas flowrate = 106 L/min @ 25°C, quench gas flowrate = 25 L/min @ 25°C) 59

5-6 Guide to Table 5-1 61

5-7 Effects of Cooled-Surface Contact in Addition to Gas Injection Upon Effluent Region Temperatures (current = 150 A, arc gas flowrate = 106 L/min @ 25°C, quench gas flowrate = 25 L/min @ 25°C) 63

5-8 Effects of Cooled-Surface Contact in Addition to Gas Injection Upon Effluent Region Temperatures (current = 150 A, arc gas flowrate = 106 L/min @ 25°C, quench gas flowrate = 90 L/min @ 25°C) 64

5-9 Effects of Cooled-Surface Contact in Addition to Gas Injection Upon Effluent Region Temperatures (current = 250 A, arc gas flowrate = 45 L/min @ 25°C, quench gas flowrate = 25 L/min @ 25°C) 65

5-10 Effects of Cooled-Surface Contact in Addition to Gas Injection Upon Effluent Region Temperatures (current = 250 A, arc gas flowrate = 45 L/min @ 25°C, quench gas flowrate= 90 L/min @ 25°C) 66

6-1 Proposed Design for Quenching Modules 69

LIST OF FIGURES (Continued)

Figure		Page
A-1	Argon Rotameter Calibration (for measurement of arc gas flowrates)	83
A-2	Argon Rotameter Calibration (for measurement of quench gas flowrates)	84
A-3	Argon Rotameter Calibration (for measurement of calorimetric probe gas sample flowrates)	85
A-4	Water Rotameter Calibration (for measurements of calorimetric probe cooling water flowrates)	86

LIST OF TABLES

Table		Page
1-1	Typical Plasma Reactions	5
1-2	Plasma Generator Characteristics	8
3-1	Advantages and Disadvantages of Each Quenching Method	29
5-1	Average Quenching Rate Estimates for Selected Operating Conditions	60
A-1	Thermocouple Calibrations	87
B-1	Variables Associated with the Calorimetric Probe Calculation of Temperature	89
B-2	Calorimetrically Determined Temperatures, Thermocouple Temperatures and Values for the Operating Variables	90

ontario hydro
research division

To Dr. D.D. Mills
Director of Research

DESIGN AND EVALUATION OF QUENCHER FOR A PLASMA REACTOR

1.0 INTRODUCTION

While matter exists in the three states: solid, liquid and gas, more attention has been directed in recent years towards the properties of matter in a fourth state called plasma.

In solid bodies, atoms and molecules are subject to rigid order, while in liquids, a greater degree of freedom of motion is attained. In gases, atoms or molecules move freely; electrons behaving according to the laws of quantum mechanics. In a plasma, where particles are highly energetic, electrons may be split off from their atoms forming a mixture of molecules, atoms, positive ions and electrons. Thus a plasma, which appears as a radiant cloud, is a gas ionized sufficiently to be electrically conducting with the degree of ionization depending on its physical and chemical properties. Its fluid-mechanical behaviour is quite complex involving interactions between electromagnetic and mechanical forces which are beyond the scope of this report.

A distinction is made between low temperature and high temperature plasmas. The former have temperatures ranging up to 20,000°C and are about two percent ionized at 10,000°C. High temperature plasmas, such as those used for fusion research, are fully ionized and can reach temperatures of 1×10^6°C /1/. Low temperature plasmas may be classified as being either "cold" or "hot" depending on their thermodynamic state. In a cold plasma, there is a lack of equilibrium between the light particle (electron) temperature, T_e, and the heavy particle (ion, atom, molecule) temperature, T_p. Typical ratios for T_e/T_p lie in the range of 10 to 100. Hot or thermal plasmas, on the other hand, indicate an equilibrium situation with ratios for T_e/T_p approximately equal to unity. Another means of differentiating between "cold" and "hot" plasmas is to consider the former as low pressure (less than 13 kPa) and the latter as high pressure (up to 1 MPa).

Common examples of man-made plasmas include the neon lighting tube and the oxyacetylene jet used for cutting and welding. The sun and stars, lightning, and the aurora borealis represent familiar examples of plasma occurring naturally.

The more common methods available for generation of plasmas are: combustion, shock waves and electrical discharges. Electrical discharge devices are capable of operating at considerably higher temperatures than combustion plasmas and for much longer time periods than plasmas produced by shock waves. Electrically generated plasmas originally established themselves a position in the aerospace field for use in simulation of atmospheric re-entry conditions. Since then, numerous commercial applications using these plasmas, such as metallurgical processing and fabrication, crystal growth, surface treatments and toxic waste destruction, have been investigated /2,3,4,5,6/. While further research in these areas continues, perhaps a field having even greater potential is that of high temperature chemical processing.

1.1 Plasmas in Chemical Processing

The ever growing use of operating conditions characterized by extremes of temperature, pressure, space velocity and reaction time is the trend in the development of today's chemical processes. With the advent of thermal plasma devices, velocities and residence times have achieved such extreme values that elementary reaction steps can be spatially resolved. Furthermore, temperature changes are abrupt enough so that reactions may not proceed along their anticipated courses. The following areas of chemical processing are particularly applicable to plasma reactors /7/:

i) highly endothermic reactions in which products are stable at relatively high or low temperatures, but less so at intermediate temperatures,

ii) reactions in which high temperatures are required for a finite reaction rate,

iii) reactions involving intermediates that do not exist at ordinary temperatures,

iv) reactions requiring heat without a large degree of dilution of the process stream,

v) reactions in which the properties of the product are enhanced by exposure to high temperatures.

In these reactions, the plasma may serve as a source of heat only or may actively participate in the reaction in the form of cations and anions.

While a wide variety of reactions has been studied /8,9,10,11/, a sampling of which is illustrated in Table 1-1, only a small percentage of them have been found economically feasible on an industrial scale. Most notably among this group is the production of acetylene from various hydrocarbons /12/ and the synthesis of ozone from oxygen /2/.

1.2 Plasma Reactors

In order to conduct a chemical reaction in a plasma, the concept of a plasma reactor is introduced. In general, such a reactor assembly consists of three distinct regions: the head or arc chamber responsible for plasma generation, an intermediate section, where reactants are mixed and the bulk of the reaction occurs, and a quenching section.

1.2.1 The Plasma Generator

For the purposes of chemical processing, most plasma generators utilize arc or high-frequency electrical discharges. In both cases, energy exchange between the plasma and surrounding environment occurs by the processes of radiation, convection and conduction. In the discharge zone, radiation predominates while convection and conduction are the major modes of transfer further downstream.

While arc discharge devices are available in a number of forms, the basic principle of operation remains the same. An arc is struck, initiated by an auxiliary high voltage supply, between electrodes in the presence of a flowing gas. The cathode emits electrons which are accelerated by the electrical field. Through collisions with ions, atoms and molecules of the gas, there is a subsequent loss of kinetic energy and increase in thermal energy. The discharge seeks the path of least resistance between electrodes, and high temperatures make the gas stream in the vicinity of the discharge very viscous. Dissipation of the thermal energy is difficult, resulting in very high temperatures being obtained along the arc path and high temperature gradients existing in the plasma. A typical plasma jet may have a centerline temperature of 10^4 to 2×10^4°K with gradients along this axis of around 400°K/mm and about 3000°K/mm in the radial direction.

Electrodes of varying geometries are utilized and may be consumable, usually carbon, or non-consumable tungsten or copper. In the non-consumable case, the electrodes are quite often water-cooled to prevent overheating. The arc, struck between electrodes, projects past the usually annular-shaped anode due to the flowing gas and is termed an arc jet.

Arc gas may be fed to the torch axially through a hollow cathode or tangentially along the generator walls. The choice of a gas or a mixture of gases is based upon the particular chemical reaction and heat transfer considerations. Some of the more commonly used gases include reactive hydrogen or nitrogen and inert helium or argon.

Arc discharges are, by nature, unstable. Control over the position of the arc between the electrodes is necessary to maximize energy transfer between the discharge and the flowing gas, minimize electrode erosion and protect the generator walls. Discharge column stabilization may be brought about by one of three methods termed: magnetic, aerodynamic or wall stabilization. Magnetic stabilization utilizes an externally applied field resulting from a solenoid, or may be self-induced through the design of the electrodes. This field increases the plasma volume by rotating the arc while constricting it by a phenomenon known as a "magnetic pinch". Aerodynamic stabilization refers to the creation of a gas vortex in the generator channel resulting from tangential arc gas injection. The vortex positions the arc near the channel's centerline and causes a rotation of the arc's striking point while heating the gas flow as it circulates along the channel.Wall stabilization refers to the phenomenon of a "thermal pinch". The arc is constricted and forced about the centerline of the channel by the placement of a series of water-cooled electrically insulated segments between the cathode and anode.

A typical arc plasma generator (plasma torch) design is illustrated in Figure 1-1(a). In this case, the cathode is a cylinder, the anode is ring-shaped and both are water-cooled. Arc gas is fed to the generator in a tangential manner allowing for aerodynamic discharge column stabilization.

High-frequency discharge plasmas are generated by an external source of radiation, usually in the radio-frequency or microwave range. Because the plasma does not make contact with electrodes, there is no risk of contamination by the eroded electrode materials and chemically reactive gases such as oxygen and chlorine may be used.

Gas-Gas Reactions Producing a Gas

CH_4 (or other Hydrocarbons) $\xrightarrow[\text{Arjet}]{H_2\text{Jet}} C_2H_2$

$CH_4 + N_2 \xrightarrow[\text{Ar} + N_2\text{Jet}]{\text{ArJet}} HCN + C_2H_2$

$CH_4 + NH_3 \xrightarrow[\text{Ar} + N_2\text{Jet}]{\text{ArJet}} HCN + C_2H_2$

$CH_4 + H_2O\ (\text{Gas}) \rightarrow CO + 3H_2$

$N_2 + O_2 \xrightarrow{N_2\text{Jet}} 2NO$

$CF_4 + N_2 \rightarrow NF_3 + CF_3NF_2$

$SF_6 + N_2 \rightarrow 2NF_3 + S$

NH_3 or CH_4 cracking rate studies

Gas-Solid Reactions Producing a Solid

$2Ti + N_2 \rightarrow 2TiN$

$3Mg + N_2 \rightarrow Mg_3N_2$

$2W + N_2 \rightarrow 2WN$

$3W + 2CH_4 \rightarrow WC + W_2C + 4H_2$

$6WO_3 + 4CH_4 \rightarrow 2WC + 2W_2C + 9O_2 + 8H_2$

$3Ta + 2CH_4 \rightarrow TaC + Ta_2C + 4H_2$

$2Ta_2O_5 + 3CH_4 \rightarrow 2TaC + Ta_2C + 5O_2 + 6H_2$

$2Ta_2O_5 + 2H_2 \rightarrow 4Ta + 5O_2 + 2H_2$

$WO_3 + 3H_2 \rightarrow W + 3H_2O$

$Al_2O_3 + 3H_2 \rightarrow 2Al + 3H_2O$

$FeO + H_2 \rightarrow Fe + H_2O$

Gas-Solid Reactions to Produce a Gas

$H_2 + S \rightarrow H_2S$

$2C + H_2 \rightarrow C_2H_2$

$4C + 2H_2 + N_2 \rightarrow 2HCN + C_2H_2$

$3C + NH_3 \rightarrow HCN + C_2H_2$

$2C + N_2 \rightarrow C_2N_2$

TABLE 1-1: Typical Plasma Reactions

The radio-frequency plasma generator is usually a quartz tube wrapped by a water-cooled, radio-frequency coil. The plasma discharge is initiated in several ways, the most common being the inductive heating of a graphite rod placed along the axis of the induction coil in the presence of a flowing gas. Figure 1-1(b) illustrates such an arrangement. When the rate of emission of electrons from the rod is sufficient, a discharge appears which is then coupled with the radio-frequency field to produce a more powerful discharge. Once the main discharge is established, the graphite rod is removed. It is then stabilized by introducing gas into the tube tangentially to create a low pressure zone at the axis of the tube. This forces a portion of the plasma to flow up the tube, opposite in direction to the main flow, creating a stable recirculation pattern.

The less common microwave plasma generators utilize an electronic vacuum tube which radiates energy in all directions from its anode. This energy is contained and transmitted by means of a waveguide or convergent metal tube which concentrates the waves by reflection with the walls of the device. This energy is aimed at a gas flowing through a quartz tube.

The characteristics of each type of plasma generator are outlined in Table 1-2.

1.2.2 The Plasma Mixing and Reaction Zone

Reactants may be mixed either prior to the discharge or after the discharge in the arc jet. By mixing upstream of the discharge, exposure of all reactants to plasma temperatures is assured and the problem of thorough mixing of a separate reactant stream with a plasma stream is reduced. For systems in which heated reactants would corrode arc electrodes or disrupt generator operation, injection of species downstream of the discharge would be necessary. In such an arrangement, some of the reactants would be introduced after the discharge. For the special case of all reactants being introduced downstream of the discharge, an inert gas would constitute the arc gas and subsequent plasma. Reactants to be processed may take the form of powders and liquids in addition to gases.

1.2.3 Product Stream Quenching

Quenching is a process which serves to withdraw excess energy from the reaction mixture. At high enthalpy levels, the course of competing chemical reactions is governed by equilibria and kinetics far different from those of more conventional processing conditions. Unstable species, such as ions, excited atoms, free radicals and molecules, are subject to decomposition or

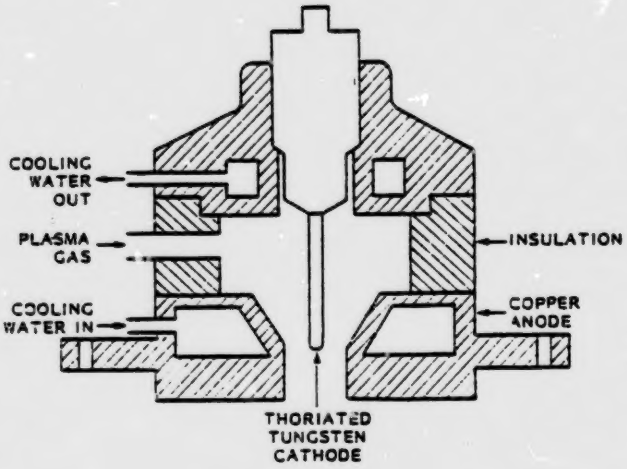
COOLING WATER OUT
PLASMA GAS
COOLING WATER IN
INSULATION
COPPER ANODE
THORIATED TUNGSTEN CATHODE

(a) An Arc Plasma Device

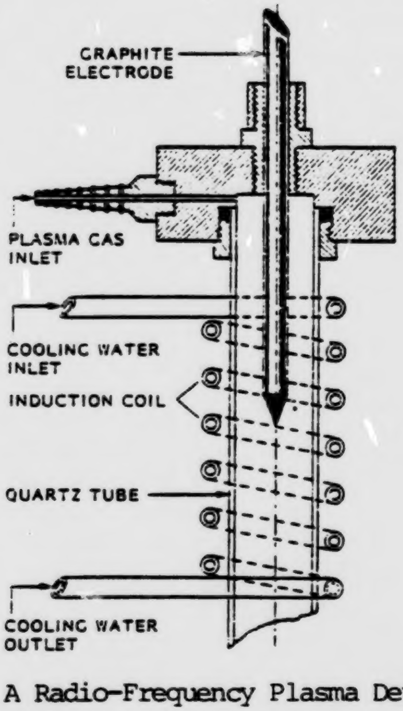
GRAPHITE ELECTRODE
PLASMA GAS INLET
COOLING WATER INLET
INDUCTION COIL
QUARTZ TUBE
COOLING WATER OUTLET

(b) A Radio-Frequency Plasma Device

FIGURE 1-1: An Arc and Radio-Frequency Plasma Generator

Reactor Type Reactor Characteristic	Direct Current Arc	Radio-Frequency	Microwave
generator configuration	tubular metal chamber with electrodes	quartz tube wrapped by r-f coil	quartz tube attached to electronic vacuum tube by waveguide
generator cooling	water	water	none
operational scale	industrial	pilot-plant	bench
plasma type	hot	hot	cold
plasma stabilization	aerodynamic, magnetic, wall	aerodynamic	aerodynamic
maximum power (kW)	10,000	1,000	5
maximum plasma jet core temperature (°K)	50,000	20,000	1,500
average plasma jet temperature (°K)	4,000 - 15,000	6,000 - 12,000	1,000
per cent thermal efficiency	<90	<50	<20
nature of reactants and products	non-reactive gases, liquids, solids	reactive or non-reactive gases, liquids, solids	reactive or non-reactive gases
processing rate of reactants (g/s)	<100	<50	<0.1
pressure range (torr)	100 - 760	10 - 760	10 - 760

TABLE 1-2: Plasma Generator Characteristics

reaction with other constituents. The quenching process influences the rates and reaction paths of these competing reactions which are responsible for the final product distribution.

There are two types of reactions where product composition is largely dependent upon quenching conditions:

i) reactions which yields in a number of intermediate compounds, some of which are desired "frozen". Not only the quenching rate, but also the moment at which the temperature starts to decrease is of prime importance. This moment depends upon the residence time of reactants in the plasma region. In one study of methane conversion to acetylene /14/, a $2x10^{-3}$ second delay in quenching resulted in a decrease of acetylene yield from 15.5 to 10 percent.

ii) reactions yielding desired compounds which are final products relatively stable at extremely high and low temperatures but less so at intermediate temperatures. Because the desired compounds are final products, quenching must not commence before reaction equilibrium has occurred. By decreasing the quench rate tenfold, investigators have observed a decrease in nitrogen oxide product concentration from 9.6 to 6.4 percent /14/.

Relatively little attention has been focused on the design of quenching systems for plasma reactors. Yet in many cases of plasma chemistry, the quenching step is the most important phenomenon determining the extent to which a desired product is formed. Because of large gaps in knowledge, research in plasma chemistry is highly empirical in nature. Because of the poor understanding of reaction kinetics, it has been speculated that higher than usual quench rates may result in new products having yields not previously thought possible.

1.3 Quenching Study Objectives

This study attempts to select the most effective quenching system from among alternatives of both the conventional and novel variety. Criteria are established upon which to judge each quencher and allow for comparisons to be made between quenchers.

1.4 Method of Investigation

The investigation was divided into two phases. In the first phase, conventional as well as novel quenching systems were selected and constructed. Conventional systems were modelled on the more frequently used designs found in the literature while a quencher of novel design was conceived by applying sound engineering principles.

The execution of carefully planned experiments, followed by analysis of the results by graphical and numerical means, constituted the second phase of the study.

2.0 PROMISING PLASMA-CHEMICAL PROCESSES

Plasma technology, in 1984 a 359 million dollar industry in the United States, is projected to climb to 10.5 billion dollars by 1995. One of several major sectors in which the impact of this technology could be felt is that of the chemical process industries. Canada has one of the largest in the world with shipments in 1981 of industrial, organic and inorganic chemicals valued at 8.2 billion dollars. It is, by its value added, the second largest manufacturing sector of the Canadian economy as well as being one of the most energy intensive.

In many instances, plasma chemical processes might prove ideally suited to replace more conventional ones by offering the following advantages:

i) efficient conversion of electrical to thermal energy,

ii) simplicity of reactor operation and potential for process flow-chart simplification,

iii) throughput of large quantities of chemicals in a small reactor,

iv) the ability to utilize feedstocks widely available but difficult to process by conventional methods (eg. air, water, coal)

A recent study was undertaken by Alvarez Cuenca /15/ to evaluate and rank in a semi-quantitative manner, those conventional processes most amenable to plasma technology. The study concluded that processes for the production of fuels from coal were most promising followed by fuels derived from municipal refuse. A number of other projects were noted as well.

2.1 Fuels From Coal

In the late 1800's, and early 1900's, coal was the basic feedstock for the production of aromatics and other petrochemicals. The advent of plentiful oil supplies, low cost natural gas and advanced technology made the use of coal by the chemical industry largely obsolete. The current prime reason for the production of petrochemicals from coal is the increasing need to find reliable supplies of an oil substitute. South Africa is the only country to have developed a fuel and petrochemical industry based on coal.

Coal gasification, followed by Fischer-Tropsch processes, has the potential to yield a wide variety of petrochemicals. However, the technology to produce chemicals such as ethylene, polyolefins and aromatics needs considerable development before commercialization.

As early as the 1960's, light speed pyrolysis of coal in a plasma reactor was considered as a source of "...a very different spectrum of products..." /13/. The production of acetylene from coal in a plasma environment has been a widely studied process while the synthesis of other products has received considerably less attention.

Amman et al /16/ processed coal for the production of light hydrocarbons in a special d.c. arc reactor. A high fraction of the coal was converted to useful products. Preliminary analyses showed 10% methane, 5% acetylene and 72% hydrogen.

Patrick and Gannon /17/ of AVCO developed a process which was economically competitive with oil based processes. Apart from acetylene, considerable amounts of C_2 and C_3 olefins were obtained. A rotating d.c. arc reactor and, particularly, a suitable propane quench contributed to the presence of important quantities of ethylene.

An indicator of the development of these processes is the insignificant effort devoted to the production of the most important petrochemicals: benzene, toluene and xylene (BTX). Only in one paper, by Szymansky et al /18/, was the presence of benzene reported from the pyrolysis of brown coal in a plasma reactor. The lack of work in this area is obvious when one considers the weight that BTX have in the petrochemical industry as either liquid fuels and octane boosters or as basic chemical feedstocks.

Methanol from coal is, in terms of energy efficiency, almost comparable to methanol from natural gas. While a vast pool of literature on the production of methanol from coal exists, information in the open literature on the production of methanol by plasma processes is meagre. Stuart et al /19/ gasified finely divided peat using a steam plasma in a co-current fashion. A H/CO ratio of 1.8 was achieved with a maximum carbon conversion of 89 percent. Reaction models developed by them showed that a 90 percent conversion and a H/CO ratio of 2 could be achieved, thus proving the viability of a commercial-scale process. The conversion to methanol and its associated products could be achieved in a subsequent step in which water would be injected into the reactor. It has been claimed that, among all the alternative fuels for automobiles, methanol would have the highest potential for world-wide use /20/.

2.2 Fuels from Municipal Refuse

As urban populations grow, garbage disposal becomes increasingly complex and costly. Water, air and soil contamination, as well as land requirements, are major obstacles to waste disposal by dumping. Projects to produce fuels from municipal waste are desirable on both an energy and environmental level. A report by Intergroup Consulting Economists Ltd. was based upon projections for 163 of the larger municipalities in Canada for the period of 1985 to 2025. It concluded that the refuse from these communities would have a total potential equivalent to 19 million barrels of oil annually /21/. Municipal refuse as a source of energy began to be developed in the early 1970's. Three cities in Los Angeles County unveiled plans to build plants to obtain steam from municipal waste and CSI Resource Systems Inc., a Boston-based engineering firm, revealed plans for 200 garbage-to-energy plants for the United States. Technical evaluations show that by the end of the century, 50% of American refuse will be burned instead of dumped in landfills. The prime motivation for such a policy is the increasing scarcity of landfill space, combined with the rising cost of trucking wastes to more-distant landfills. These projects raise a public concern: the emission of highly toxic pollutants. C.O. Velzy, in a report for Argonne National Laboratory /22/, stated that in urban areas or regions with air pollution problems, the addition of acid-gas removal devices, along with ultra-high-efficiency (99% plus) particulate removal devices, should be considered essential. J.L. Kuester, professor of chemical engineering at Arizona State University, has analyzed the pyrolysis of municipal refuse. Some of the pyrolysis methods include the use of microwaves, incomplete combustion and indirect heating. Although no process could be called trouble-free, Kuester felt that pyrolysis development was of major importance with regard to producing synthesis gas appropriate for indirect processes that included a downstream conversion step.

The use of plasma incinerators for the pyrolysis of municipal waste and generation of fuels has received little attention relative to the destruction of toxic materials. A process was developed in 1983, however, at the University of Manchester (10) to transform municipal refuse into oil with a calorific value of 40,000 MJ/Ton.

2.3 Other Processes

In addition to the previously discussed areas of plasma application, the fixation of nitrogen, synthesis of phosphorous and phosphoric acid and the production of cement have been examined as well by Alvarez Cuenca /15/.

Nitrogen fixation is a well established technology. Thus, improvements in productivity will come either from the introduction of new catalysts or better energy management. Because profit margins are already small, any important increase in productivity is bound to come through a drastic departure from the conventional technology now in place. The fixation of nitrogen in a plasma reactor may be the sought technology. The theoretical energy required to produce NO from air is about 0.9 kWh/kg NO while plasma arc processes consume about 33 kWh/kg NO. New plasma processes being developed, appear to increase the yield of NO while reducing the energy requirements. Fauchais and Baronnet claim that plasma processes could be developed with energy requirements along the order of 7 kWh/kg NO (comparable to conventional processes) /16/. Moreover, increases in the cost of natural gas could soon make plasma processes in France competitive .

Phosphorous is produced by reducing phosphate rock with coke in electric furnaces. Phosphoric acid, on the other hand, is obtained by the reaction of phosphate rock with sulphuric acid or by burning elemental phosphorous and reacting it with water. The technologies of these processes are advanced and, hence, improvements in productivity will come from radically different processes. The application of plasma to the production of elemental phosphorous is relatively unexplored. Goldberger and Baroch used a plasma jet to fluidize a bed of coke and silica to reduce phosphate rock /24/. Another plasma process developed by Foex et al /25/, incorporated a sophisticated reactor design in which a rotating furnace was heated by a discharge resulting from two plasma jets located at opposite ends of the furnace. The feeding of the rock, silica and coke took place at the top, while the molten slag containing phosphorous was removed from the bottom of the furnace.

In a recent paper, Chase et al /26/ showed that the continuous operation of a hot graphite plasma reactor, using methane as the phosphate rock reducing agent, could yield up to 80% phosphorous. The net power requirements were surprisingly large (24 kWh/lb of phosphorous) when compared to the theoretical value (7 kWh/lb of phosphorous). This difference was attributed to the large heat losses observed in bench scale experimental setups.

Cement manufacturing technology has not radically changed over the last few decades. In response to this, the application of high temperature plasmas to the cement industry has been proposed by Tylko /27/, Ettlinger et al /28/ and more recently by Drouet /29/. Tylko developed a plasma reactor for the production of a wide range of hydraulic cements. Such a reactor could be installed into existing plants to provide thermal energy to prevent contamination in the rotary kiln. Preliminary estimates indicated that cement could be produced 25 percent cheaper by incorporating plasma technology. It was further predicted that replacement of the kiln by a plasma furnace could mean a 40 percent reduction in capital costs /28/.

3.0 LITERATURE REVIEW ON QUENCHING

The quenching rate may be defined as a change in temperature occurring over a defined period of time. Additionally, a quenching temperature may be denoted as the gas temperature at which the quenching process is initiated. In a simple reaction between dissociated species, any increase in the temperature beyond that required to produce complete dissociation would only serve to slow down the quenching step.

The quenching mechanism for a given system is very complex and poorly understood. Experimental or theoretical quench rates commonly on the order of 10^5 to 10^9 °K/s have been reported. If the rate of cooling is below some critical value, commonly taken as 10^5 °K/s, predictable equilibrium reaction paths dominate and less desirable products usually result.

According to Polak and Sthchipatchev /14/, the quenching rate is a function of the plasma's temperature. That is,

$$\frac{dT}{dt} = f(T) \tag{3-1}$$

where T = plasma temperature
t = time

Figure 3-1 illustrates this law for the case of nitrogen oxide quenching. An English translation of this work was not available and could not be obtained.

The four quenching methods which have received the greatest attention by investigators and which are reviewed in this study are:

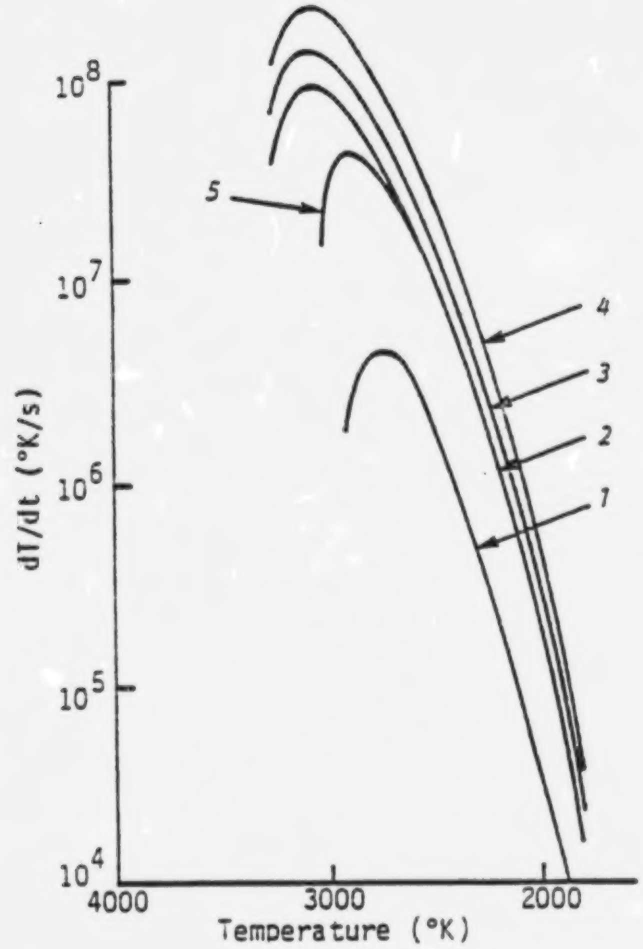

CURVE 1: $T_{initial}$ = 3000 K ; T_{final} = 1800 K ; P = 1.1 atm

CURVE 2: $T_{initial}$ = 3300 K ; T_{final} = 1800 K ; P = 10 atm

CURVE 3: $T_{initial}$ = 3300 K ; T_{final} = 1800 K ; P = 20 atm

CURVE 4: $T_{initial}$ = 3300 K ; T_{final} = 1800 K ; P = 50 atm

CURVE 5: $T_{initial}$ = 3100 K ; T_{final} = 1800 K ; P = 20 atm

FIGURE 3-1: The Quenching Law for Nitrogen Oxides

i) injection of liquids or gases into the quench region,
ii) contact of the product stream with cooled surfaces,
iii) product stream interaction with a fluidized bed,
iv) passage of the product stream through a De Laval nozzle.

3.1 Fluid Injection

A very effective quenching can be achieved by mixing a hot gas stream with a stream of cold liquid or gas. Liquid sprays offer the advantages of higher specific heats and heats of vapourization. Liquid drops of smaller diameter give greater quench rates because of their greater surface areas per unit mass. Gaseous jets, however, tend to mix much faster in a more dispersed manner.

The diameter of the plasma jet is a very important factor in fluid injection quenching. As the jet diameter is increased, more time is required for the mixing process to penetrate to the core of the jet. The quenching stream may enter the reactor through slits or holes and contact the plasma stream in a parallel or perpendicular fashion.

The interaction of cool fluid with a plasma stream may result in either a chemical or a thermal quench.

The process of a chemical quench is characterized by a highly endothermic reaction between the plasma stream and an injected fluid. This selectively removes one or more excited species from the plasma stream, to facilitate product synthesis or to prevent undesirable chemical recombinations. At the same time, considerable quantities of heat are consumed.

In a series of experiments conducted by Harnish, Heymer and Schallus /30/, the quenching device consisted of a cylindrical tube through which the plasma flowed and into which a liquid was injected through slots located directly beneath the anode outlet. To avoid introducing chemical species detrimental to the desired reaction, one of the reactants was injected and served as the coolant as well.

Stokes and Streng /31/ synthesized ozone in an arc plasma reactor using liquid oxygen in a similar manner. Ozone formed in the helium plasma was rapidly removed from the reaction zone and quenched by excess liquid oxygen. The stability of ozone was favoured at low temperatures and thus quenching of the high temperature oxygen radicals was necessary. A stainless steel feed ring, connected directly to the exit of the torch, was 10 cm in diameter and 1.6 cm thick with a removable annular insert containing sixteen equally spaced entrance ports, each 0.8 mm in diameter.

Elsewhere, Honda, Takahira and Kanzawa /32/ have reported on the injection of hydrogen gas through a cooling ring in their experimental and analytical investigations of carbon dioxide decomposition in an argon plasma.

Thermal quenching, a purely physical process of heat transfer between plasma and coolant streams, introduces the problem of additional species in the plasma mixture resulting in considerable dilution of the plasma stream. Such a problem may be overcome by recycling a portion of the cooled product stream for quenching. This was demonstrated by Freeman /33/ who, in a synthesis of hydrogen cyanide by admixture of methane in a nitrogen plasma jet, chilled the products by injecting a portion of the cooled product gas. Quenching by this method was claimed by the author to be the fastest of several methods he had investigated.

Many studies have been performed on the mixing of cool gases and plasma steams with the intent being focused on aerospace applications as opposed to plasma chemistry /34,35,36,37,38/. In one such study, Grey et al /34/ performed analytical and experimental studies on the interactions between a laminar argon jet and a coaxial flow of cool helium. It was found experimentally that stream mixing, and thus transition from laminar to turbulent flow, was enhanced by increasing the helium velocity and confining the flow in a duct. It was further reported that jet mixing, and thus heat transfer, was dominated by the inflow of cool helium as opposed to dispersion of the argon jet or loss of energy directly by radiation or ionization.

Mixing of the plasma and coolant streams is a critical factor in the quenching process with higher rates of heat transfer possible for increasingly turbulent mixing. At internal plasma jet temperatures, the viscosity is very high (approximately ten times greater than that of the cool gas) so that penetration of a cold stream into the plasma is difficult. Some investigators (2) claim that if the flowrate of quenching fluid is sufficiently high, an originally laminar stream of arc gas will be sharply disrupted with the resulting turbulence facilitating rapid mixing.

Mazza and Pfender /39/ have reported on the numerical modelling of an arc plasma reactor used extensively for the experimental production of fine powders of metal carbides and nitrides. A quenching ring, located at the end of the reaction duct, allowed for the injection of cold gas to quench the reaction products. Calculations were performed for typical operating conditions considering the simple case of pure argon used in the roles of arc, reactant and quench gas. From the calculated velocity and temperature distributions in the reactor channel and plasma jet, quench rates of 10^8 to 10^9 °K/s resulted. It was also reported that the injection of cold gas did not penetrate the highly viscous core of the plasma but remained close to the reactor walls instead, even at relatively high injection flowrates.

A study was conducted by Anderson and Case /40/ who quenched a hydrogen/methane plasma to form acetylene by circumferentially spraying the stream with water. Experimental yields were compared with an analytical model making use of available thermodynamic and kinetic data. From the model, it was concluded that the reaction contact time and quenching speeds were not as important as the speed of mixing between the hydrogen plasma and methane feedstream. The authors stressed, however, that in other reactions, contact times and quenching speeds could be extremely important.

As a result of modelling the radial feed of a reagent in tube confined plasma flow, Freeman and Skrivan (13) have indicated the potential for gas injection to serve as a method of quenching. A diffusion-rate-limited model describing the reaction kinetics was developed. Results of the model allowed estimation of, among other quantities, axial temperature profiles of the effluent plasma. The slope of a calculated temperature versus time curve indicated a temperature decay rate of 5×10^7 °K/s. It was predicted that one half of the cool stream's molecules would have diffused into the hot core of the plasma jet in sixty microseconds or within one centimeter from the coolant injection point. In the experiments, reactants entered the reaction section through a 3 mm radial feed tube centered 14 mm from the section inlet.

In the Soviet Union, where considerable effort has been expended in the field of plasma chemistry, Khait /14/ has mathematically modelled the case of liquid injection at right-angles to the plasma jet and produced a quenching rate equation. The unavailability of specifics, however, precludes any further discussion of his work.

3.2 Cooled Surface Contact

Investigations of chemical syntheses commonly utilize cooled surface quenching devices such as tubular probes /40,42,43,44,45,46,47,48/, cold fingers /49/, rotating drums /30/, funnels /50/ and the reactor walls /51,52/. While devices such as these frequently make use of water for cooling, liquid nitrogen and solid carbon dioxide have been used. In all geometries, quenching occurs at the cooled surface and in the immediate surrounding region.

By far the most popular configuration is a water-cooled quenching probe such as that one illustrated in Figure 3-2. While water is circulated through a cooling jacket, a sample stream is withdrawn through the innermost tube allowing for simultaneous quenching and sample recovery. High pressure, high volume water flowrates are necessary to prevent ablative damage to the probe. Experience has shown that most of the quenching occurs at and near the inlet to the probe with maximum product yields being obtained by a probe placed at a minimum distance to, and facing directly at, the plasma discharge /46,53/. This distance is limited by the maximum heat transfer sustainable by the probe without damage. The probe's outer diameter is typically in the range of 5 to 15 mm and the innermost tube is of the hypodermic tubing variety. Plooster and Reed /54/ reported that sampling tube inner diameters smaller than the optimum had gas flowrates too low for good heat transfer. Those larger than the optimum had inadequate surface contact area for fast quenching. Probes are typically made from quartz, stainless steel, copper or brass. While some materials may be superior in regards to heat transfer, other factors such as susceptibility to corrosion, fouling or catalytic effects must be considered as well. For reaction environments in which corrosion of the probe becomes significant, platinum or alumina-silica coatings become necessary.

Although probes may be easily placed at different points in the reactor and act as both a quencher and sampler, serious drawbacks exist. Because of problems associated with fouling and plugging of the small diameter sampling tube, probes are unsuitable for reactions in which solids participate . Baddour and Blanchet /44/ in an investigation of carbon vapour reactions with hydrogen or methane, experienced the problem of plugging by carbon deposits.

Small probes can achieve fairly high quench rates. However, use is impractical on an industrial scale as only a fraction of the product stream is recovered. As tube diameter increases, the surface area to volume ratio decreases resulting in poorer heat transfer and lower quench rates. An alternative to probe scaleup, although expensive, is the use of banks of small diameter tubes.

Skrivan and Von Jaskowsky /55/ conducted a study on the heat transfer from a plasma to the confining walls of a tubular test section. The test section consisted of individually cooled segments separated by insulating materials. An empirical equation based upon heat transfer data for argon, nitrogen and hydrogen in test sections of various diameters, led to an expression for the mean axial enthalpy, and subsequently, mean temperature profiles. The equation was written as:

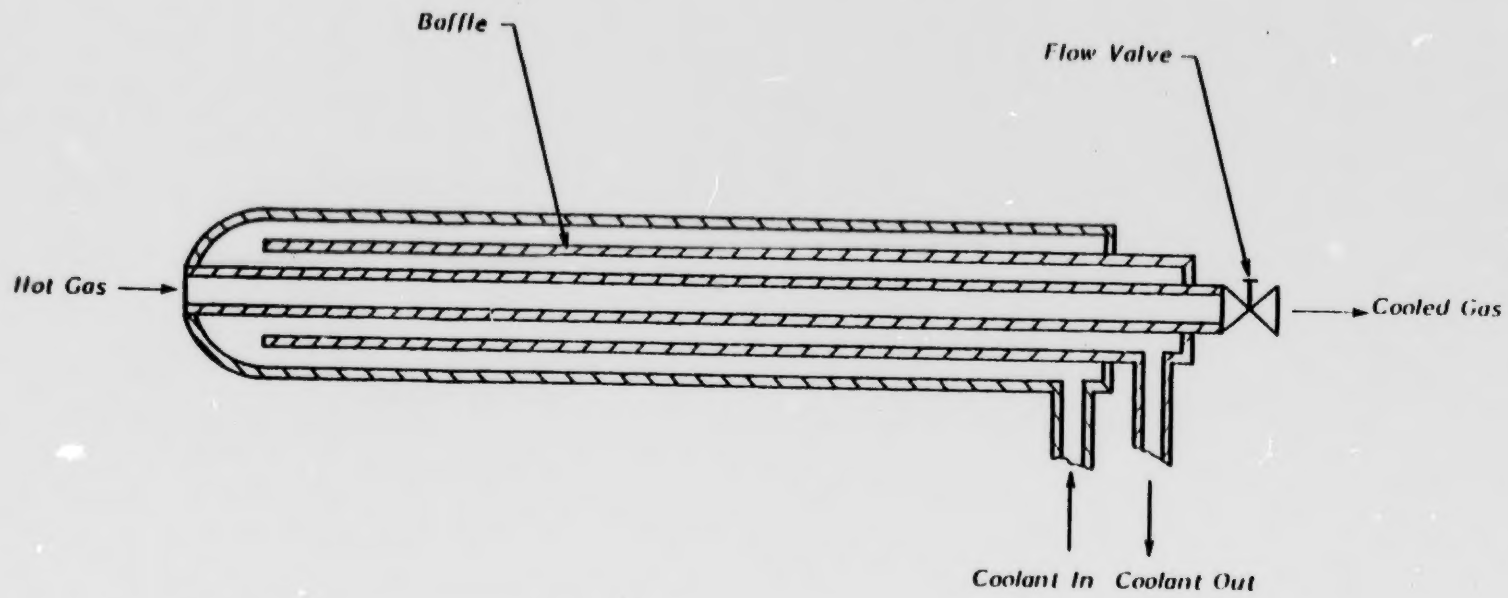

Baffle
Flow Valve
Hot Gas
Cooled Gas
Coolant In
Coolant Out

FIGURE 3-2: The Water-Cooled Quenching Probe

$$\int c_p \, dT = \frac{1.49 \quad H' \quad \alpha}{(x+S)^{0.67}} \qquad (3\text{-}2)$$

where c_p = specific heat capacity (Btu/lb°R)

T = plasma temperature (°R)

H' = plasma core enthalpy (Btu/lb)

x = axial dimension (ft)

S = length of transition section placed prior to water-cooled section (ft)

α = a variable dependent upon reactor geometry (ft 0.67)

The equation was used for the construction and comparison of temperature profiles obtained under different conditions. However, it did not allow the calculation of quench rates.

In a similar manner, Wethern and Brodkey /56/, studying heat and momentum transfer in a helium plasma, calculated average temperature profiles in water-cooled copper tubes.

Ammann and Timmins /43/ developed a model to study high temperature chemical reactions occurring in oxygen/nitrogen mixtures during quenching in small diameter, water-cooled probes. The reaction mechanisms were determined to be a function of the initial temperature and composition, the pressure, probe diameter, reactivity of the probe surface and the temperature-time history of the gas. Rates of quenching, as calculated by an energy balance, were found to cause reacting species to follow a non-equilibrium path if their magnitudes exceeded 10^7°K/s. Based upon the assumption that energy lost from the gas was equivalent to the energy convected to the tube walls and energy associated with chemical reactions occurring at the tube surface, the following quench equation was derived:

$$\frac{-d(c_p \; T)}{dT} = \frac{4h(T - T_w)[1 + \sum_{i=1}^{N} \lambda_i \; W_{i-N}/h(T - T_w)]}{\rho D\bar{M}} \qquad (3\text{-}3)$$

where c_p = specific heat capacity (cal/g°K)

T = plasma temperature (°K)

t = time (s)

h = convective heat transfer coefficient (cal/cm^2 s °K)

T_w = quench tube surface temperature (°K)

D = quench tube diameter (cm)

$\bar{M}$ = average molecular weight (g/gmol)

W = heterogeneous rate of loss of the ith component (gmol/cm^2 s)

N = total number of species

ρ = molar gas density (gmol/cm^3)

λ = energy of surface reactions (cal/gmol)

Solution of the equation by numerical integration and utilization of published physical and thermodynamic properties allowed construction of temperature-time histories of the gas stream. In the equation, c_p, h, ρ, $\bar{M}$ and W_{i-N} were all functions of temperature.

Huczko /57/ has studied the decomposition of carbon dioxide in an argon plasma. The product stream was withdrawn from the reactor through small diameter channels of a multi-channel, water-cooled sampling probe located at different longitudinal positions. It allowed measurement of the spatial distribution of both temperature and fractional conversion. These measurements made possible an estimation of the quenching rate in the probe's channel. For the particular system under study, the quench rate was given by:

$$\frac{dT}{dt} = \frac{1.61 \times 10^{-2}(T_I - T_{II})^2[\tilde{w}_{Ar}+\tilde{w}_{CO_2}(1+0.5\bar{X})]}{\ln\left(\frac{T_I}{T_{II}}\right)} \qquad (3\text{-}4)$$

where t = time (s)

T_I , T_{II} = plasma temperature in measuring zones I, II (°K)

$\tilde{w}$ = molar flowrate (mol/s)

$\bar{X}$ = average fractional conversion

Quenching rate equations, derived from the conservation equations, require an estimation of heat transfer coefficients. To this end, studies of plasma heat transfer to water-cooled tubes have been undertaken /55,56,58,59/.

Quenching rate correlations, specific to the process occurring in water-cooled tubes, are abundant in the Russian literature, covering a wide variety of heat exchange configurations. However, no English translations of these works are available.

Ultimately, the quenching rate is limited by the thermal conductivity of the cooled surface. The maximum heat flux through a surface is about 500 W/cm^2, with higher heat fluxes resulting in significant damage to even the most heat-resistant materials available /60/. Because heat fluxes in plasmas tend to be much higher, cooled surface quenchers are limited in their ability to cool the plasma.

The use of cold-fingers, rotating drums, funnels and other unique cooled-surface geometries in a quenching capacity has been restricted to specialized applications, accounting for the scarity of information available on these devices.

3.3 Fluidized Beds

Quenching of the product stream by a fluidized bed involves a complex exchange of energy between the plasma, the entrained gas and solids of the fluidized bed and the reactor walls. Particle diameter strongly influences the quenching ability of a fluidized bed with higher quench rates attainable with smaller particles. These smaller diameter particles circulate throughout the bed easier in addition to having a higher surface area per unit mass available for heat transfer. Increasing the fluidizing gas velocity also improves quenching by increasing entrainment of the gas into the plasma jet.

The jet may exhaust into a fluidized bed in a horizontal manner or may be fired vertically up or down into the bed. Amouroux and Cavadias /61/ fired a plasma horizontally into a fluidized bed of tungsten oxide particles to study quenching and catalytic effects. Encouraging yields of nitrogen oxides were reported from feedstocks of nitrogen and oxygen. Goldberger and Oxley utilized a bed of fluidized alumina to quench an argon plasma /62/. Using the apparatus of Figure 3-3, the plasma was injected upward directly into the bed of fluidizing solids with additional cool argon gas being provided to maintain a uniform degree of fluidization. Temperature profiles, taken during operation with the column free of solids, were compared with profiles taken during fluidized bed operation under similar conditions. An increase in the quench rate due to the presence of solids was observed. Greater bed temperature uniformity was reported for lower arc gas flowrates, higher fluidizing gas flowrates and deeper beds. These investigators found that a semi-logarithmic plot of the difference between the centerline and bulk bed temperature versus the distance from the plasma jet opening, approximated a straight line. Upon algebraic manipulation and differentiation of the resulting correlation, with respect to time the following quench equation was obtained:

$$\frac{dT_{cl}}{dt} = \frac{(\bar{T}_o - T_B)\ (C)\ (e^{Cy})\ (Q^{o}T_{cl})}{(60\ A\ T^{o})} \qquad (3\text{-}5)$$

where T_{cl} = centerline temperature of jet (°K)

t = time (s)

$\bar{T}_o$ = average plasma temperature at $y=0$ (°K)

T_B = bulk temperature of fluidized bed (°K)

C = a coefficient determined from a semi-logarithmic plot (ft^{-1})

y = vertical distance above jet opening (ft)

Q^{o} = arc gas volumetric flowrate at reference conditions (ft^3/min)

A = area of jet opening (ft^2)

T^{o} = reference temperature (20°C)

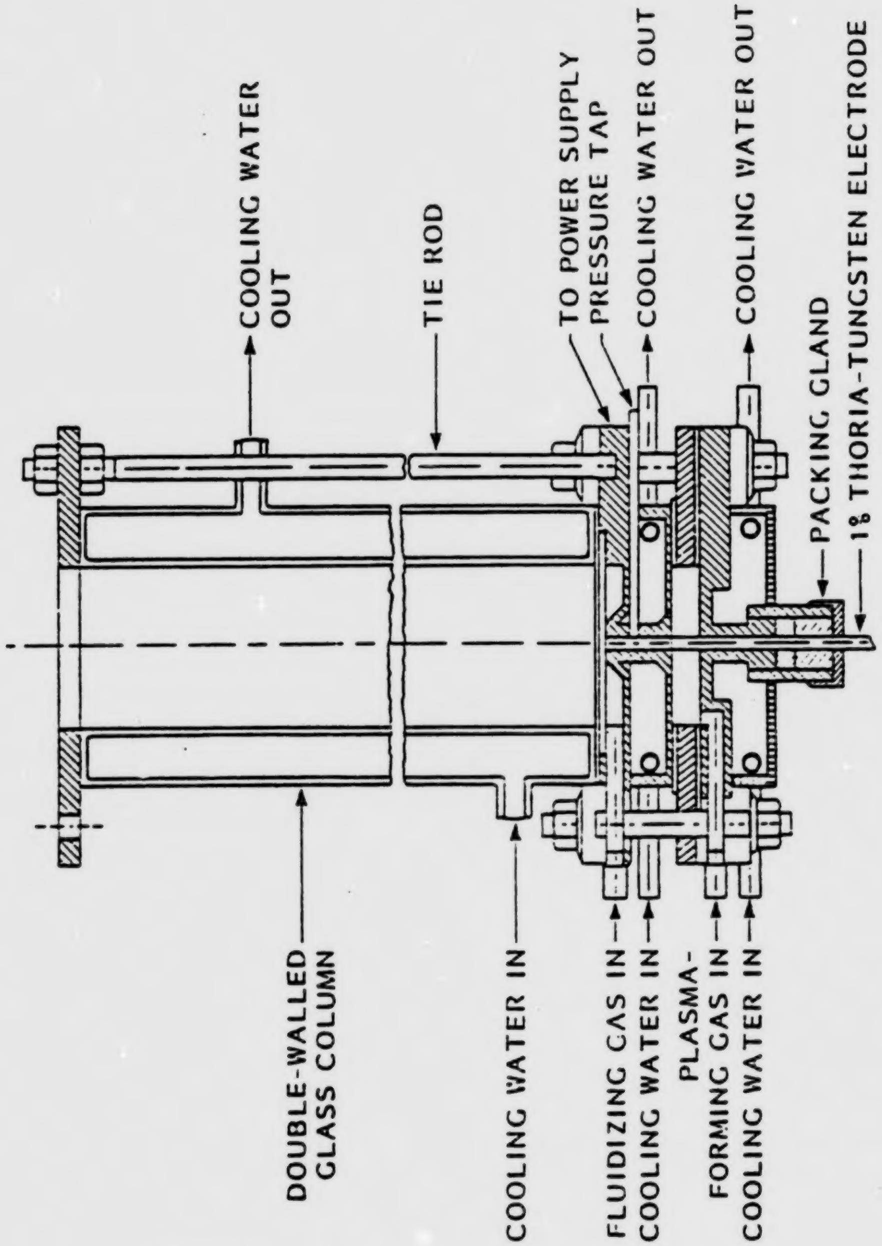

COOLING WATER OUT
TIE ROD
TO POWER SUPPLY
PRESSURE TAP
COOLING WATER OUT
COOLING WATER OUT
PACKING GLAND
1% THORIA-TUNGSTEN ELECTRODE
DOUBLE-WALLED GLASS COLUMN
COOLING WATER IN
FLUIDIZING GAS IN
COOLING WATER IN
PLASMA-FORMING GAS IN
COOLING WATER IN

FIGURE 3-3: A Fluidized Bed Quenching System

Average quench rates for cooling to below 1000°C were found to exceed 10^6°K/s and initial temperature decay rates were estimated to be about 5×10^7°K/s under ordinary experimental conditions.

In addition to its quenching characteristics, the fluidized bed offers advantages not found in other reactors. Fluidized solids may act as reactants, catalysts, or sites for product adsorption. The agglomeration of solids formed during the cooling process would pose little danger in terms of reactor fouling and erosion; a situation likely in some other types of quenchers. The economical recovery of energy may be possible, as well, by using energy stored in the bed solids in a direct contact heat transfer system to preheat reactants or provide heat for endothermic reactions.

Additional work on the quenching of plasmas using fluidized beds has been carried out by German investigators /63/.

3.4 De Laval Nozzles

By forcing a hot gas stream to accelerate through a nozzle, a good degree of the stream's thermal energy is converted to kinetic energy resulting in a significant temperature decrease. The highest discharge velocity is obtained by using a convergent/divergent (De Laval) nozzle having the geometry illustrated in Figure 3-4. The shape of the converging section is similar to that of a simple converging nozzle, while the shape of the diverging section must be of a special design so as to obtain a uniform, parallel, shock-free, supersonic exit stream.

Quenching in the nozzle entrance region, where cooling is initiated, may be described by the following relationship developed from thermodynamics /64/:

$$\frac{dT}{dt} = \frac{2\,\bar{v}\,\tan\phi}{r[\tilde{c}_p/\bar{M}\bar{v}^2 - 1/\,T(\gamma-1)]} \qquad (3\text{-}6)$$

where T = plasma temperature

t = time

$\bar{v}$ = average velocity

r = radius of an arbitrary nozzle cross section

$\tilde{c}_p$ = molar heat capacity

$\bar{M}$ = average molecular weight

Ø = some angle less than the half-angle of the converging or diverging cones forming the nozzle

γ = ratio of specific heat at constant pressure to specific heat at constant volume

The cooling rate found elsewhere in the nozzle may be calculated from the equation:

$$\frac{dT}{dt} = \frac{2\tan\delta(2\bar{c}_p T_c{}^3/\bar{M})^{0.5}}{\{0.5(1-T/T_c)^{-1.5} - T_c[(\gamma-1)T(1-T/T_c)\ 0.5]\}^{-1/r}} \qquad (3\text{-}7)$$

where T_c = reaction chamber temperature

δ = half-angle of the converging or diverging cones forming the nozzle

Results of calculations done with these equations, under representative operating conditions, indicate a quenching rate on the order of 10^7 °K/s. However, few, if any, experimental results have been described in the literature.

The major obstacle to nozzle utilization is reheating of the exiting stream to near its original temperature as it decelerates from supersonic speeds. To prevent this reversal of the cooling process, it has been suggested that the nozzle be coupled to a turbine to allow removal of translational energy from the gas stream by having it do work /64/. Electricity generated by the turbine's action could be used to augment the plasma generator's power supply. Of concern, would be the relatively high temperatures to which the blades of the turbine would be exposed. In response to this, the use of transpiration-cooled blades has been proposed /65/. These ideas have even been incorporated in a proposed process for the production of nitric oxide from nitrogen and oxygen /66/, the schematic diagram of which is illustrated in Figure 3-5. Unlike fluid injection or bed quenching, the De Laval nozzle causes no dilution of the product stream, although it may be susceptible to plugging in reactions involving solids.

The merits and drawbacks of all four quenching techniques are summarized in Table 3-1.

	Fluid Injection	Cooled Surfaces	Fluidized Bed	De Laval Nozzle
Typical Quenching Rates (°K/s)	$10^6 - 10^7$	$10^5 - 10^6$	$10^6 - 10^7$	$10^7 - 10^8$
ADVANTAGES	- injected fluid may serve as a reactant or adsorbant as well as a quenching medium	- no product stream dilution - simultaneous quenching and product recovery in probes	- advantageous where solid products are formed - bed solids may act as reactants, catalysts or sites for product adsorption as well as a heat sink - potential exists for energy recovery	- no product stream dilution - potential exists for energy recovery
DISADVANTAGES	- potential for product stream dilution - energy recovery is impractical	- probe scaleup problems - heat transfer is limited by materials of construction - reactions with solids may cause fouling or plugging of the quencher - energy recovery is impractical	- product stream dilution by fluidizing gas	- special heat-resistant materials required for a turbine and nozzle - reactions with solids may cause fouling or plugging of the nozzle - extreme pressures required

TABLE 3-1: Advantages and Disadvantages of Each Quenching Method

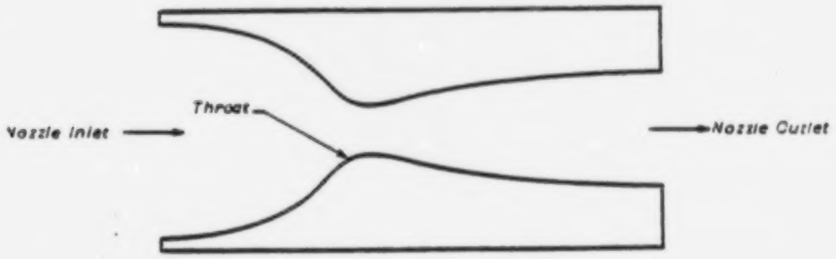
Throat
Nozzle Inlet
Nozzle Outlet

FIGURE 3-4: The De Laval Nozzle

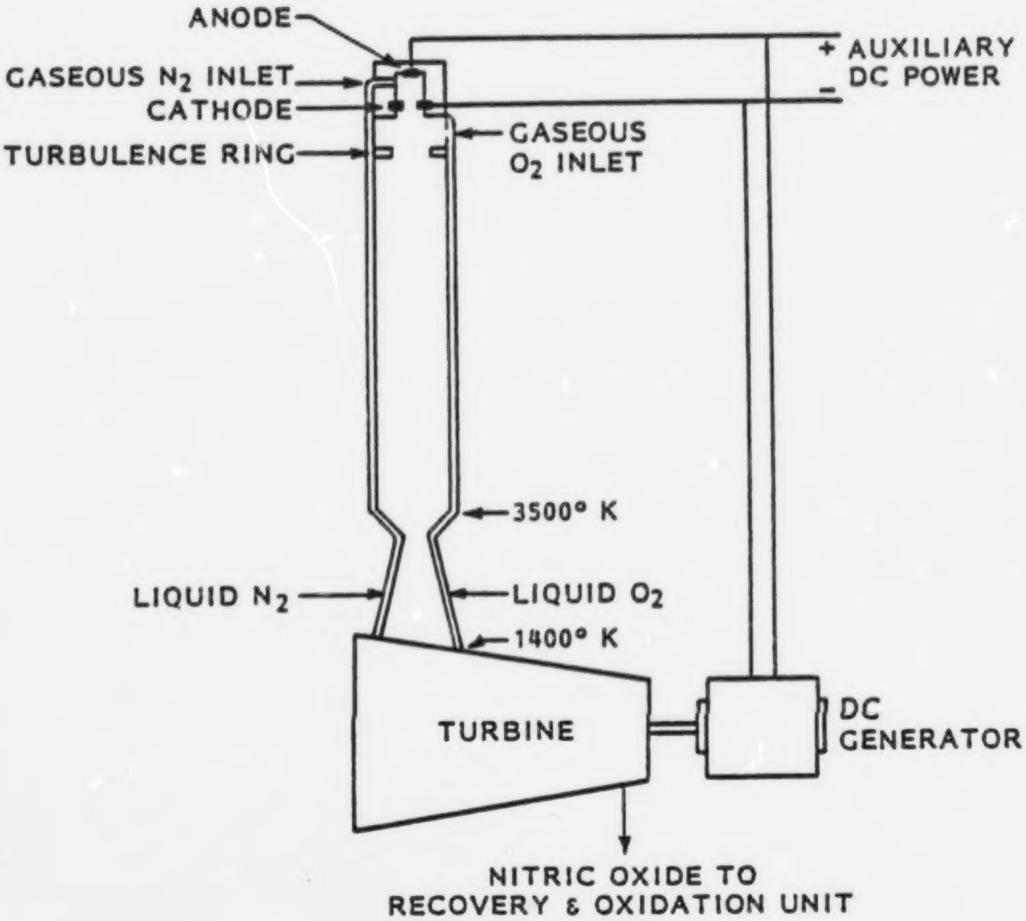
ANODE
GASEOUS N2 INLET
CATHODE
TURBULENCE RING
+ AUXILIARY
_ DC POWER
GASEOUS
O2 INLET
3500° K
LIQUID N2
LIQUID O2
1400° K
TURBINE
DC
GENERATOR
NITRIC OXIDE TO
RECOVERY & OXIDATION UNIT

FIGURE 3-5: A Proposed Plasma Process for Nitrogen Oxide Production Utilizing a Nozzle/Turbine Quencher

Quenching systems, consisting of various combinations of the basic quenching methods, have received little attention owing to the limited focus on the quenching process in general. Propositions have been made, for example, to link a De Laval nozzle/turbine quencher to a liquid spray injection quencher /65/ but experimental follow-up has been lacking. One exception, however, is a water-cooled probe having an unconventional inner geometry resulting in an aerodynamic quench /67/. Such a device, illustrated in Figure 3-6, has been successfully tested in flames. Flow entering the probe is choked at the entrance orifice and then quickly accelerated to a supersonic speed in the region of the diffuser-shaped probe tip. Supersonic flow is maintained in a constant area section located immediately downstream of the probe tip until the stagnation temperature of the stream is reduced sufficiently by heat transfer with the probe walls. Upon return to subsonic flow conditions caused by a sudden expansion in flow area, the aerodynamic quenching process is complete. In an investigation of acetylene synthesis from fluidized methane in an arc discharge /53/, a similar probe design reportedly gave quench rates of 10^8°K/s. It was also concluded that this form of probe aperture was less susceptible to blockage by solid products than was a constant diameter probe.

Few studies have been done to compare the performances of different types of quenchers. In one such undertaking, Sundstrom and De Michiell /68/ chose to mathematically model cold gas mixing, liquid spray evaporation, injection into a fluidized bed and cooled-surface contact. The effects of process variables were examined and quenching rates calculated for each method. Models chosen to represent the four quenching processes were adapted from those of the literature with quenching rates evaluated over a range of operating conditions considered typical. Comparison of the quenching methods was difficult owing to the specific variables associated with each technique. The study rated each quencher's performance in order of increasing quench rates as: cooled-surface contact, liquid spray evaporation, injection into a fluidized bed and cold gas mixing. Typical temperature-time profiles which summarized the findings of the study are illustrated in Figure 3-7. Magnitudes of the initial quenching rates for cold gas mixing, liquid spray evaporation and the fluidized bed were similar. As time proceeded, cold gas mixing gave the *highest quench rates* attributable to turbulent mixing effects. Conversely, liquid spray evaporation gave the lowest quench rates because liquid drops were accelerated by the faster moving hot gas stream. This resulted in decreased heat and mass transfer coefficients. All techniques were able to provide initial cooling rates in excess of 10^6°R/s.

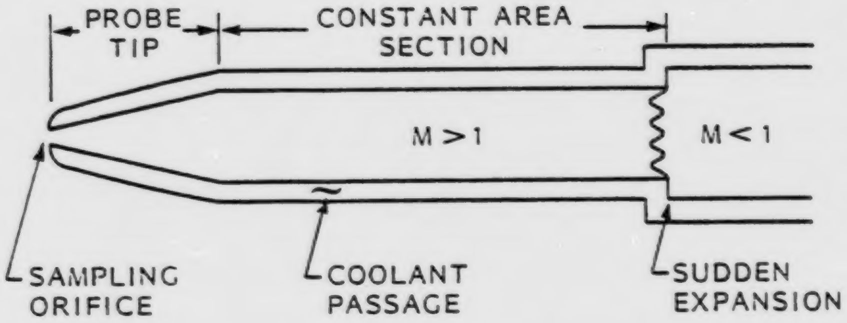
PROBE TIP
CONSTANT AREA SECTION
M > 1
M < 1
SAMPLING ORIFICE
COOLANT PASSAGE
SUDDEN EXPANSION

FIGURE 3-6: The Aerodynamic Quench Probe

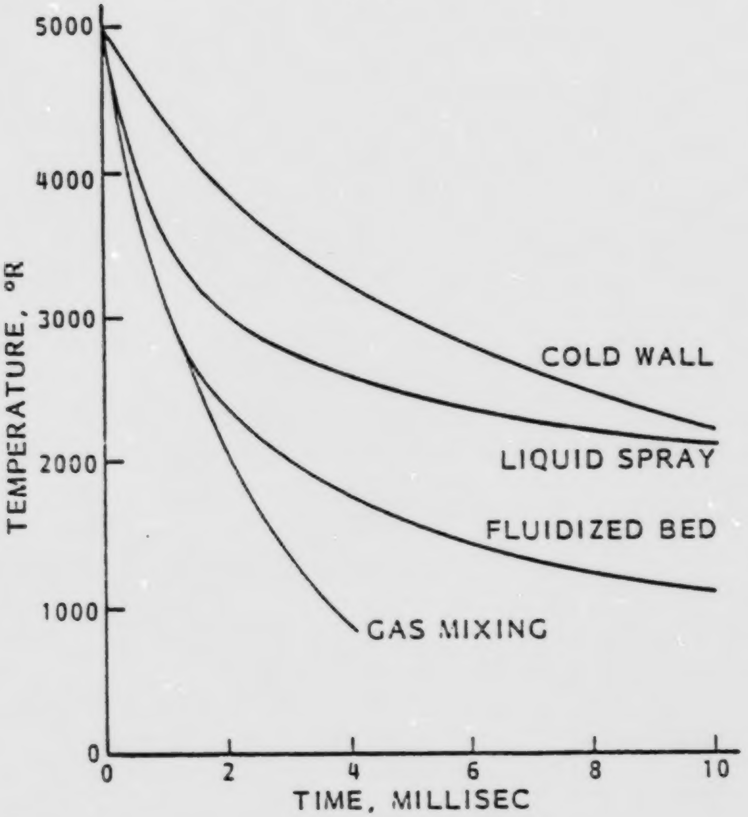

FIGURE 3-7: Comparison of Quenching Processes Under Typical Conditions

4.0 THE QUENCHING EXPERIMENTS

The experimental apparatus used in this investigation, including the selection and design of the quenching systems, is outlined in the following sections. Based upon this information, an experimental procedure was formulated.

4.1 The Experimental Apparatus

The experimental portion of the investigation was conducted at the W.R. Dobson laboratories of Ontario Hydro in Toronto. The apparatus described herein is classified as either an integral subsystem of the plasma chemical reactor or as a diagnostic tool.

4.1.1 The Plasma Chemical Reactor

The plasma chemical reactor can be thought of as a system composed of the following subsystems:

i) the plasma torch
ii) the diagnostic chamber
iii) the power supply
iv) the gas supply system
v) the cooling water network
vi) the data acquisition and control system
vii) the quenching system

A schematic of the experimental set up is presented in Figure 4-1.

a) The Plasma Torch

Plasma was generated for these experiments by an electrical discharge arc plasma device. The plasma torch was an 80 kw direct current arc generator proven capable of operating on air, argon, nitrogen, or hydrogen gases. The unit, illustrated in Figure 4-2, was modular in construction allowing for individual sections to be added or removed. Each disc-shaped copper section was water-cooled to prevent thermal failure. Combinations of modules were fastened together by four bolts and sealed tightly by O-rings. Those sections placed between the anode and cathode were electrically insulated from neighbouring sections by boron nitride spacers. The basic torch configuration consisted of, in order of their assemblage: cathode, gas injection, arc column and anode modules.

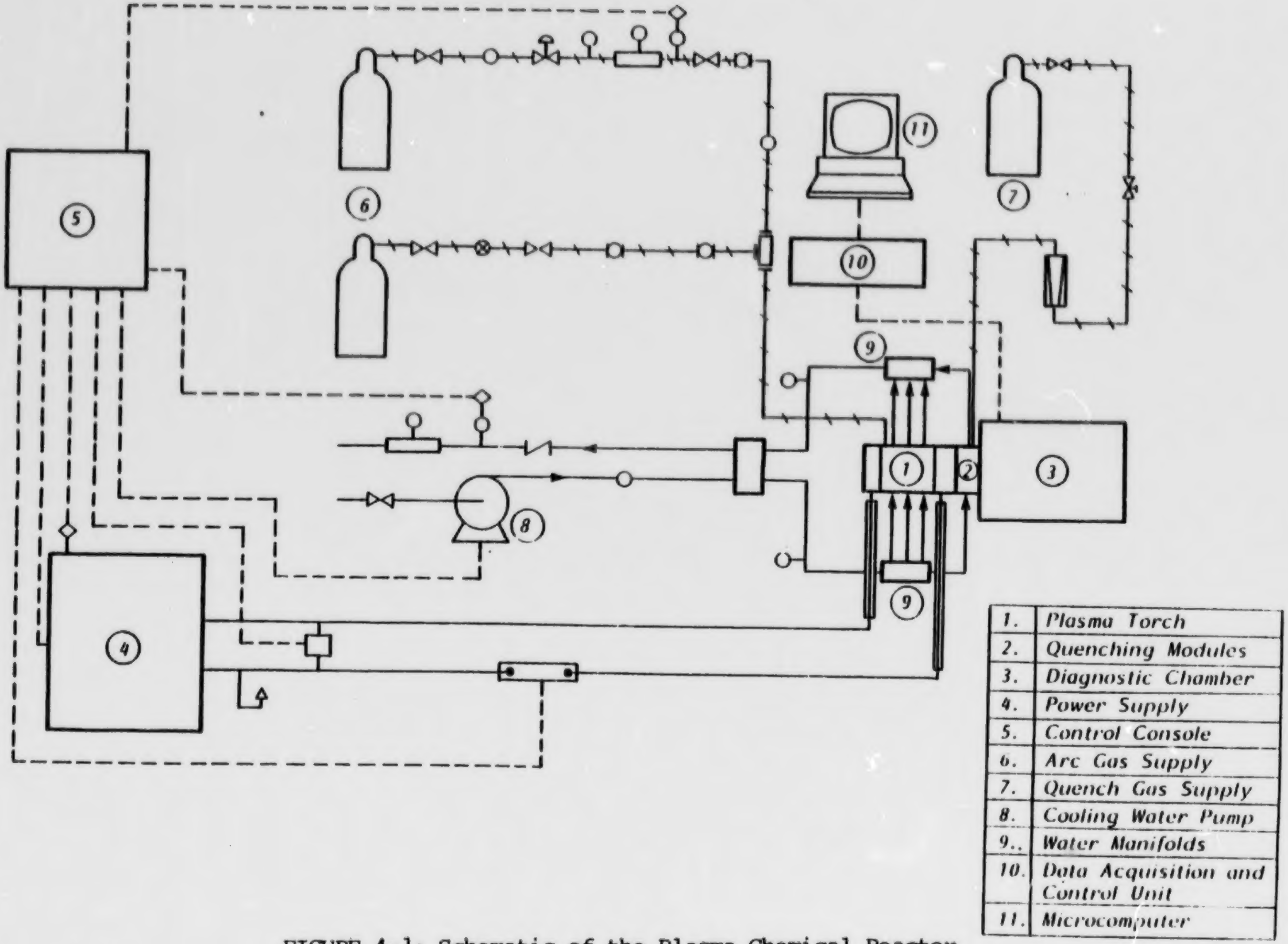

1.	Plasma Torch
2.	Quenching Modules
3.	Diagnostic Chamber
4.	Power Supply
5.	Control Console
6.	Arc Gas Supply
7.	Quench Gas Supply
8.	Cooling Water Pump
9..	Water Manifolds
10.	Data Acquisition and Control Unit
11.	Microcomputer

FIGURE 4-1: Schematic of the Plasma Chemical Reactor

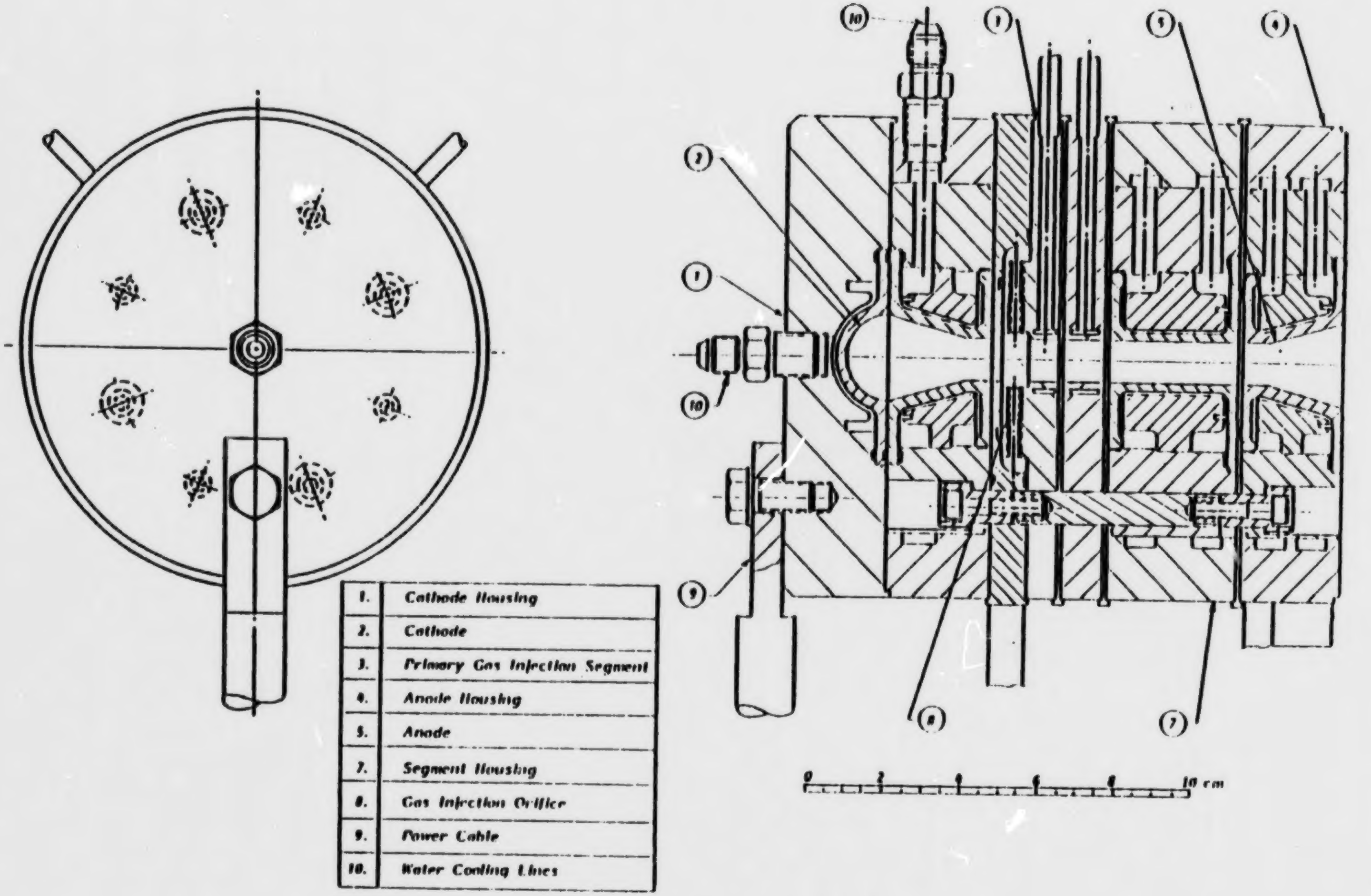
10
3
5
4
2
1
10
9
8
7
0
2
4
6
8
10 cm

1.	Cathode Housing
2.	Cathode
3.	Primary Gas Injection Segment
4.	Anode Housing
5.	Anode
7.	Segment Housing
8.	Gas Injection Orifice
9.	Power Cable
10.	Water Cooling Lines

FIGURE 4-2: The Plasma Torch

The cathode section used either a copper bell-shaped or tungsten button-shaped electrode. The anode section used the copper conical-shaped electrode. In operation, the arc was struck from the cathode to the surface of the anode, through the electrically insulated segments Arc stabilization was provided by the vortex resulting from tangential arc gas injection.

In the case of a chemical synthesis, an injection module for the introduction of solid, liquid or gaseous reactants, and a mixing plenum module, in which separate streams would be mixed and subsequently reacted, could be added to the basic torch configuration.

b) The Diagnostic Chamber

The chamber, illustrated in Figure 4-3, provided an environment in which the stream issuing from the torch could be studied. Insertion of the torch through the chamber entrance was limited to the point at which its gas or water-cooling lines interfered with the front face of the vessel. The forward portion of the torch rested on a support welded to the chamber while the cavity between the torch and support was sealed to minimize the inflow of air. The chamber was outfitted with six viewing ports of pyrex glass (three on each side of the vessel). In addition to this, there were nine sampling ports, each 11 mm in diameter, located at varying distances along its top. Effluent from the chamber was removed via a fumehood.

The absence of a cooling system in the diagnostic chamber resulted in run times of less than 20 minutes to minimize chamber heating.

c) The Power Supply

The plasma torch power supply was rated for up to 80 kW of continuous direct current output. The supply consisted of a three phase semi-converter bridge and a constant voltage output transformer. By controlling the firing angle on the semi-converter bridge, the current could be varied over the entire operating range. Forced air cooling was used to control the power supply's temperature.

d) The Gas Supply System

Gas, to be used as arc gas or injected as a quenching medium, was drawn from commercial grade gas cylinders. The arc gas flow was routed through the control panel which

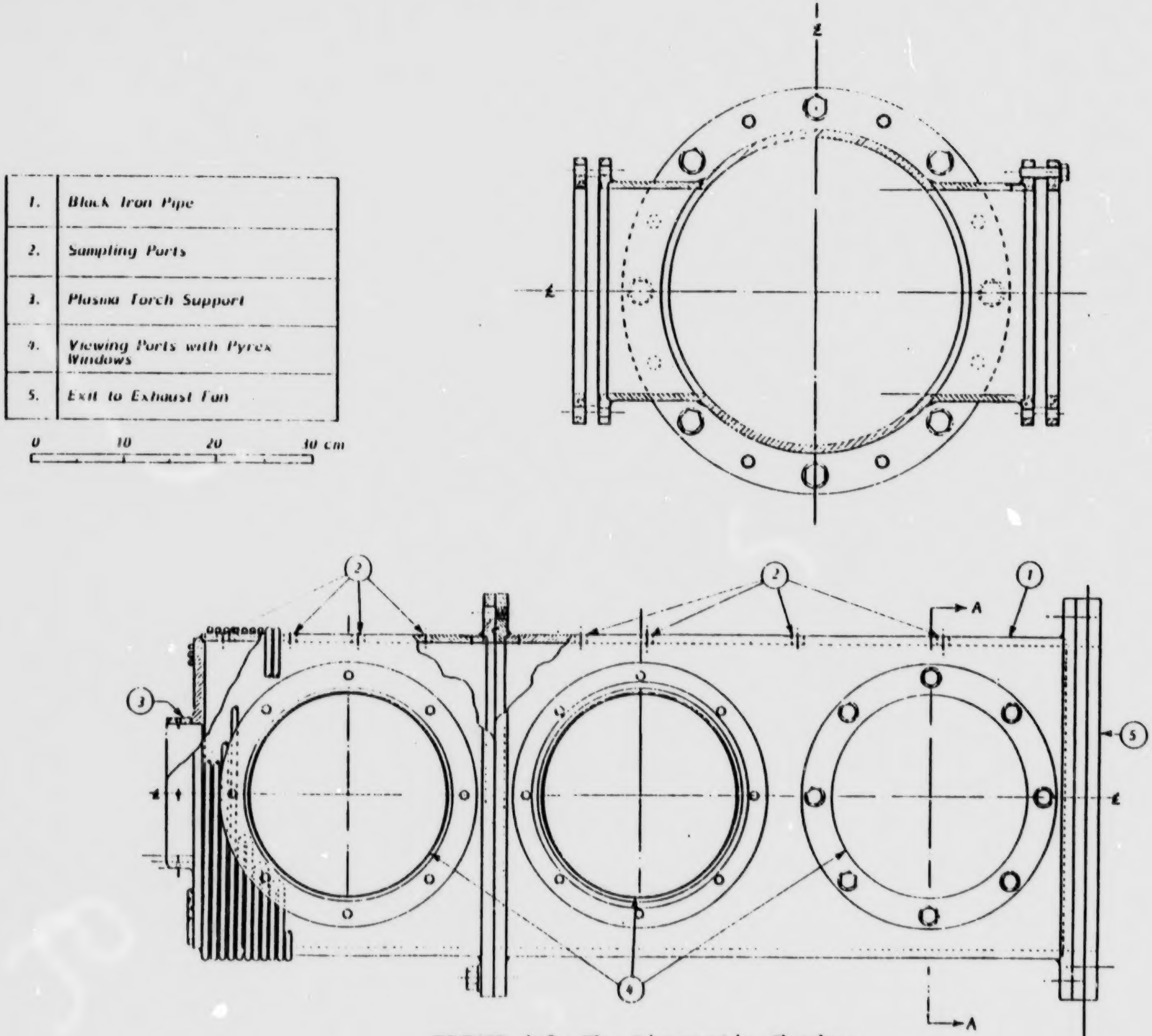
1. Black Iron Pipe
2. Sampling Ports
3. Plasma Torch Support
4. Viewing Ports with Pyrex Windows
5. Exit to Exhaust Fan
0
10
20
30 cm
1
2
3
4
5
A
A

FIGURE 4-3: The Diagnostic Chamber

controlled flowrate by a series of metering and shutoff valves. The panel also included a regulator to set the gas load pressure and a calibrated rotameter to observe the gas flowrate.

Quench gas flow was routed from a gas cylinder to the appropriate torch module. In between, gas flowrate was monitored by a calibrated rotameter with appropriate valve arrangements for flow control. Results of the rotameter calibrations are presented in Appendix A.

e) The Cooling Water Network

Water, from the city supply, was drawn through a 25 μm filter into a 6.5 horsepower pump capable of delivering 76 L/min of water at a gauge pressure of 1725 kPa. Flow was discharged through a flexible coupling to an aluminum inlet manifold connected to each torch module by high pressure water hoses. Upon distribution in the cooling passages of each torch module, the coolant exited through a second manifold and then a calibrated rotameter before being sent to a drain. Ball and check valves were used to isolate various parts of the system in the event of a leak or break. A differential thermopile, consisting of ten copper/constantan thermocouples, was positioned between the inlet to the first water manifold and the outlet of the second to measure water temperature changes. This allowed energy balance calculations to be made about the torch.

f) The Data Acquisition and Control System

Variables associated with arc gas flowrate, power supply to the torch and water pump operation were monitored and displayed by the control panel. Arc current was set at the turn of a dial while arc length, and thus arc voltage, was determined by the arc gas flowrate, arc current and torch configuration. Voltage and current were displayed on analog meters alongside a digital display of the torch cooling water temperature rise. The steadystate value for each variable was recorded manually during a run.

Thermocouple signals were processed by a data acquisition and control unit capable of accepting each analog input signal with an accuracy of ±10 μV. Operation of the data acquisition system was under the control of an interfaced 64K RAM microcomputer with dual disk drives and printer. The computer software allotted each thermocouple a predetermined, set period of time (based upon preliminary measurements) for attainment of a steadystate reading. The following ten readings, taken approximately 1.5 seconds apart, were averaged and the result stored for later retrieval.

g) The Quenching Systems

The type of quenching system selected for study was strongly influenced by the degree to which it satisfied the following criteria:

i) did the quencher provide a quenching rate of sufficient magnitude to interrupt equilibrium reaction paths?

ii) could the quenching rate be varied with considerable ease to allow optimization of the quenching process?

iii) was the design simple enough to ensure easy construction and trouble-free operation?

iv) could the quenching system be adapted to other torches and diagnostic chambers having different geometries?

v) was the quenching system adaptable to a wide range of chemical reactions?

vi) could the device be manufactured and operated for a reasonable cost?

Based upon these guidelines, and the more practical constraints of a technical, time and cost nature, attention was focused exclusively on the proven methods of fluid injection and cooled-surface contact. This meant that each quencing system design was to utilize some aspect of either the gas supply system and/or the cooling water supply network.

The incorporation of a De Laval nozzle in a quenching system would have necessitated extremely high upstream to downstream pressure ratios for which the torch and diagnostic chamber were not designed. The extensive modifications to the diagnostic chamber and exhaust hood, necessary to install a fluidized bed quenching system, were considered impractical for this investigation.

Quenchers, based soley upon the injection of a cool gas, provided the startpoint for subsequent designs.

To represent a conventional fluid injection quenching system, the following aspects of design were considered:

i) orientation of gas injection (radial, tangential, axial),

ii) size, shape and number of injection orifices,

iii) geometry of the stream passageway (converging, diverging, constant diameter),

iv) materials of construction.

Two fluid injection devices, for comparative purposes, were chosen for study. The first, henceforth called injection ring #1, is shown in relation to the plasma reactor in Figure 4-4. Made of copper, the ring had an outer diameter of 140 mm, an inner diameter of 38 mm and a total thickness of 17 mm. Fluid was injected radially into the plasma stream through 16 evenly spaced orifices, each having a diameter of 0.8 mm. A flexible stainless steel tube, affixed to the outer edge of the ring, allowed easy connection to the quenching fluid supply. The ring was mounted on the front end of the torch by the same four bolts used to hold the torch modules together. Injection ring #1 was originally designed for use with liquid injectants thus explaining the absence of any direct water cooling. For use with gaseous injectants, the module was to be cooled primarily by conduction with adjacent cool surfaces.

The second fluid injection quencher (designated injection ring #2) is illustrated as part of the overall chemical reactor in Figure 4-5 and was, originally a module of the torch designed for the injection of powders by entrainment in a carrier gas stream. In the quenching experiments, gas alone was injected radially into the plasma stream through the two 5 mm diameter orifices positioned opposite one another. The ring had an outer diameter of 140 mm, an inner diameter of 25 mm, an overall thickness of 22 mm and was directly water-cooled through connection to the water manifolds.

The first quenching system incorporating both gas injection and cooled-surface contact is shown as part of the plasma reactor in Figure 4-6. A cooled-surface constant diameter flow passage was attached to the outlet of gas injection ring #2 to enhance mixing and heat transfer and to conduct heat away, all by confinement of the flow. Both modules were fastened directly to the plasma torch. The cooled-surface module, of copper construction, had an outer diameter of 140 mm, an inner diameter of 38 mm and a thickness of 17 mm. Cooling water, from the water manifolds, flowed to and from the disk through two 13 mm O.D. flexible

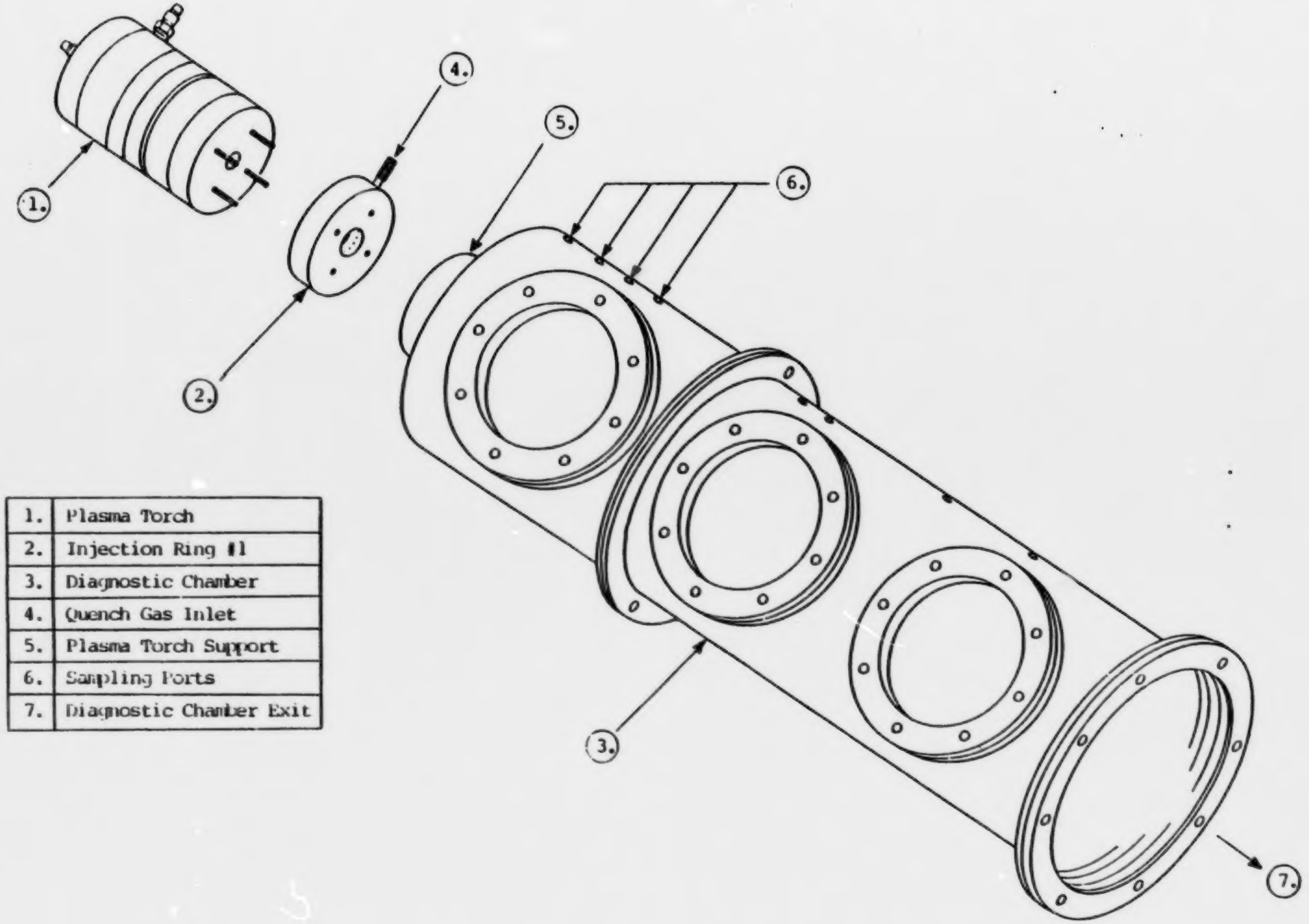

1.	Plasma Torch
2.	Injection Ring #1
3.	Diagnostic Chamber
4.	Quench Gas Inlet
5.	Plasma Torch Support
6.	Sampling Ports
7.	Diagnostic Chamber Exit

FIGURE 4-4: The Plasma Reactor Assembly for Gas Injection Ring #1

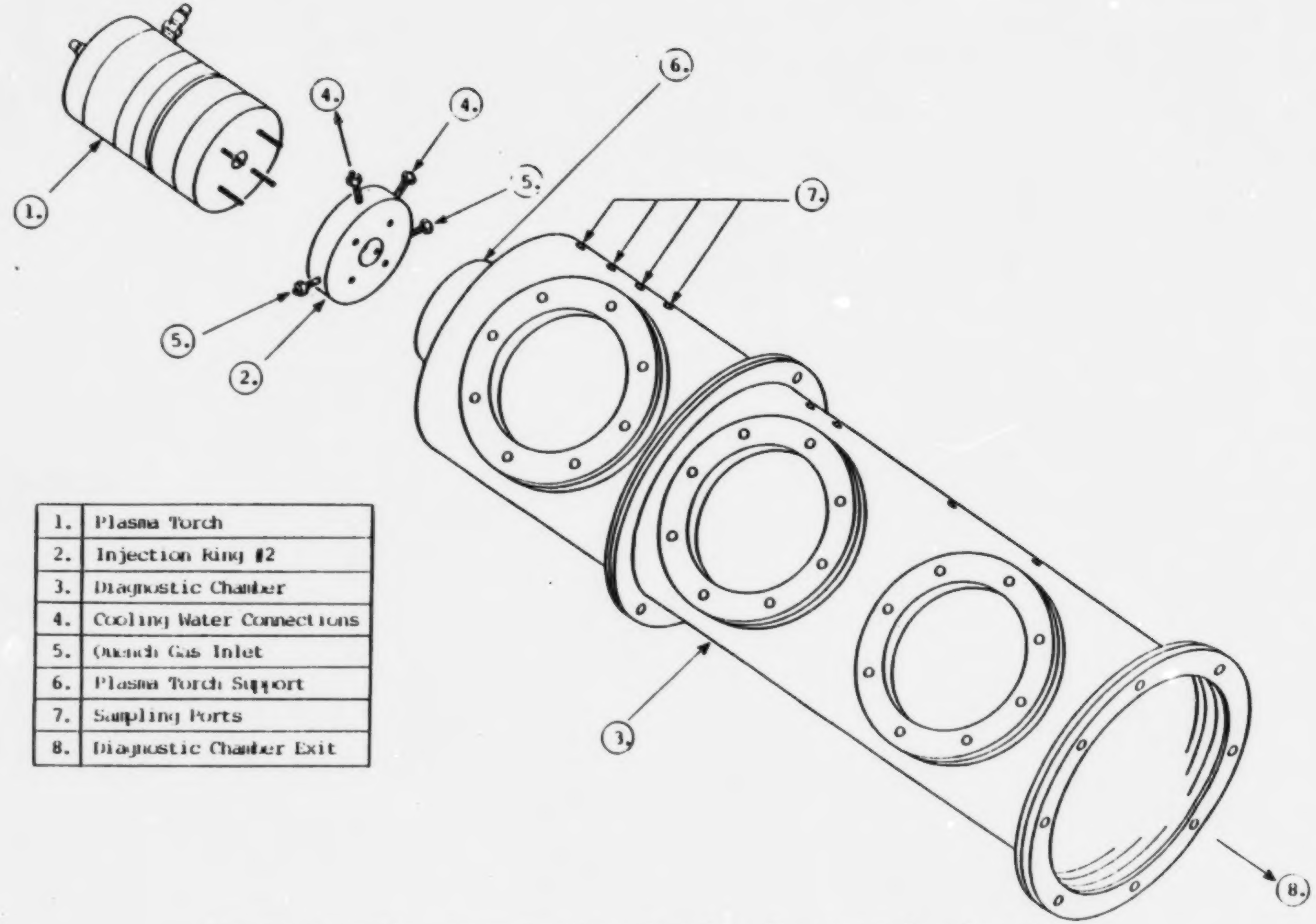

1.	Plasma Torch
2.	Injection Ring #2
3.	Diagnostic Chamber
4.	Cooling Water Connections
5.	Quench Gas Inlet
6.	Plasma Torch Support
7.	Sampling Ports
8.	Diagnostic Chamber Exit

FIGURE 4-5: The Plasma Reactor Assembly for Gas Injection Ring #2

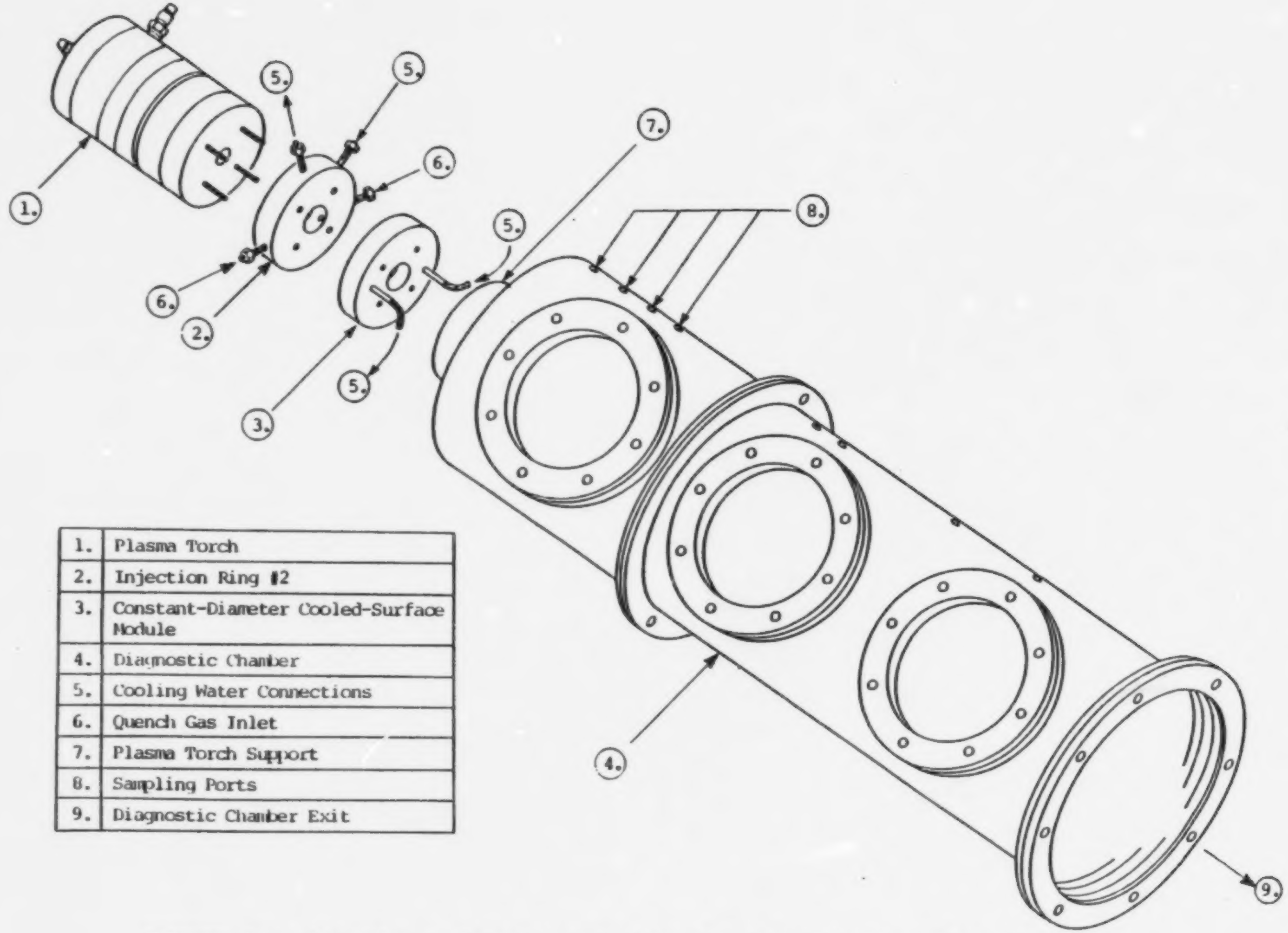

1.	Plasma Torch
2.	Injection Ring #2
3.	Constant-Diameter Cooled-Surface Module
4.	Diagnostic Chamber
5.	Cooling Water Connections
6.	Quench Gas Inlet
7.	Plasma Torch Support
8.	Sampling Ports
9.	Diagnostic Chamber Exit

FIGURE 4-6: The Plasma Reactor Assembly for Gas Injection Ring #2 Plus the Cooled-Surface, Constant-Diameter Flow Passage

stainless steel tubes soldered to the outer face of the disk. This permitted easy insertion and removal of the torch assembly from the diagnostic chamber. The auxiliary equipment, with the addition of water hoses for the cooled-surface module, remained the same as that for the gas injection ring alone.

The second quenching system to use gas injection and cooled-surface contact was the novel design. Since the constant-diameter flow passage could not force the degree of mixing between hot and cold streams desired for improved quenching, it was replaced with a flow passage of a convergent nature. No previous work on this type of quencher was reported in the literature. In addition to cooling the plasma, the flow of quench gas served as a buffer between the plasma core and passageway walls. Thus, the potential for ablative damage to the exposed surfaces of the passage was considerably lessened. The water-cooled, convergent flow passage, or nozzle, was constructed with an outer diameter of 140 mm and a thickness of 33 mm. It is shown together with the water-cooled gas injection ring in Figure 4-7. The nozzle module was an unused component of the torch designed for stream diffusing applications. By mounting the disk backwards onto the gas injection ring, a convergent flow passage was created. The module was designed with a removable nozzle insert to allow for substitution of nozzles having different inlet to outlet area ratios. In this investigation, the nozzle had a ratio of 4. The quenching system's auxiliary equipment was identical to that of the first gas injection/cooled-surface quencher. Surface areas, exposed to the flow of plasma for both cooled-surface modules, were chosen identical in magnitude to allow a comparison of the effects of geometry alone upon quenching.

4.1.2 Quench Experiment Diagnostics

It would have been ideal to measure temperatures within the quencher itself without significantly disrupting the flow in the quenching region. However, the inaccessibility of diagnostic tools to the internal flow passages of most quenchers makes this a very hard task. Consequently, temperatures are monitored within a defined area, termed the effluent region, located immediately downstream of the quencher.

These temperatures can be classified, by their method of measurement, into two categories:

i) those values exceeding approximately 2000°C
ii) those values less than approximately 2000°C

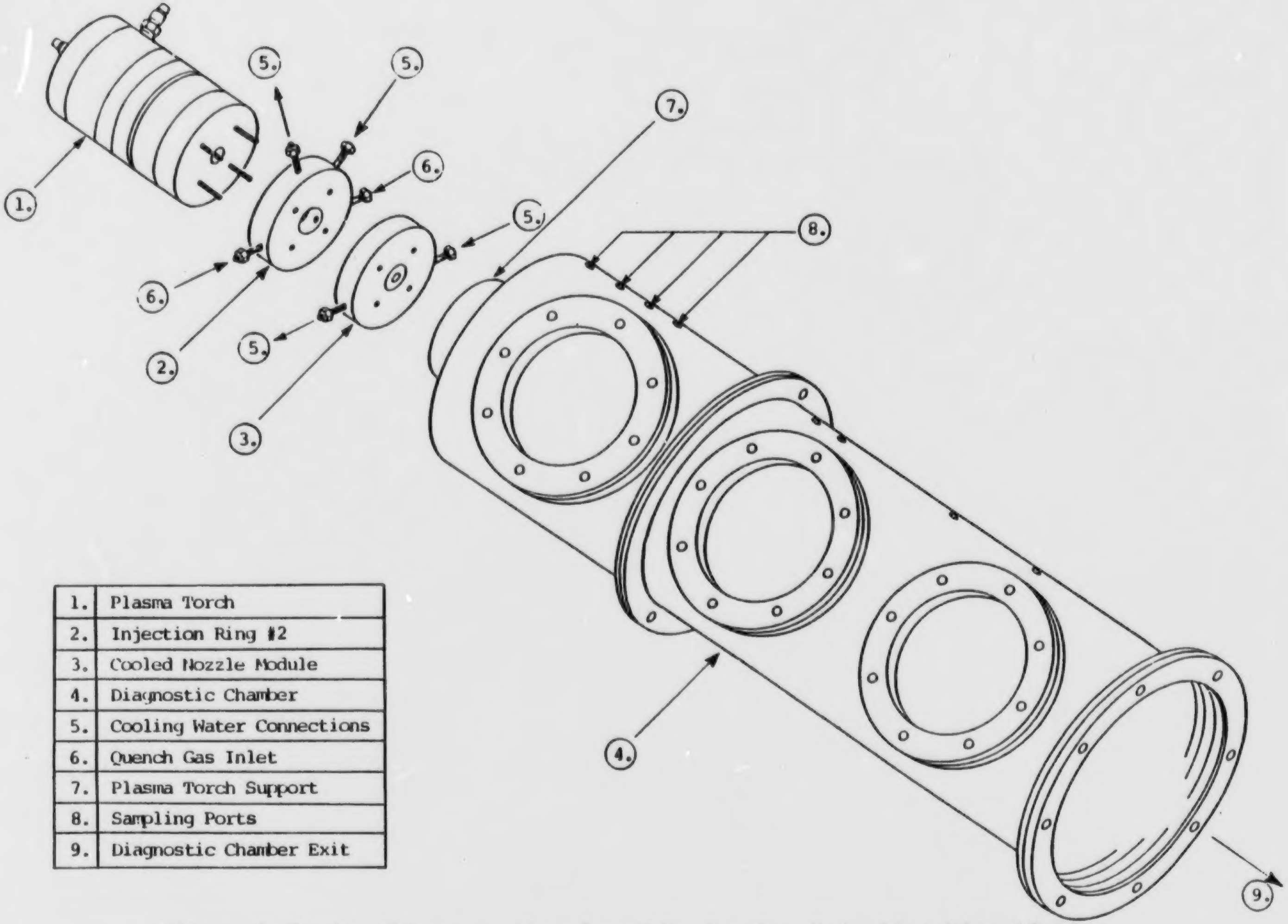

1.	Plasma Torch
2.	Injection Ring #2
3.	Cooled Nozzle Module
4.	Diagnostic Chamber
5.	Cooling Water Connections
6.	Quench Gas Inlet
7.	Plasma Torch Support
8.	Sampling Ports
9.	Diagnostic Chamber Exit

FIGURE 4-7: The Plasma Reactor Assembly for Gas Injection Ring #2 Plus the Cooled-Surface, Convergent Flow Passage (Nozzle)

For temperatures exceeding 2000°C, conventional devices, which function on the basis of their thermal and electrical properties, would soon melt. Instead, there are two generally accepted methods for temperature measurement in this range.

The first of these is spectroscopic and is based upon measurement of one of the following quantities: absorption of radiation of known intensity, spectral line broadening, absolute intensity of a spectral line, relative intensities of different spectral lines or of a single line and the intensity of continuum radiation. An in-depth discussion of the underlying theory of spectroscopic techniques is to be found in the literature /69,70/. An optical multi-channel analyzer, consisting of a monochromator and vidicon tube under computer control, is a diagnostic tool designed for such measurements. Such a device, made available for the investigation, was restricted to the measurement of temperatures representing on average value encompassing the luminous zone of the plasma jet. An even greater drawback was the general limitation of spectroscopic techniques to the measurement of temperatures exceeding approximately 9000°K.

A second option was the water-cooled calorimetric probe whose accuracy was found to be comparable to that of spectroscopic methods /71/. A probe, illustrated in Figure 4-8, was constructed using three concentric stainless steel tubes having inner diameters of 0.8, 4.6 and 9.4 mm. This permitted cooling water, from the high pressure water manifolds to circulate through the outermost coolant channel to the probe tip and back via the inner coolant channel. The diameter of the innermost tube dictated the spatial resolution of measured temperatures. A clamp and calibrated retort stand, fastened to the diagnostic chamber, held the probe motionless in the sampling port. The nature of the chamber required a ninety degree bend in the probe. A copper/constantan thermocouple had its junctions located at the probe coolant channel inlet and outlet, to allow for the measurement of coolant water temperature rise. A calibrated water rotameter measured the flowrate of cooling water through the probe. The central tube of the probe carried a steady flow of sample gas past a chromel/alumel thermocouple, located near the probe exit to measure the outlet gas temperature. A variable speed, flow-through pump, in line with a calibrated rotameter, was used to draw gas samples through this tube. Results of the cooling water and gas sample rotameter calibrations are presented in Appendix A. Cooling of the calorimetric probe also cooled the gas sample stream passing through it, revealing a second function of the probe as a cooled-surface quenching device.

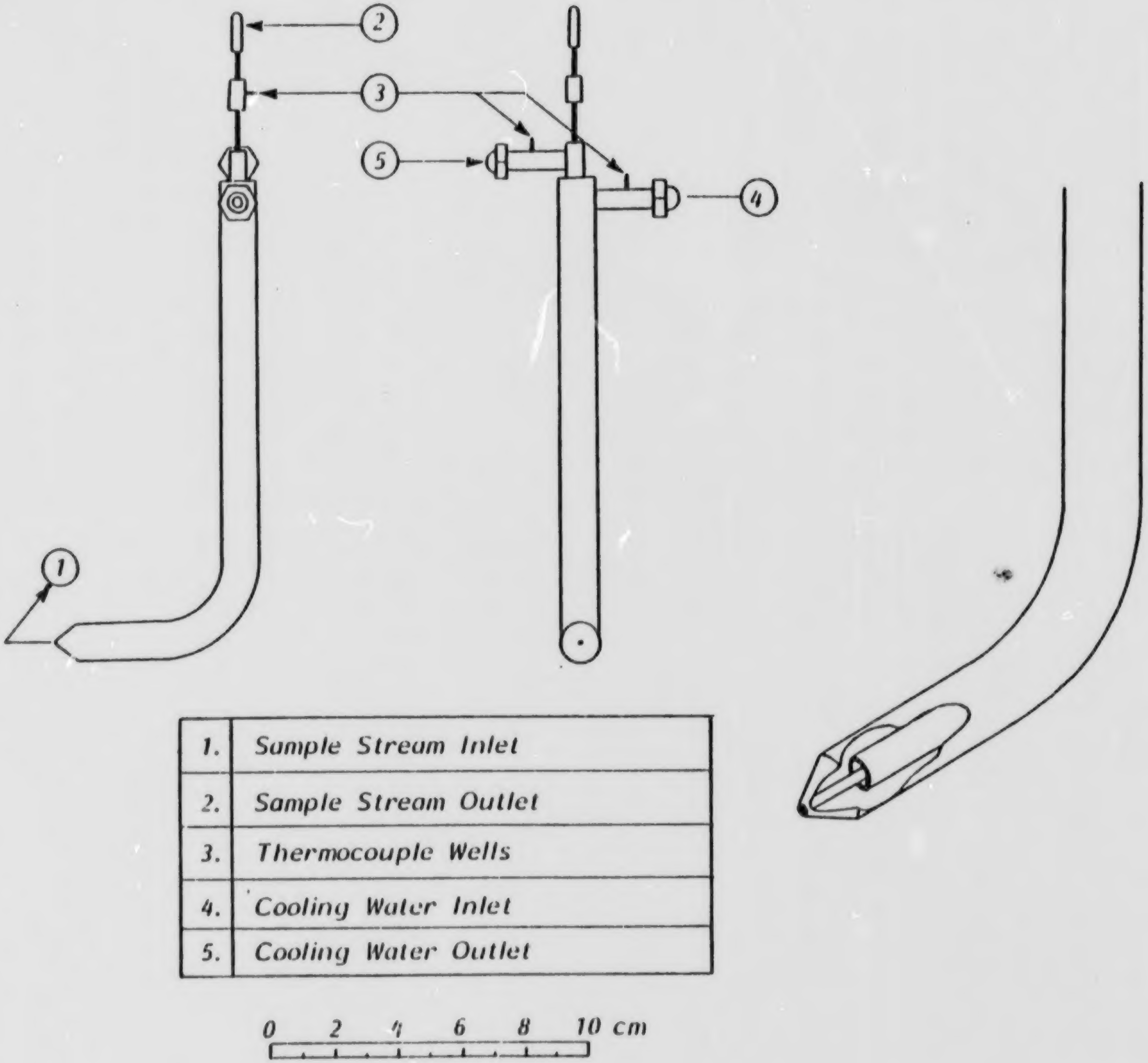

1.	*Sample Stream Inlet*
2.	*Sample Stream Outlet*
3.	*Thermocouple Wells*
4.	*Cooling Water Inlet*
5.	*Cooling Water Outlet*

FIGURE 4-8: The Calorimetric Probe

In operation, the calorimetric probe was positioned in the path of the plasma flow with the probe tip facing the discharge. The probe utilized a tare measurement which not only eliminated the error due to heat transfer from the outer surface of the probe jacket, but also the error due to radiation heating of the probe. During the tare measurement, gas was prevented from flowing through the probe and observations of steady state water temperature rise and flowrate were made. Following this tare procedure, gas flow was initiated through the probe and the same measurements were repeated together with those of the gas sample exit temperature and flowrate. The rate of heat removal from the gas sample was thus given by the difference between the two coolant rates. That is,

$$(wc_p\Delta T)_{gas} = \left\{(wc_p\Delta T)_{\substack{\text{cooling}\\ \text{water}}}\right\}_{\text{flow}} - \left\{(wc_p\Delta T)_{\substack{\text{cooling}\\ \text{water}}}\right\}_{\text{no flow}} \qquad (4\text{-}1)$$

or,

$$\Delta T_{gas} = \frac{\left\{(wc_p\Delta T)_{\substack{\text{cooling}\\ \text{water}}}\right\}_{\text{flow}} - \left\{(wc_p\Delta T)_{\substack{\text{cooling}\\ \text{water}}}\right\}_{\text{no flow}}}{(wc_p)_{gas}} \qquad (4\text{-}2)$$

where w = mass flowrate
c_p = specific heat capacity
ΔT = temperature rise

The mass flowrate of water did not fluctuate appreciably between the two modes of measurement. In addition, the specific heat capacity of water remained essentially constant over the range of temperatures encountered. Thus, it could be rewritten as:

$$T_{\substack{\text{probe}\\ \text{tip}}} = \frac{\left\{(wc_p)(\Delta T_{\text{flow}} - \Delta T_{\text{no flow}})\right\}_{\text{cooling water}}}{(wc_p)_{gas}} + T_{\substack{\text{probe}\\ \text{exit}}} \qquad (4\text{-}3)$$

There are two disadvantages associated with the tare measurement technique. A steady state environment or duplication of the test conditions for the flow and no-flow modes is a necessity. More importantly, flow conditions near the probe tip with no gas sample flowing, should be closely repeated when the gas sample is being extracted. This is ensured by selecting a sufficiently small gas smaple flowrate. Implicit in equation 403 is the assumption of flow duplication at the probe-tip which has been the subject of considerable discussion with regard to the probe's suitability for high temperature measurement. Studies, which have compared calorimetric techniques with other methods of temperature estimation /71,72/, have concluded that minor differences in external flow at the probe tip, between the flow and no-flow modes, were insignificant. Alternatives to probes which operated on the tare measurement principle in the form of multi-jacketed probes /73/, tended to introduce more complications than they resolved. Unlike spectroscopic methods, the calorimetric probe necessarily disturbed flow in the plasma stream. However, based upon the relatively simple theoretical background and support equipment and the satisfaction of probe miniaturization and high-temperature durability constraints, the calorimetric method was applied to this investigation.

The flowrate of water to the probe was a function of that deliverable by the water manifold. The gas sample flowrate chosen, was the lowest value for which the difference in cooling water temperature rise between the flow and no-flow modes became significant.

The measurement of temperatures not exceeding 2000°C was accomplished by using two different types of thermocouples, each positioned at a sampling port by a clamp and calibrated retort stand fastened to the diagnostic chamber. A chromel/alumel thermocouple was used to measure temperatures up to approximately 1200°C while a tungsten-5% rhenium/tungsten-26% rhenium thermocouple measured temperatures up to 2000°C. Thermocouples were chosen based upon their proven performance in research and industrial applications. They are inherently simple and rugged devices, useful over wide ranges of temperatures and operating environments. All of the thermocouples used, including those of the calorimetric probe, were tested for accuracy using the freezing and boiling points of water. Results of the calibrations are found in Appendix A.

In actual operation, each transducer was connected in the same manner with its leads fastened to junctions of an enclosed isothermal block. Copper leads, from the corresponding junctions, were connected at the opposite end to a card which inserted into the data-logger. The datalogger was interfaced to a microcomputer which was responsible for on-line processing of the incoming thermocouple signals. Cold junction compensation, based upon the temperature of the enclosed isothermal block, was provided through the software. This allowed voltage-to-temperature conversions directly by interpolation of thermocouple tables read in as software data. The copper/constantan thermocouple of the probe, unlike the others, measured a temperature difference and was, therefore, not subject to cold junction compensation.

4.2 Experimental Procedure

Following initiation of cooling water flow to the water manifold and arc gas flow to the torch, an arc was struck between electrodes, initiated by a pulse of the radio-frequency starter. The arc current was adjusted to 150,200 or 250 amperes and the argon arc gas flowrate assumed a value of 45, 75 or 106 L/min @ 25°C. These parameters were representative of the operating range of argon in this torch as determined from preliminary tests. Temperatures of the plasma exiting the torch were comparable to those required for many reactions of potential commercial interest. The flowrate of argon quenching gas (25 or 90 L/min @ 25°C) was set next. This quantity was based upon those of published plasma/cool gas injection studies /32,38,41, 74/. The choice of argon (99.997 percent pure) over other types of gas was due to its inertness which allowed quenching comparisons to be made without reference to specific chemical reactions.

After a brief period was allotted for attainment of steady state operating conditions, the observation of temperatures downstream of the quencher exit, in the effluent region, would commence. Only a portion of the designated locations could be sampled during the course of each run. These locations formed a vertical, rectangular plane which varied in length, depending upon the configuration of quencher, from 105 to 120 mm and was 45 mm in width with its bottom edge resting on the centerline of the reactor. Specifically, measurements were taken at five axial positions along the centerline; at three of these locations, an additional three radial measurements were taken. Reactor operating variables were periodically monitored during the run, as well.

Shutdown of the experimental system was accomplished by extinguishing the arc and ceasing the flow of gas and, eventually, cooling water to the reactor. After suitable time for cooling of the diagnostic chamber had elapsed, the procedure was repeated.

4.3 Analysis of Data

The degree or range of cooling and the rate of cooling provide a basis upon which to compare the performances of the different quenching systems. Conclusions may be drawn regarding quenching performance by a qualitative comparison of the effluent region temperatures. Their magnitudes and distribution give some indication of the degree of cooling. Calculating, where possible, the rate of cooling provide a quantitative means for comparison between systems.

4.3.1 Examination of Effluent Region Temperatures

The graphical representation of temperatures in the effluent region allows a number of general observations to be made concerning the effects of operating variables. Changes in current or gas flowrates are manifested in the magnitudes and distribution of these temperatures. More importantly, by providing a visual interpretation of the results of the quenching process, more or less desirable characteristics of a quencher are clearly discernable.

4.3.2 Calculation of Average Quenching Rates

Unlike the quenching rate equations of Chapter 3, which were often based upon models for a particular situation, a less rigorous approach utilizes heat balances about the torch and about the torch and quencher. Each balance, in turn, gives rise to the following expression for an average or equilibrium temperature representative of conditions over a vertical plane at the quencher entrance (torch exit) or quencher exit.

$$\bar{T} = \frac{IV - (wc_p\Delta T)_{\text{cooling water}}}{(w_{\text{arc gas}} + w_{\text{quench gas}})\, c_{p_{\text{gas}}}} + T^\circ \qquad (4\text{-}4)$$

where $\bar{T}$ = average or equilibrium temperature

I = arc current

V = arc voltage

w = mass flowrate

c_p = specific heat capacity (calculated at the arithmetic mean temperature)

ΔT = temperature rise

T° = reference temperature (25°C)

Given an average temperature, and knowledge of the volumetric flowrate of the gas at reference conditions, the corresponding velocity is given by:

$$\bar{v} = Q^\circ \left(\frac{\bar{T}}{T^\circ}\right) \left(\frac{1}{A}\right) \qquad (4\text{-}5)$$

where $\bar{v}$ = average velocity

Q° = gas volumetric flowrate at reference conditions

A = cross-sectional flow area

The form of the temperature correction used is substantiated by argon's near-ideal behaviour at elevated temperatures /75/76/.

By denoting conditions at the quencher entrance with the subscript 1 and those at the quencher outlet with the subscript 2, the following expression for average quenching rate can be written.

$$\frac{\Delta\bar{T}}{\Delta t} = \left(\frac{\bar{T}_1 - \bar{T}_2}{\Delta x} \right) \left(\frac{\bar{v}_1 + \bar{v}_2}{2} \right) \tag{4-6}$$

where $\frac{\Delta\bar{T}}{\Delta t}$ = average quenching rate

Δx = quencher thickness

$$\begin{aligned}
\frac{\Delta\bar{T}}{\Delta t} = \frac{1}{2\Delta x \rho^{o}_{gas} T^{o}} \Bigg[\Bigg(& \frac{IV_1 - (w_1 c_p \Delta T_1)_{H_2O}}{w_{\substack{arc\\gas}} (c_{p_1})_{gas}} + T^{o} \Bigg) - \\
\Bigg(& \frac{IV_2 - (w_2 c_p \Delta T_2)_{H_2O}}{(w_{\substack{arc\\gas}} + w_{\substack{quench\\gas}}) (c_{p_2})_{gas}} + T^{o} \Bigg) \Bigg] \times \\
\Bigg[\frac{w_{\substack{arc\\gas}}}{A_1} \Bigg(& \frac{IV_1 - (w_1 c_p \Delta T_1)_{H_2O}}{w_{\substack{arc\\gas}} (c_{p_1})_{gas}} + T^{o} \Bigg) + \\
\frac{(w_{\substack{arc\\gas}} + w_{\substack{quench\\gas}})}{A_2} \Bigg(& \frac{IV_2 - (w_2 c_p \Delta T_2)_{H_2O}}{(w_{\substack{arc\\gas}} + w_{\substack{quench\\gas}}) (c_{p_2})_{gas}} + T^{o} \Bigg) \Bigg]
\end{aligned} \tag{4-7}$$

4.3.3 Uncertainty Analysis

Estimates of experimental uncertainty are necessary to give some idea as to how reliable the results are. In the present investigation, an uncertainty analysis, described by Holman /77/ was performed to estimate the error in calorimetric probe calculations of temperature and in average quenching rate calculations. Samples are presented in Appendix C.

Values for the uncertainties associated with the thermocouples used in free-stream measurements were supplied by the manufacturer. Under controlled conditions, the tungsten -5% rhenium/tungsten-26% rhenium thermocouple was said to have a ± 1 percent error limit for the range of temperatures studied while that for the chromel/alumel thermocouple was reported as ± 2.2°C /78/.

5.0 RESULTS AND DISCUSSION

Analysis of the reactor operating variables and temperatures in the effluent region of the plasma reactor permitted comparisons to be made between quenching systems. A comprehensive collection of the experimental data is presented in Appendix B.

Effluent region temperatures, for which no prior data was available for this reactor, were reliable indicators of the effects of changes in operating variables. The temperature contour plots employed to represent these observations, were constructed based upon an assumption of axially symmetric effluent region temperatures. Attempts to radially probe the effluent region with diagnostic equipment through planes other than the vertical, were prevented by the awkward location of diagnostic chamber windows in relation to the would-be sampling ports. Axial symmetry of the temperatures was assumed given the configuration and characteristics of the reactor. In each of the contour plots, the anode exit was chosen as the datum from which longitudinal distances were measured.

The magnitude of the temperatures was found to be influenced considerably by changes in arc current. As Figure 5-1 illustrates, increases in current translated into higher effluent temperatures.

Increases in arc gas flowrate were observed to be accompanied by modest increases in voltage. The net result was a lessening of temperatures within the torch but an increase in effluent region temperatures (Figure 5-2) due to the elongated nature of the plasma jet.

TEMPERATURE CONTOUR PLOTS
(Degrees Kelvin)

Quencher: Gas Injection Ring #2 + Nozzle Module
Arc Gas Flowrate: 45 l/min @ 25°C
Quench Gas Flowrate: 25 l/min @ 25°C

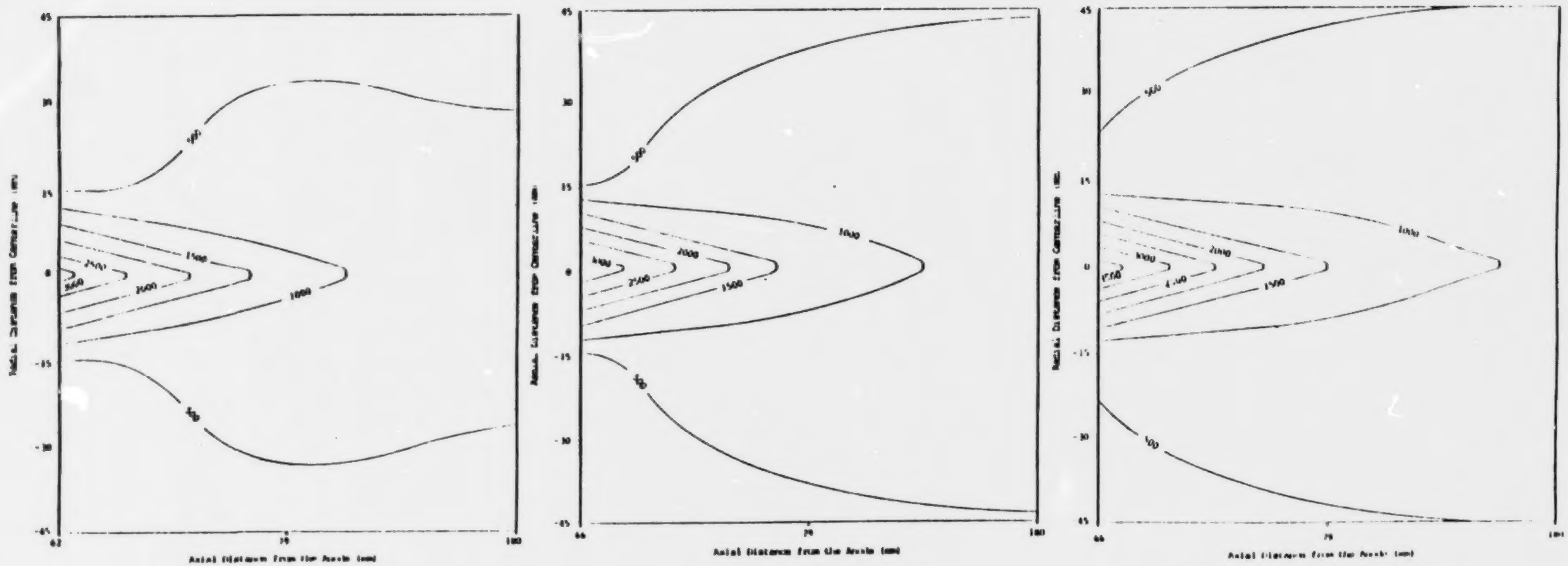

Current: 150 Amperes

Current: 200 Amperes

Current: 250 Amperes

FIGURE 5-1: The Effect of Current on Temperatures
In the Effluent Region

As would be expected, increases in quenching gas flowrate lowered temperatures in the effluent region. In all cases, core temperatures remained relatively high. Figure 5-3 provides an illustration of this point.

Analysis of quencher performance was undertaken in two stages. Furthermore, because a large amount of data was accumulated, representative operating conditions were chosen throughout to illustrate findings. In the first stage, gas injection rings 1 and 2 were examined by considering those conditions which gave minimum and maximum values for effluent region temperatures (current = 150 A, arc gas flowrate = 45 L/min @ 25°C and current = 250 A, arc gas flowrate = 106 L/min @ 25°C respectively). A quenching gas flowrate of 25 L/min @ 25°C was used in both cases. Relative performance was appraised by comparison of individual axial temperature profiles. For each profile, temperatures were measured at various axial distances from the anode for fixed radial distance from the reactor centerline. As Figures 5-4(a) and 5-5(a) show, core temperatures for both quenchers were approximately equal in value. A general trend in differences between quenchers was not in evidence until radial distances of 30 mm or more. In this peripheral region, illustrated by Figures 5-4(c), (d) and 5-5(c), (d) temperatures for gas injection ring #2 were approximately 5 percent lower than comparable temperatures for ring #1. These lower values were attributed to gas injection ring #2's water-cooled walls in contact with the flowing stream. The absence of cooling in ring #1 caused it to act as a heat sink, presumably pre-heating the quenching gas prior to injection. Consequently, gas injection ring #2 was judged a marginally better quencher.

In the second stage of quenching system evaluation, the performance of gas injection ring #2 was compared to that of the ring used in conjunction with a cooled-surface, constant-diameter flow passage or a cooled-surface, convergent flow passage (nozzle). Operating conditions inferring minimum and maximum temperatures within the torch (current = 150 A, arc gas flowrate = 106 L/min @ 25°C and current = 250 A, arc gas flowrate = 45 L/min @ 25°C respectively) for both quenching gas flowrates (25 and 90 L/min @ 25°C) were selected for discussion. Average quenching rates were estimated for these conditions in Table 5-1, which refers to the information contained in Figure 5-6. In these calculations, it was assumed that, for given operating conditions, the average quenching rate calculated about the gas injection ring remained constant regardless of whether additional modules were present or not downstream. This allowed separate cooling rates to be calculated for either of the cooled-surface quenching modules, in addition to the rates determined for combinations of modules.

TEMPERATURE CONTOUR PLOTS
(Degrees Kelvin)

Quencher: Gas Injection Ring #1
Current: 250 Amperes
Quench Gas Flowrate: 25 l/min @ 25°C

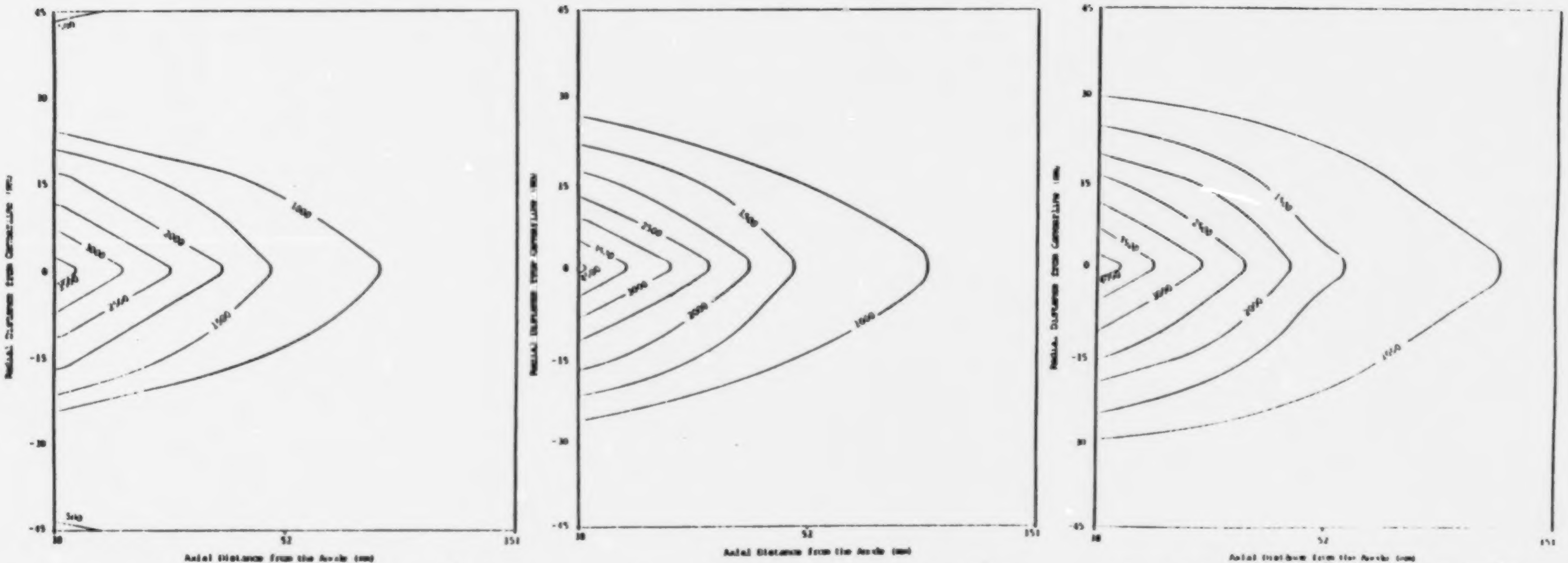

Arc Gas Flow: 45 l/min @ 25°C

Arc Gas Flow: 75 l/min @ 25°C

Arc Gas Flow: 106 l/min @ 25°C

FIGURE 5-2: The Effect of Arc Gas Flowrate on Temperatures in the Effluent Region

TEMPERATURE CONTOUR PLOTS
(Degrees Kelvin)

Quencher: Gas Injection Ring #2 + Cooled-Surface,
Constant-Diameter Flow Passage Module
Current: 150 Amperes
Arc Gas Flowrate: 45 1/min @ 25°C

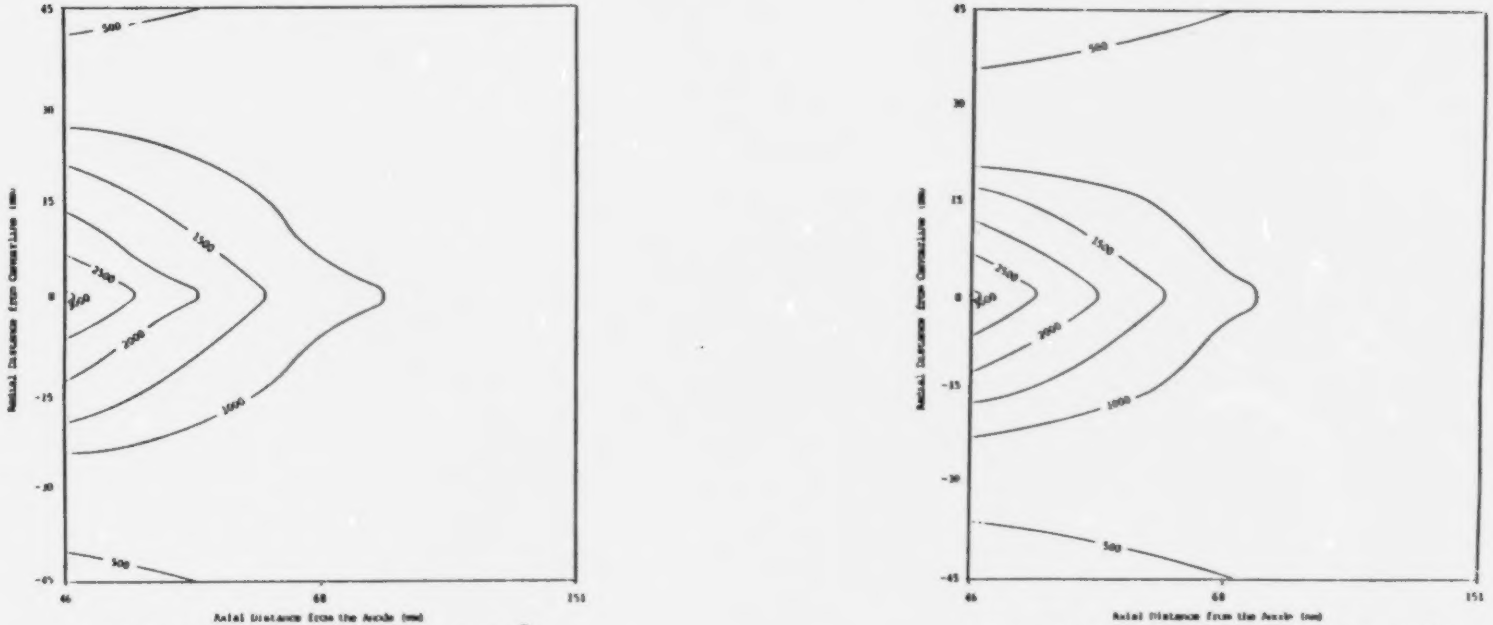

Quench Gas Flow: 25 1/min @ 25°C

Quench Gas Flow: 90 1/min @ 25°C

FIGURE 5-3: The Effect of Quench Gas Flowrate on Temperatures in the Effluent Region

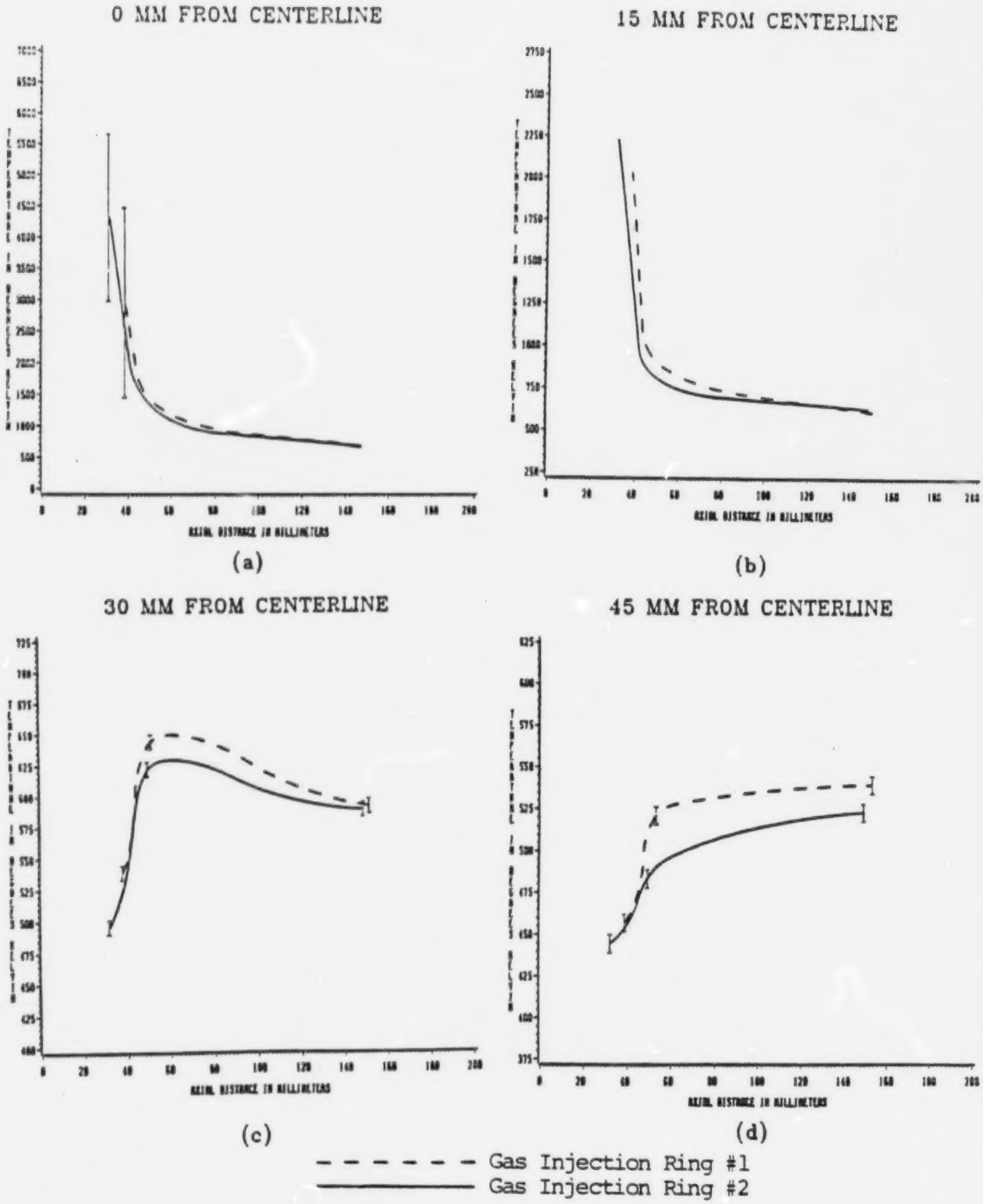

FIGURE 5-4: Effluent Region Axial Temperature Profiles for Gas Injection Rings 1 and 2 (current=150 A, arc gas flow=45 l/min @ 25°C, quench gas flow=25 l/min @ 25°C)

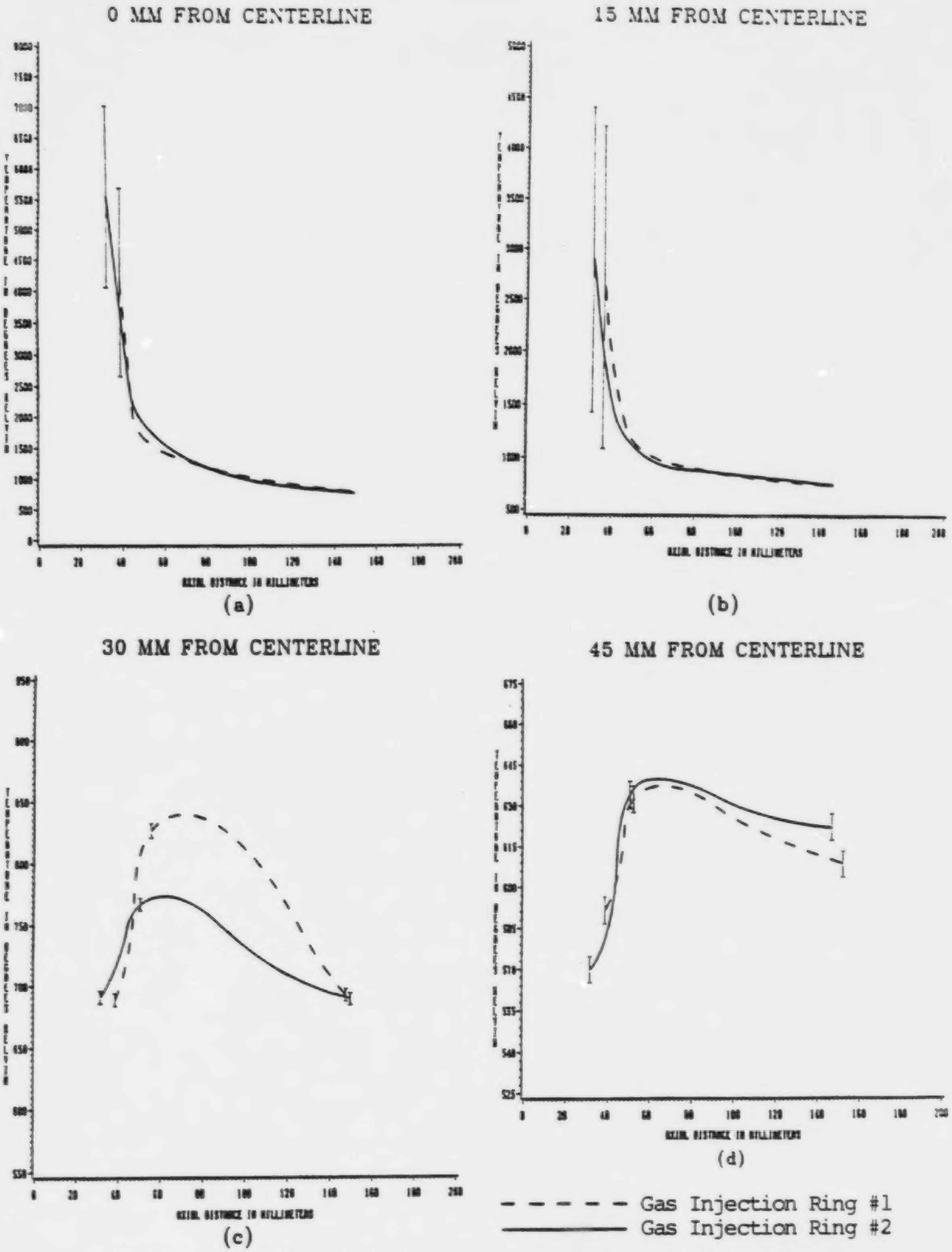

0 MM FROM CENTERLINE

15 MM FROM CENTERLINE

(a)

(b)

30 MM FROM CENTERLINE

45 MM FROM CENTERLINE

(c)

(d)

FIGURE 5-5: Effluent Region Axial Temperature Profiles for Gas Injection Rings 1 and 2 (current=250 A, arc gas flow=106 l/min @ 25°C, quench gas flow=25 l/min @ 25°C)

Quencher #	Current (Amperes)	Arc Gas Flowrate (L/Min @ 25°C)	Quench Gas Flowrate (L/Min @ 25°C	Boundaries	Estimated Average Quenching Rate (°K/s)
1	150	106	25	A-B	4.14×10^5
1 + 2	150	106	25	A-B	4.14×10^5
				B-C	1.06×10^5
				A-C	2.03×10^5
1 + 3	150	106	25	A-B	4.14×10^5
				B-C	2.49×10^5
				A-C	5.78×10^5
1	150	106	90	A-B	4.25×10^6
1 + 2	150	106	90	A-B	4.25×10^6
				B-C	2.30×10^6
				A-C	2.31×10^6
1 + 3	150	106	90	A-B	4.25×10^6
				B-C	2.68×10^6
				A-C	5.72×10^6
1	250	45	25	A-B	1.92×10^5
1 + 2	250	45	25	A-B	1.92×10^5
				B-C	1.10×10^5
				A-C	1.08×10^5
1 + 3	250	45	25	A-B	1.92×10^5
				B-C	8.73×10^4
				A-C	2.65×10^5
1	250	45	90	A-B	4.22×10^6
1 + 2	250	45	90	A-B	4.22×10^6
				B-C	3.86×10^6
				A-C	2.29×10^6
1 + 3	250	45	90	A-B	4.22×10^6
				B-C	4.08×10^6
				A-C	7.22×10^6

TABLE 5-1: Average Quenching Rate Estimates for Selected Operating Conditions

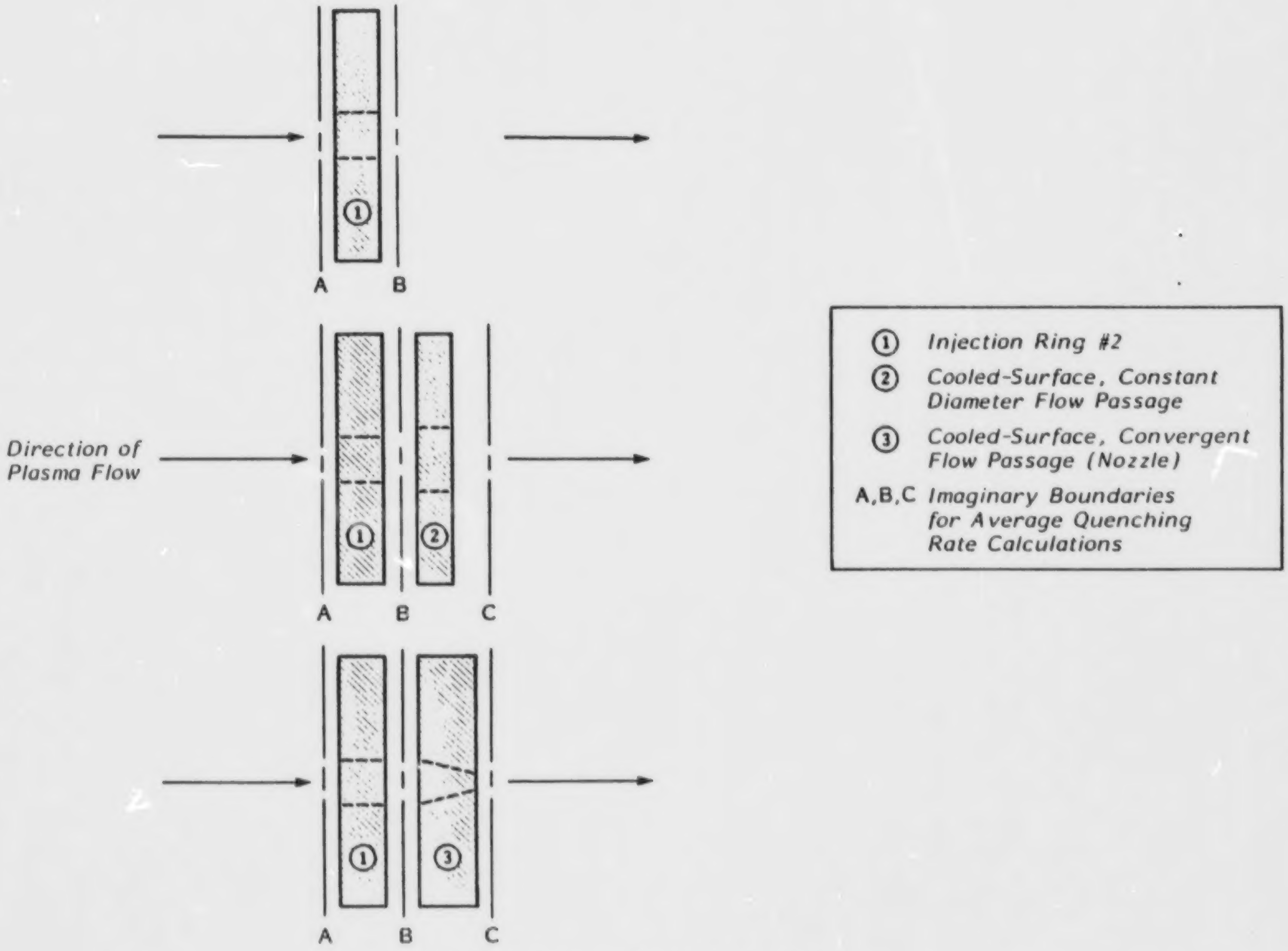
A
B
C
①
②
③
Direction of Plasma Flow
① Injection Ring #2
② Cooled-Surface, Constant Diameter Flow Passage
③ Cooled-Surface, Convergent Flow Passage (Nozzle)
A,B,C Imaginary Boundaries for Average Quenching Rate Calculations

FIGURE 5-6: Guide to Table 5-1

While the addition of a cooled-surface quenching module affected quenching locally, this was not necesarily reflected in the average cooling rates. The combination of the gas injection ring and constant-diameter flow passage gave average quenching rates lower than those resulting from the gas injection ring alone. This was due partly to the constant-diameter flow passage's inner diameter which was 50 percent greater than that for the gas injection ring. The larger diameter was suggested as a precautionary measure against ablative damage /79/; advice which would later be proved unwarranted.

The injection ring plus nozzle exhibited consistently higher average quenching rates relative to other quenchers. In most cases, each quenching system, even at a low quenching gas flowrate had cooling rates exceeding the benchmark value of 10^5°K/s considered necessary for disruption of equilibrium reaction paths.

While the values of Table 5-1 provided a basis upon which to compare quenchers, no light was shed regarding the distribution of quenching rates within the quencher. Nor was any indication given as to the extent of mixing between hot and cold streams. Bearing in mind the inability to gather any more information from within the quencher, focus was turned to the effluent region to examine the degree of cooling.

Contour plots were employed to best illustrate differences in effluent region temperatures associated with each quencher's use. As Figures 5-7 to 5-10 show, the addition of a cooled-surface, constant diameter flow passage to the gas injection ring lessened temperatures and radial temperatures gradients somewhat throughout the effluent region. This was a strong indication of an increased degree of mixing between the hot and cold streams. These same figures show the effect of adding a cooled-surface, convergent flow passage to the gas injection ring. While maximum temperatures were comparable, regions of high temperature for the ring plus nozzle were much smaller in size, constituting a lesser proportion of the effluent region. Radial temperature gradients were substantially higher with nozzle use.

Tests conducted with a nozzle having an inlet to outlet area ratio of 26 were unsuccessful. Pressure within the torch channel was unavoidably high, causing excessive heating of the channel walls. A second nozzle, with an inlet to outlet area ratio of 4, was shown to cause little or no disruption in torch operation and was used throughout the investigation. Concern arose only at the highest torch power level studied, in which case the arc would occasionally strike at locations past the anode. Torch operation, and hence data acquisition, was restricted to lower power levels.

TEMPERATURE CONTOUR PLOTS
(Degrees Kelvin)

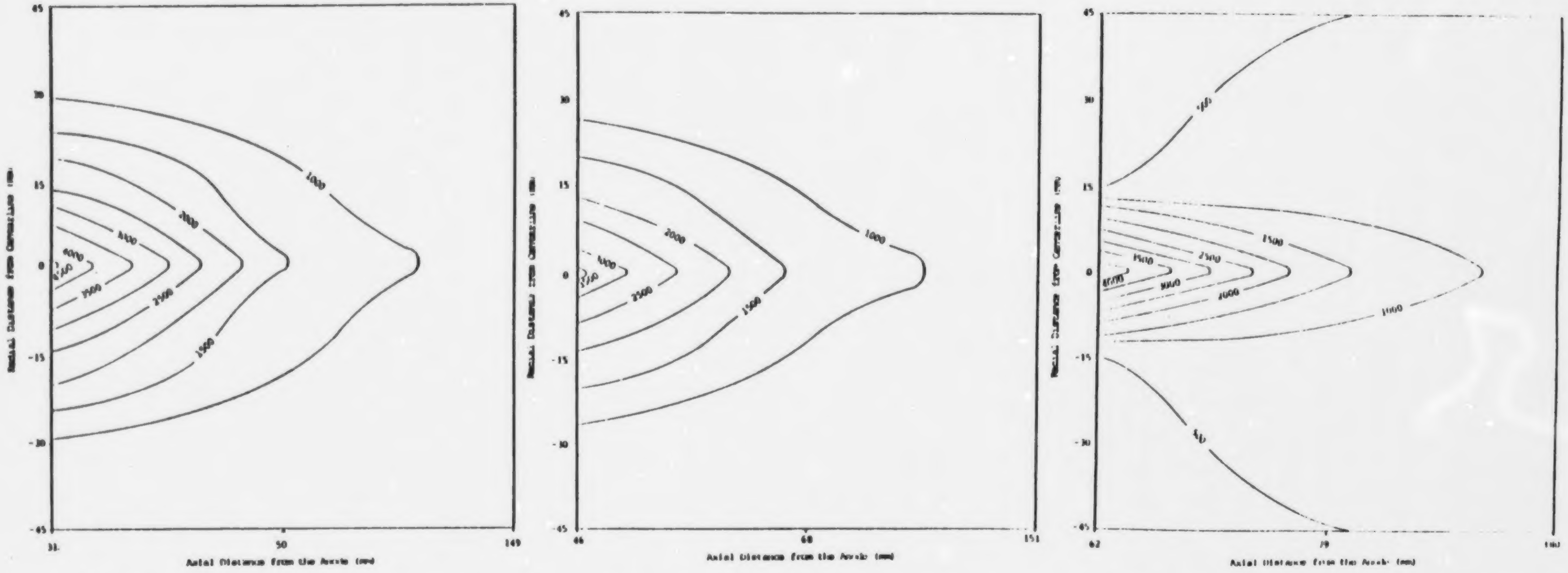

Quencher: Gas Injection Ring #2

Quencher: Gas Injection Ring #2 + Cooled-Surface, Constant-Diameter Flow Passage

Quencher: Gas Injection Ring #2 + Cooled Nozzle

FIGURE 5-7: Effects of Cooled-Surface Contact in Addition to Gas Injection Upon Effluent Region Temperatures (current=150 A, arc gas flowrate=106 l/min @ 25°C, quench gas flowrate=25 l/min @ 25°C)

TEMPERATURE CONTOUR PLOTS
(Degrees Kelvin)

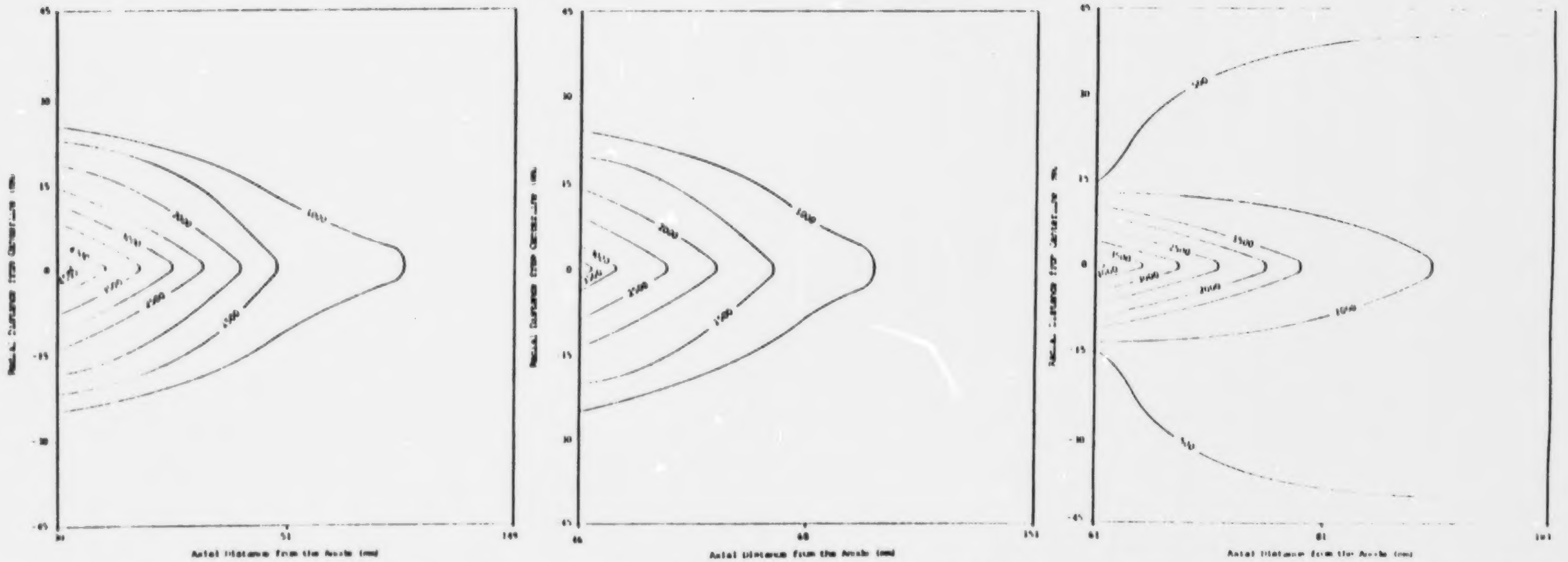

Quencher: Gas Injection Ring #2

Quencher: Gas Injection Ring #2 + Cooled-Surface, Constant-Diameter Flow Passage

Quencher: Gas Injection Ring #2 + Cooled Nozzle

FIGURE 5-8: Effects of Cooled-Surface Contact in Addition to Gas Injection Upon Effluent Region Temperatures (current=150 A, arc gas flowrate=106 l/min @ 25°C, quench gas flowrate=90 l/min @ 25°C)

TEMPERATURE CONTOUR PLOTS
(Degrees Kelvin)

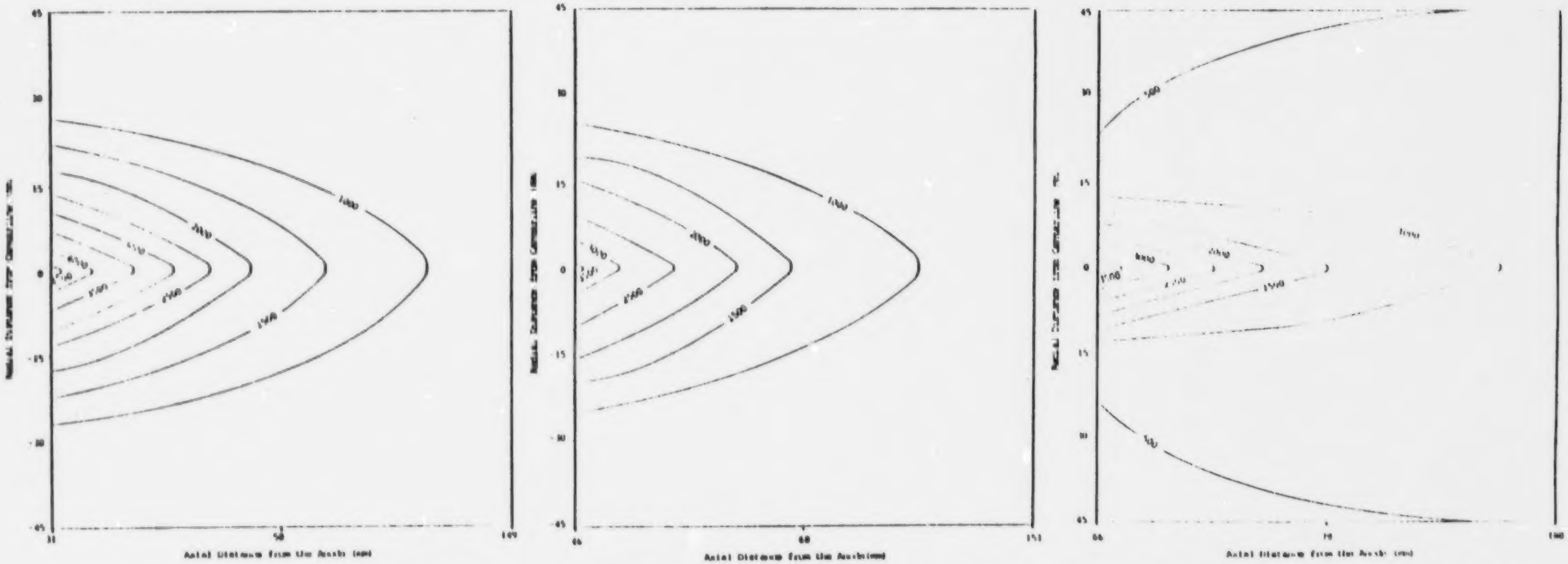

Quencher: Gas Injection Ring #2

Quencher: Gas Injection Ring #2 +
Cooled-Surface, Constant-
Diameter Flow Passage

Quencher: Gas Injection Ring #2 +
Cooled Nozzle

FIGURE 5-9: Effects of Cooled-Surface Contact in Addition to Gas Injection Upon Effluent Region Temperatures (current=250 A, arc gas flowrate=45 l/min @ 25°C, quench gas flowrate=25 l/min @ 25°C)

TEMPERATURE CONTOUR PLOTS
(Degrees Kelvin)

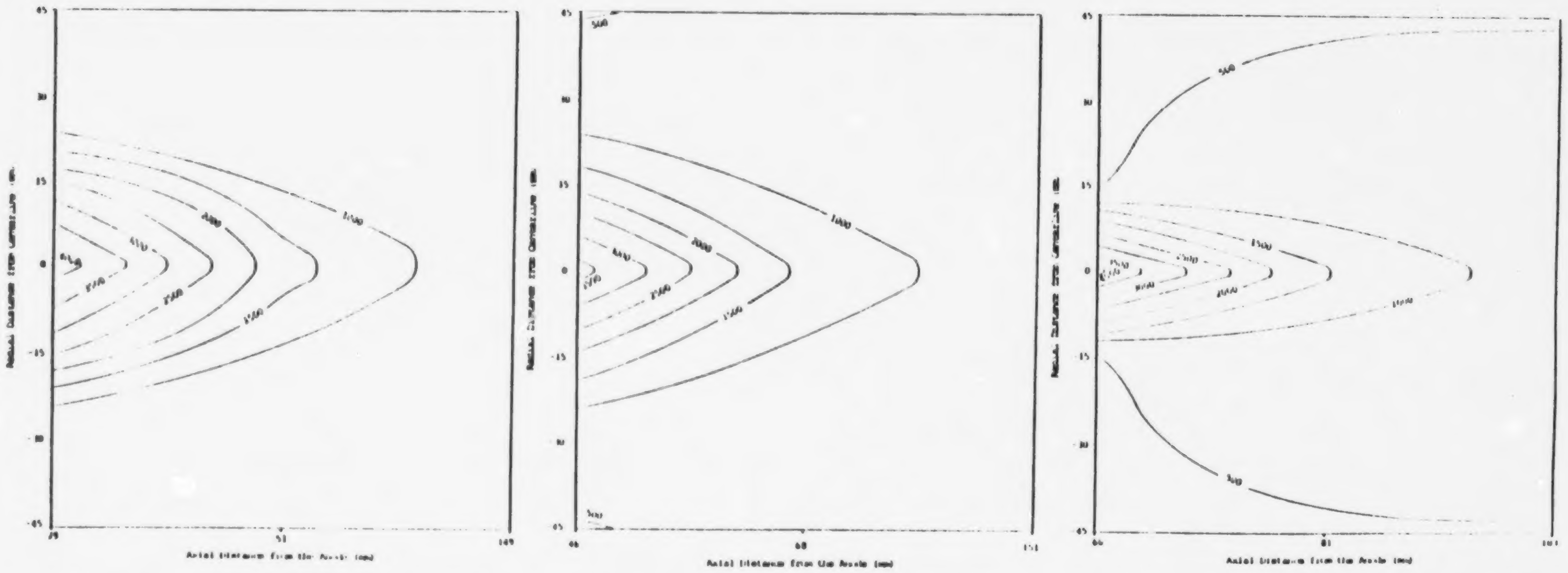

Quencher: Gas Injection Ring #2

Quencher: Gas Injection Ring #2 +
Cooled-Surface, Constant-
Diameter Flow Passage

Quencher: Gas Injection Ring #2 +
Cooled Nozzle

FIGURE 5-10: Effects of Cooled-Surface Contact in Addition to Gas Injection Upon Effluent Region Temperatures (current=250 A, arc gas flowrate=45 l/min @ 25°C, quench gas flowrate=90 l/min @ 25°C)

Based upon that portion of the data analyzed in this chapter, estimates of the uncertainties associated with the calculations were made.

Values of temperature obtained by the calorimetric probe were subject to experimental uncertainties along the order of 40 percent. However, the relative size of this uncertainty decreased as calculated temperatures increased in value. Sizable uncertainties were reported, as well, in another investigation /71/ in which a similar method of analysis was applied to a colorimetric probe. Given the absence of any suitable alternatives for the measurement of temperature in this range, such considerable errors had to be tolerated.

It was unlikely that the magnitude of the uncertainties, such as those calculated in Appendix C, were significant enough to affect the conclusions which were to be drawn regarding quencher performance.

6.0 CONCLUSIONS AND RECOMMENDATIONS

6.1 Conclusions

Four different quenching systems were assembled and tested with a plasma chemical reactor for which argon was used as arc and quench gas. The results of this investigation show that:

1. The magnitude of temperatures in the effluent region of the reactor is strongly influenced by the parameters: arc current, arc gas flowrate and quench gas flowrate. Increases in current and/or arc gas flowrate yielded higher temperatures while increases in the flowrate of quench gas gave lower temperatures.

2. Direct watercooling of a gas injection ring is largely responsible for lower temperatures in the periphery of the effluent region.

3. The highest average quenching rates were found in the novel quencher identified as the water-cooled gas injection ring plus the cooled-surface, convergent flow passage (Figure 4-7). The same gas injection ring, used in conjunction with a cooled-surface, constant-diameter flow passage (Figure 4-6), resulted in the lowest quenching rates. Operation of the gas injection ring alone (Figure 4-5), yielded values which fell in the range between the two extremes. In most cases, values for the quenching rate exceeded 10^5 °K/s.

4. The highest degree of cooling, as determined by examination of effluent region temperatures, was observed for the water-cooled gas injection ring used together with the cooled-surface, constant-diameter flow passage. Maximum temperatures were comparable for the gas injection ring and the gas injection ring plus cooled-surface convergent flow passage. However, the undisturbed core of the plasma jet was significantly smaller in the latter case indicating a higher degree of cooling.

5. The best design of a quencher, utilizing gas injection and cooled-surface contact, would incorporate a cooled-surface flow passage whose geometry lies somewhere in-between that of the two modules tested. Such a design would allow for the rate of cooling and the degree of cooling to be optimized. Employing fluid injection and cooled-surface contact guarantees a device which is simple, inexpensive and adaptable, although subject to the limitations discussed in Chapter 3.

6.2 Recommendations

The present study represents a first step towards the development of better quenching system. Research into methods of quenching far removed from those existing should continue and be encouraged. One aspect that might be examined would be the use of external magnetic fields to disperse the plasma in order to allow a more thorough mixing with a quenching fluid.

Much work remains to be done as follow-up to the present investigation. To these ends, the following recommendations are made:

1. A gas injection ring of minimum thickness should be tested with a cooled-surface module incorporating features found in both the constant-diameter and convergent flow passages. A module having the geometry illustrated in Figure 6-1 would fulfill these requirements by providing a high quenching rate and high degree of cooling. The optimization of the length together with the inlet and outlet diameters would follow.

2. The design of every quenching module should include strategically placed, threaded sampling ports of various sizes; sealable when not in use. Together with changes to the probe of the optical multi-channel analyzer presently available, temperatures in small, well-defined regions of the quenching zone could be evaluated in a non-intrusive manner. This would permit a much clearer understanding of those processes occurring in the quenching region.

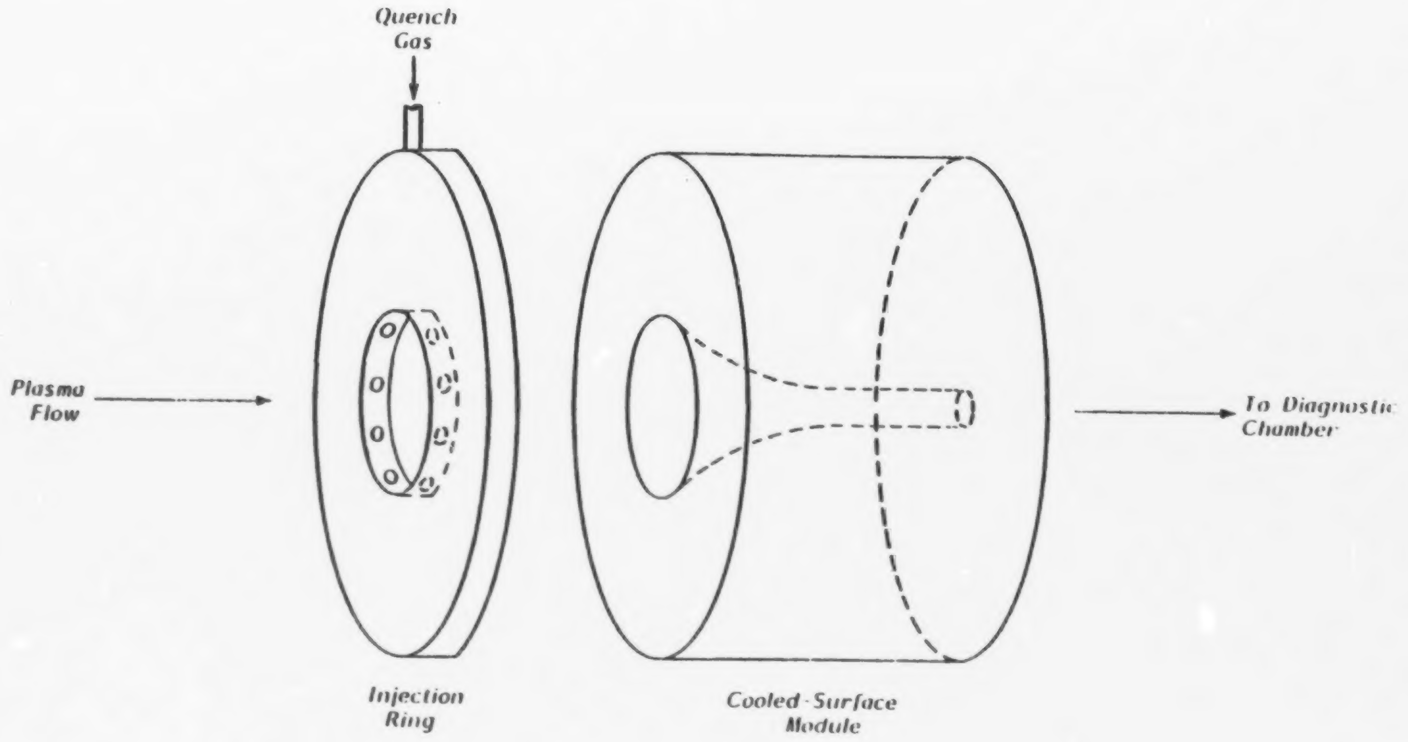
Quench Gas
Plasma Flow
Injection Ring
Cooled-Surface Module
To Diagnostic Chamber

FIGURE 6-1: Proposed Design for Quenching Modules

3. The diagnostic chamber is inadequate for reactor research and should be redesigned. The chamber does not allow for a proper fit with the plasma torch, is not water-cooled and is restrictive as to the locations at which diagnostic tools may be placed. A more suitable design would consist of a series of modules, similar to those comprising the torch. By water-cooling each module, reactor run times could be prolonged considerably. Separating each module with high-temperature insulative material would permit individual heat balance calculations. Every unit would have a series of strategically placed, threaded sampling ports of various sizes; sealable when not in use. The diagnostic chamber could thus be "made-to-order" by using the most appropriate combination of modules.

Approved by:

MRBooth

M.R. Booth
Acting Manager
Chemical Research Department

Prepared by:

DD for

M. Alvarez-Cuenca
Engineer
Process Chemistry Section

DD for.

G.P. Kushla
M.A.Sc. Candidate
Process Chemistry Section

Reviewed by:

DJRDodd

D.J. Dodd
Supervising Engineer
Process Chemistry Section

MAC:am

REFERENCES

1. Ibberson, V.J., Plasmas Cut the Cost of Industrial Chemistry, New Scientist, 1414, p 19 (July 26, 1984).

2. Parsons, R.J., Progress Review No. 61: The Use of Plasmas in Chemical Synthesis, Journal of the Institute of Fuel, 43, 359, p 524 (December 1970).

3. Suryakumar, K. and Subramanien, V., Plasma Technology - Application to Chemical Processing, Chemical Age of India, 26, 3, p 185 (March 1975).

4. Tennankore, K., A Review of the Application of High Temperature Plasma Arcs in Thermal Processing, Report No. WNRE-582., Atomic Energy of Canada Ltd. (March 1984).

5. Zanetti, R.J., Plasma: Warming Up to New CPI Applications, Chemical Engineering, 90, 26, p 14 (December 26, 1983).

6. Fauchais, P. and Baronnet, J., State of the Art of Plasma Chemical Synthesis of Homogeneous and Heterogeneous Products, Pure and Applied Chemistry, 52, p 1669 (1980).

7. Freeman, M.P. and Skrivan, J.F., Plasma Jet...New Chemical Processing Tool!, Hydrocarbon Processing and Petroleum Refiner, 41, 8, p 124 (August 1962).

8. Ibberson, V.J. and Thring, M.W., Plasma Chemical and Process Engineering, Ind. Eng. Chem., 61, 11, p 48 (November 1969).

9. Williams, M., Flame and Plasma Reactors, Transactions of the Institute of Chemical Engineers, 51, p 225 (1973).

10. Kubanek, G.R. and Gauvin, W.J., Recent Developments in Plasma Jet Technology, The Canadian Journal of Chemical Engineering, 45, p 251 (October 1967).

11. Stokes, C.S., Chemistry in High Temperature Plasma Jets, American Chemical Society Advances in Chemistry Series 80, p 390 (1969).

12. Gladish, H., How Huels Makes Acetylene by D.C. Arc, Hydrocarbon Processing and Petroleum Refiner, 41, 6, p 159 (June 1962).

13. Baddour, R.F. and Timmins, R.S., ed., The Application of Plasmas to Chemical Processing, 206 p, The M.I.T. Press, Cambridge, Mass. (1967).

14. Polak, L., ed., *Kinetics and Thermodynamics of Chemical Reactions in Low Temperature Plasma*, Nauka, Moscow (1965).

15. Alvarez-Cuenca, M., *Application of Plasma Technology to Selected Chemical Processes*, report no. 85-119-K, Ontario Hydro, Toronto, Ontario (September 1985).

16. Ammann, P.R., Baddour, R.F., Johnson, M.M., Mix, F.W, and Timmins, R.S., *Coal Conversion in an Electric Arc*, Chemical Engineering Progress, 60, 6, p 52 (June 1964).

17. Patrick, A.J. and Gannon, R.E., *A 1 MW Prototype Arc Reactor For Processing Coal to Chemicals*, Proceedings of the Industrial Opportunities for Plasma Technology Symposium, D-1.1 (October 21, 1982).

18. Szymanski, A., Plotczyk, W.W., Reszlak, A. and Huczko, A., *Brown Coal Pyrolysis in Hydrogen Plasma Jet*, Proceedings of the Sixth International Symposium on Plasma Chemistry, 1 (July 1983).

19. Stuart, P.R., Munz, R.J. and Gauvin, W.H., *Synthesis Gas Production from Peat Using a Steam Plasma*, Plasma Chemistry and Plasma Processing, 4, 4 (December 1984).

20. Anderson, E., *Methanol Touted as Best Alternate Fuel for Gasoline*, Chemical and Engineering News, 62, 23, p 14 (June 1984).

21. The Corporate Planning Group, *The Energy Brief: Comments on Alternative Energy*, Department of the Environment, Ottawa (1982).

22. Ryser, J., *Don't Discard Garbage as a Source of Energy*, Chemical Engineering, 91, 6, p 38 (March 19, 1984).

23. Chementator, Chemical Engineering, 90, 16, p 9 (August 8, 1983).

24. Goldberger, W.M. and Baroch, C.J., U.S. Patent 3247014 (1966).

25. Foex, M., Dumon, R., Bot-Langet, Y. and Verouchalmi, D., French patent 2079746 (1971).

26. Chase, J.D., Skrivan, J.F., Hyman, D. and Longfield, J.E., *Plasma Jet Process for Making Elemental Phosphorous*, Ind. Eng. Chem. Proc. Des. Dev., 18, 2, p 261 (1979).

27. Tylko, J.D., Tech. Transf., 6, 52 (1977).

28. Ettlinger, L.A., Nainan, T.D. and Ouellette, R.P., Applications of High Temperature Plasmas, Report No. MR-79W00166, The MITRE Corporation (June 1979).

29. Drouet, L.A., Plasma Technology: Review of the State of the Art and its Potential in Canada, Report No. 126 U 322, IREQ (March 1984).

30. Harnish, H., Heymer, G. and Schallus, E., Inorganic Reactions With Arc Heated Gases, Angew. Chem. Int. Ed., 2, 5, p 238 (1963).

31. Stokes, C.S. and Streng, L.A., Production of Ozone by the Use of a Plasma Jet, Ind. Eng. Chem. Prod. Res. Dev., 4, 1, p 36 (March 1965).

32. Honda, T., Takahira, S. and Kanzawa, A., Thermal Decomposition and Quenching of CO_2 in Argon Thermal Plasma, Sixth International Symposium on Plasma Chemistry Proceedings, 1, p 264 (July 1983).

33. Freeman, M.P., Production of Hydrogen Cyanide from Methane in a Nitrogen Plasma Jet, American Chemical Society Advances in Chemistry Series 80, p 406 (1969).

34. Grey, J., Sherman, M.P., Williams, P.M. and Fradkin, D.B., Laminar Arcjet Mixing and Heat Transfer: Theory and Experiments, AIAA Journal, 4, 6, p 986 (June 1966).

35. Grey, J. and Jacobs, P., Experiments on Turbulent Mixing in a Partially Ionized Gas, AIAA Journal, 2, 3, p 433 (March 1964).

36. O'Connor, T.J., Comfort, E.H. and Case, L.A., Turbulent Mixing of an Axisymmetric Jet of Partially Dissociated Nitrogen with Ambient Air, AIAA Journal, 4, 11, p 2026 (November 1966).

37. Smith, D.L., Kadlec, R.H. and Churchill, S.W., Mass and Energy Transfer Between a Confined Plasma Jet and a Gaseous Coolant, AIChE Journal, 17, 2, p 482 (March 1971).

38. Kobayashi, M., Honda, T. and Kanzawa, A., The Effect of Gas Injection on a Thermal Argon Plasma Flow in a Water-Cooled Tube, Plasma Chemistry and Plasma Processing, 5, 1, p 39 (1985).

39. Mazza, A. and Pfender, E., Modelling of an Arc Plasma Reactor for Thermal Plasma Synthesis, Sixth International Symposium on Plasma Chemistry Proceedings, 2, p 41, (July 1983).

40. Anderson, J.E. and Case, L.K., An Analytical Approach to Plasma Torch Chemistry, AIChE Journal, 1, 3, p 161 (July (1962).

41. Freeman, M.P. and Skrivan, J.F., Rate Studies of the Decomposition of Ammonia and Methane in a Plasma Jet, AIChE Journal, 8, 4, p 450 (September 1962).

42. Nishimura, Y., Takenouchi, T. and Sakai, W., The Dissociation of Carbon Monoxide in an Induction-Coupled Argon Plasma Jet, Bulletin of the Chemical Society of Japan, 47, 9, p 2331 (1974).

43. Ammann, P.R. and Timmins, R.S., Chemical Reactions During Rapid Quenching of Oxygen/Nitrogen Mixtures from Very High Temperatures, AIChE Journal, 12, p 957 (September 1966).

44. Baddour, R.F. and Blanchet, J.L., Reactions of Carbon Vapour with Hydrogen and with Methane in a High Intensity Arc, AIChE Journal, 3, 3, p 258 (July 1964).

45. Bronfin, B.R. and Hazlett, R.N., Synthesis of Nitrogen Fluorides in a Plasma Jet, AIChE Journal, 5, 4, p 472 (November 1966).

46. Baddour, R.F. and Iwasyk, J.M., Reactions Between Elemental Carbon and Hydrogen at Temperatures Above 2800°K, Ind. Eng. Chem. Proc. Des. Dev., 1, p 169 (July 1962).

47. Bronfin, B.R., Hydrogen Cyanide Synthesis in a Thermal Radio-Frequency Induction Plasma, American Chemical Society Advances in Chemistry Series 80, p 423 (1969).

48. Meubus, P., High Temperature Propane Cracking in an Argon Plasma with the Presence of Aluminum Vapour and Tungsten Particles, Can. J. Chem. Eng., 53, p 653 (December 1975).

49. Stokes, C.S. and Knipe, W.W., The Plasma Jet in Chemical Synthesis, Ind. Eng. Chem., 52, 4, p 287 (1960).

50. Leutner, H.W., The Production of Cyanogen from the Elements, Using a Plasma Jet, Ind. Eng. Chem. Proc. Des. Dev., 1, 3, p 166 (July 1962).

51. Plotczyk, W.W., Effect of Quenching Temperature of the Reaction on the Synthesis of Acetylene from Methane in Hydrogen Plasma Jet, Sixth International Symposium on Plasma Chemistry Proceedings, 1, p 300 (July 1983).

52. Giacobbe, F.W. and Schmerling, D.W., Production of Carbon Monoxide from Carbon and Carbon Dioxide in a Plasma Arc Reactor, Plasma Chemistry and Plasma Processing, 3, 4, p 383 (1983).

53. Colver, G.M. and Weinberg, F.J., Quenching Magnetically Rotated Augmented Flames and Plasma Jets in Mixtures Containing Methane, Oxygen and Nitrogen, Proceedings of the Royal Society of London, A.326, p 383 (1972).

54. Plooster, M.M. and Reed, T.B., Carbon-Hydrogen-Acetylene Equilibrium at High Temperatures, J. Chem. Phys., 31, 1, p 66 (July 1959).

55. Skrivan, J.F. and Von Jaskowsky, W., Heat Transfer from Plasma to Water-Cooled Tubes, Ind. Eng. Chem. Proc. Des. Dev., 4, 4, p 371 (October 1965).

56. Wethern R.J. and Brodkey, R.S., Heat and Momentum Transfer in Laminar Flow: Helium Initially at Plasma Temperatures, AIChE Journal, 9, 1, p 49 (January 1963).

57. Huczko, A., Plasma Decomposition of Carbon Dioxide, AIChE Journal, 30, 5, p 811 (September 1984).

58. Johnson, J.R., Choksi, N.M. and Eubank, P.T., Entrance Heat Transfer from a Plasma Stream in a Circular Tube, Ind. Eng. Chem. Proc. Des. Dev., 7, 1, p 34 (January 1968).

59. Gambill, W.R., An Evaluation of Recent Correlations for High-Flux Heat Transfer, Chemical Engineering, 74, 16, p 147 (August 28, 1967).

60. Goldberger, W.M., An Evaluation of High Temperature Chemical Technology, Brit. Chem. Eng., 8, 9, p 610 (September 1963).

61. Amouroux, J. and Cavadias, S., Heating of a Fluidized Bed by the Injection of a Thermal Plasma: Application to the Synthesis of Nitrogen Oxides, Sixth International Symposium on Plasma Chemistry Proceedings, 1, p 169 (July 1983)

62. Goldberger, W.M. and Oxley, J.H., Quenching the Plasma Reaction by Means of the Fluidized Bed, AIChE Journal, 9, 6, p 778 (November 1963).

63. Wicke, E., Chem. Eng. Sci., 6, p 160 (1957).

64. Penner, S.S., *Chemistry Problems In Jet Propulsion*, 316 p., Pergamon Press, New York (1957).

65. Marynowski, C.W., Phillips, R.C., Phillips, J.R. and Heister, N.K., *Thermodynamics of Selected Chemical Systems Potentially Applicable to Plasma Jet Synthesis*, Ind. Eng. Chem. Fund., 1, 1, p 52 (February 1962).

66. Phillips, R.C. and Ferguson, F.A., *High Temperature Chemical Synthesis*, Symposium on High Temperature Technology Proceedings, p 192, McGraw-Hill, New York (1959).

67. Colkert, M.B., Chiappetta, L., Guile, R.N., Zabielski, M.F. and Seery, D.J., *Internal Aerodynamics of Gas Sampling Probes*, Combustion and Flame, 44, p 3 (1982).

68. Sundstrom, D.W. and De Michiell, R.L., *Quenching Processes for High Temperature Chemical Reactions*, Ind. Eng. Chem. Proc. Des. Dev., 10, 1, p 114 (1971).

69. John, R.E., *Spectroscopic Measurements of the Temperature of Plasma Jets*, Proceedings of the Fifth International Conference on Ionization Phenomena in Gases, 1, p 955 (August 1961).

70. Eckert, E.R.G. and Goldstein, R.J., eds., *Measurements in Heat Transfer*, 2nd ed., 400 p, Hemisphere Publishing Co., Washington, (1976).

71. Incropera, F.P. and Leppert, G., *Investigation of Arc Jet Temperature-Measurement Techniques*, ISA Transactions, 6, 1, p 35 (January 1967).

72. Grey, J., Jacobs, P.F. and Sherman, M.P., *Calorimetric Probe for the Measurement of Extremely High Temperatures*, Rev. Sci. Instrum., 33, 7, p 738 (July 1962).

73. Katta, S., Lewis, J.A. and Gauvin, W.H., *Plasma Calorimetric Probe*, Rev. Sci. Instrum., 44, 10, p 1519 (October 1973).

74. Nishimura, Y. and Haraguchi, T., *Analysis of a Plasma Jet Reactor by a Two-Layer Model*, Ind. Eng. Chem. Fund., 22, p 202, (1983).

75. Amdur, I. and Mason, E.A., Properties of Gases at Very High Temperatures, The Physics of Fluids, 1, 5, p 370 (September/October 1958).

76. Hilsenrath, J. et al, Tables of Thermodynamic and Transport Properties, 478 p, Pergamon Press, New York, (1960).

77. Holman, J.P., Experimental Methods for Engineers, 3rd ed, 493 p, McGraw-Hill, New York, (1978).

78. Omega Engineering, One Omega Drive, Box 4047, Stamford CT, 06907, Temperature Measurement Handbook and Encyclopedia, (1985).

79. Chu, F.Y., personal communication, (September 1984).

NOMENCLATURE

A = area of jet opening

C = coefficient determined from a semi-logarithmic plot

$\tilde{c}_p$ = molar heat capacity

c_p = specific heat capacity

D = quench tube diameter

H' = plasma core enthalpy

h = convective heat transfer coefficient

I = arc current

M = molecular weight

N = total number of species

Q = volumetric flowrate

r = radius of an arbitrary nozzle cross section

S = length of transition section placed prior to water-cooled section

T = temperature

t = time

V = arc voltage

v = velocity

w = mass flowrate

$\tilde{w}$ = molar flowrate

W = heterogeneous rate of loss of the i^{th} component

X = average fractional conversion

x = axial dimension

y = vertical distance above jet opening

Greek Symbols

α = a variable dependent upon reactor geometry

γ = ratio of specific heat at constant pressure to specific heat at constant volume

δ = half-angle of the converging or diverging cones forming the nozzle

λ = energy of surface reactions

ρ = density

σ = uncertainty

ϕ = some angle less than the half-angle of the converging or diverging cones forming the nozzle

Subscripts

B = bulk

c = reaction chamber

cl = centerline

e = electron

o = axial distance=0

p = heavy particle (ion, atom, molecule)

w = quench tube surface

Superscripts

$-$ = average

' = core

o = reference or at reference conditions

APPENDIX A

INSTRUMENTAL CALIBRATIONS

A-1 Rotameter Calibration

The two rotameters, used to meter argon arc gas and quench gas flowrates, were calibrated by using a standard dry test meter. Air at 25°C was passed through each rotameter connected in series with the meter. A correction factor was applied to determine the volumetric flowrate of argon based upon the flowrate of air. Specifically,

$$Q_{Ar} = Q_{air} \sqrt{\frac{M_{air}}{M_{Ar}}} \tag{A-1}$$

where Q = volumetric flowrate
M = molecular weight

Results of these rotameter calibrations are presented in Figures A-1 and A-2.

The rotameter employed to measure the rate at which a sample stream is withdrawn through the calorimetric probe, was calibrated by the manufacturer. Based upon that calibration, the curve of Figure A-3 was constructed.

Cooling water to the calorimetric probe was metered by a rotameter calibrated by a direct weighing technique. This technique entailed the passage of known masses of water in measured time intervals through the rotameter. The resulting calibration curve is presented in Figure A-4. A second water rotameter, designed and used for the metering of torch cooling water flowrates, had been calibrated by the manufacturer.

A-2 Thermocouple Calibration

Each thermocouple was calibrated by immersing its junctions in containers of ice water and boiling water. Distilled water was employed and efforts were made to minimize temperature gradients in each container through mixing action. Thermocouple lead wires were connected directly to the digital readout data logger. The two calibration points represented only a small portion of the operating range of temperatures for the thermocouples. The degree of accuracy afforded by a more exacting calibration method was deemed unnecessary. Random comparisons of freestream temperatures, at chosen points in the effluent region of the plasma reactor, indicated good agreement between the high temperature and chromel/alumel thermocouples.

Where possible, thermocouples were re-calibrated during the course of the experiments. Results of the calibrations are presented in Table A-1.

ARGON ROTAMETER CALIBRATION
(FOR MEASUREMENT OF ARC GAS FLOWRATES)

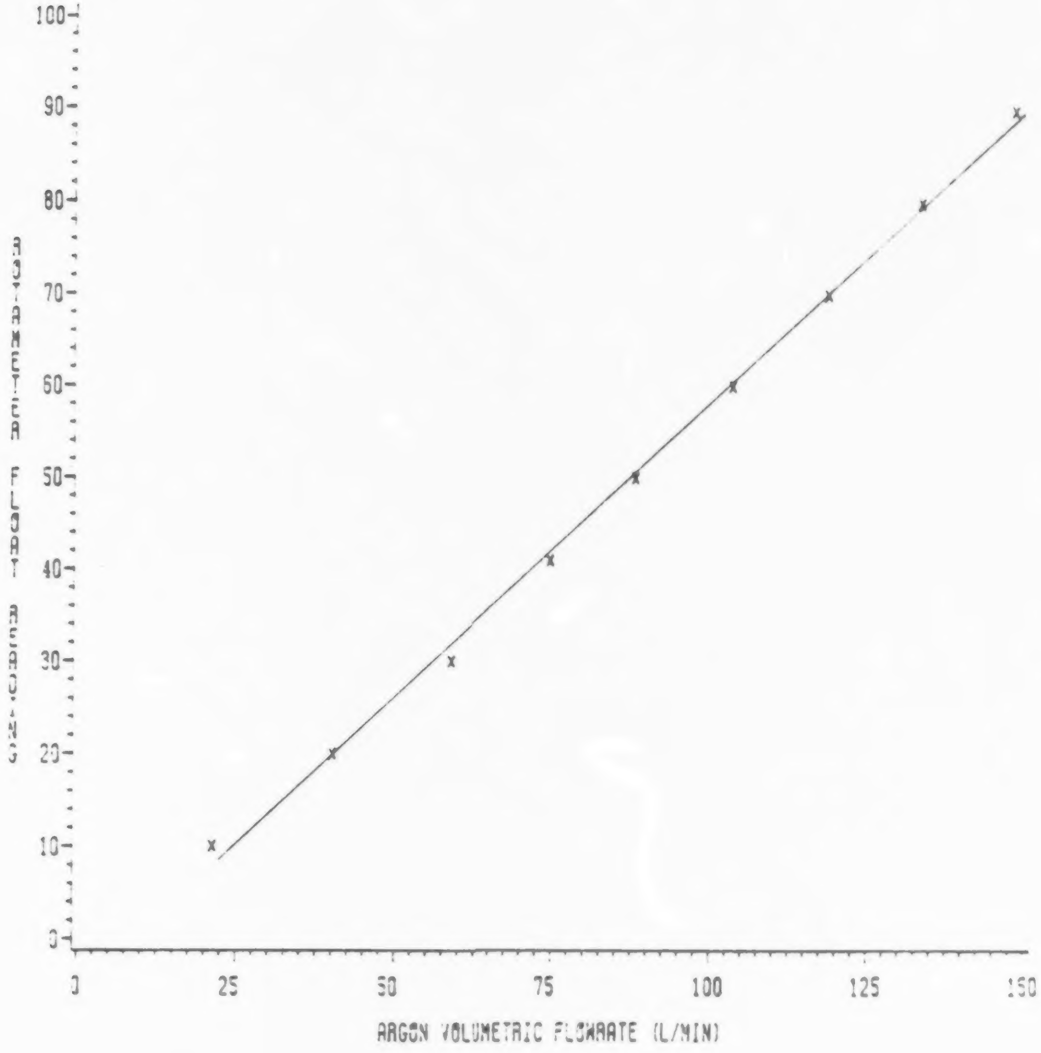

FIGURE A-1

ARGON ROTAMETER CALIBRATION
(FOR MEASUREMENT OF QUENCH GAS FLOWRATES)

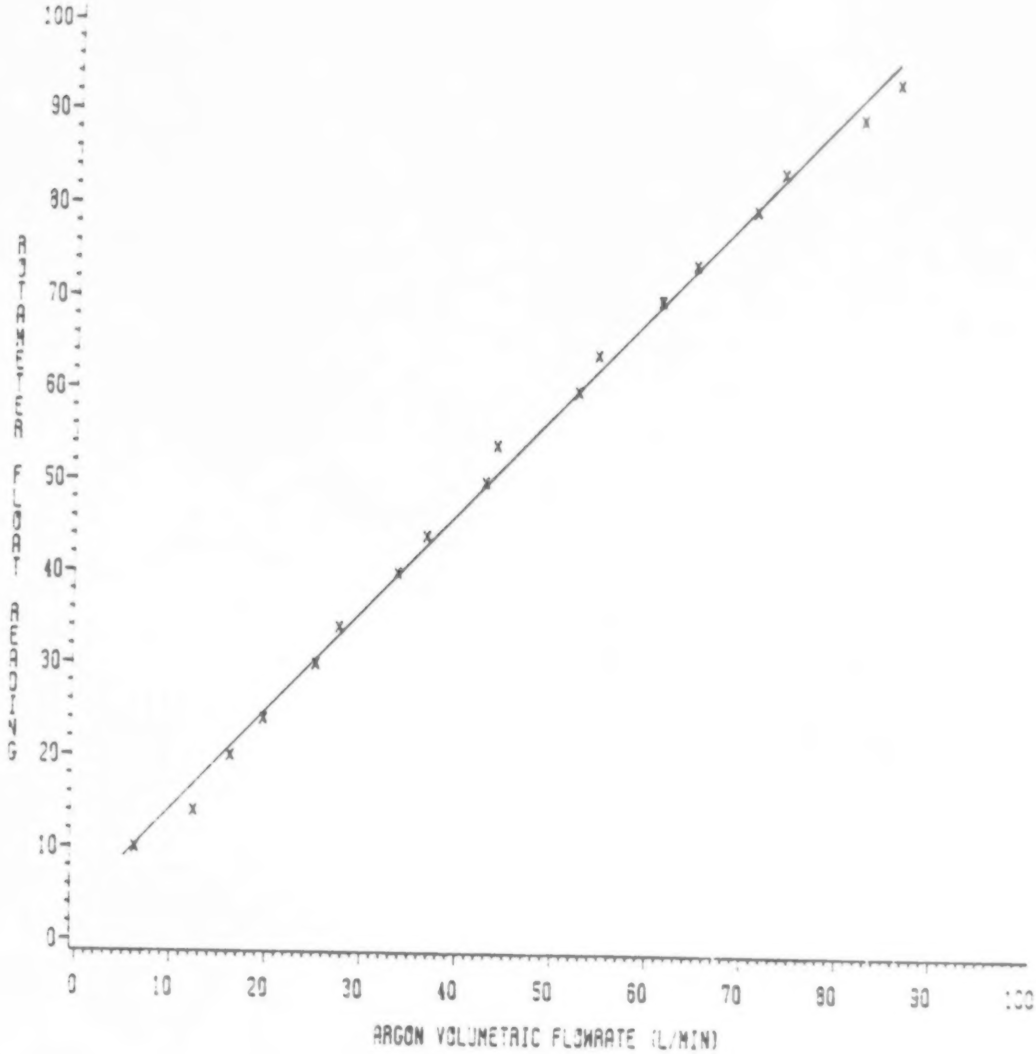

FIGURE A-2

ARGON ROTAMETER CALIBRATION

(FOR MEASUREMENT OF CALORIMETRIC PROBE GAS SAMPLE FLOWRATES)

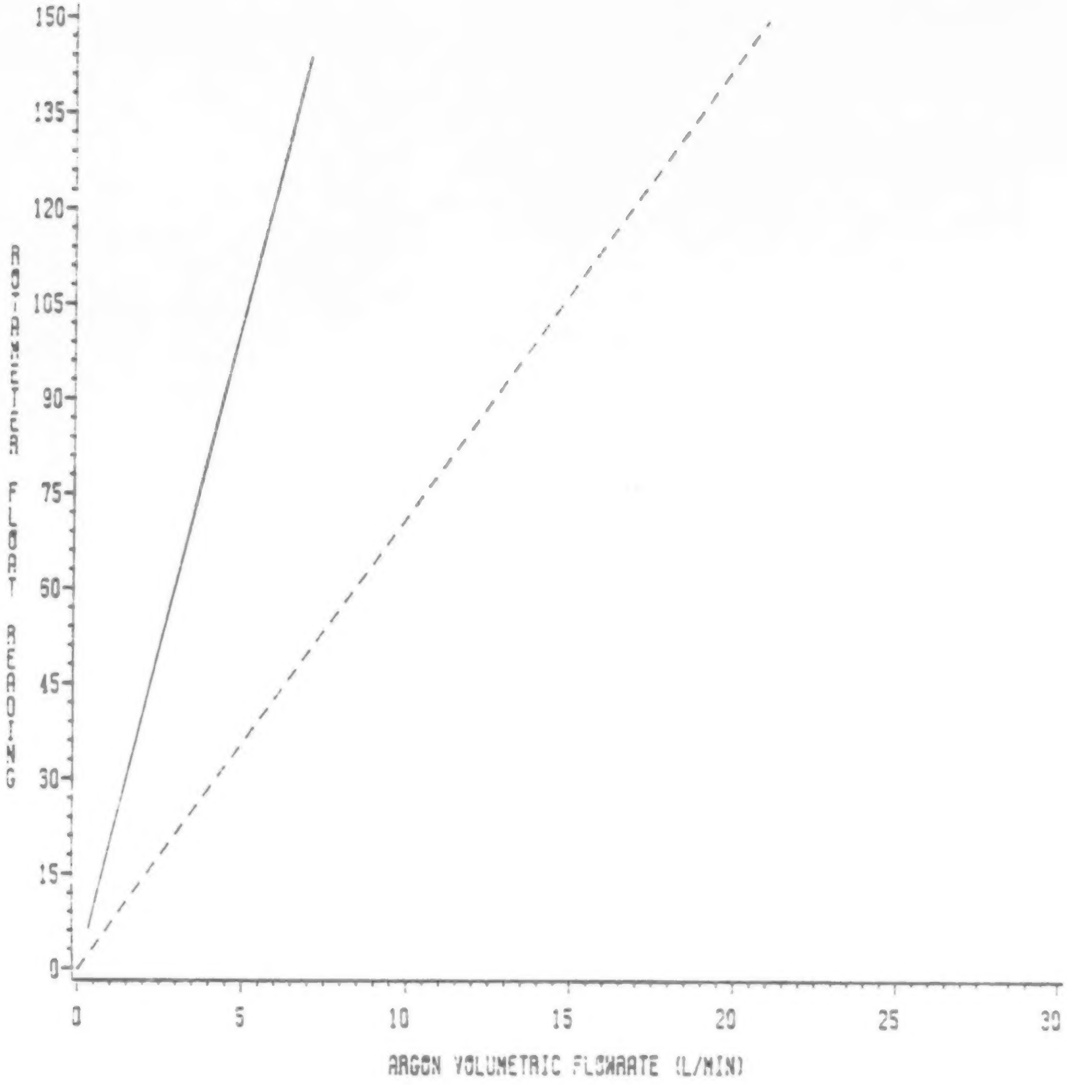

SOLID LINE: GLASS FLOAT
DASHED LINE: TANTALUM FLOAT
(NOTE: ARGON GAS TEMPERATURE = 25°C)

FIGURE A-3

WATER ROTAMETER CALIBRATION

(FOR MEASUREMENT OF CALORIMETRIC PROBE COOLING-WATER FLOWRATES)

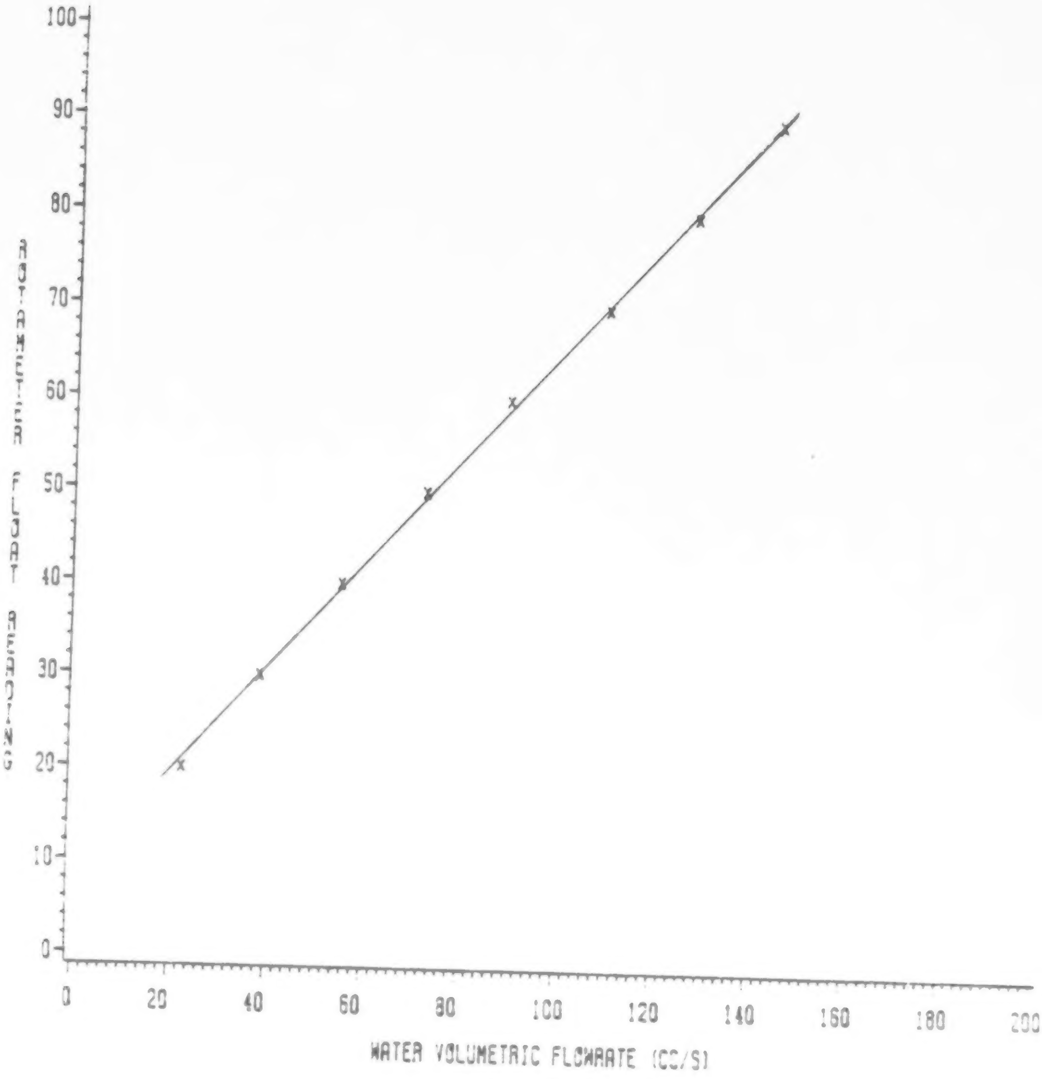

NOTE: WATER TEMPERATURE= 12°C

FIGURE A-4

THERMOCOUPLE DESCRIPTION	TRIAL NUMBER	HOT JUNCTION TEMPERATURE (°C)	COLD JUNCTION TEMPERATURE (°C)	MEASURED VOLTAGE (mV)	TABULATED VOLTAGE* (mV)
chromel/alumel (free stream)	1	0	0	-0.06	0.000
		100	0	4.02	4.095
	2	0	0	-0.02	0.000
		100	0	4.05	4.095
	3	0	0	-0.07	0.000
		100	0	4.02	4.095
tungsten-5% rhenium/ tungsten-26% rhenium (free stream)	1	0	0	-0.04	0.000
		100	0	1.40	1.451
	2	0	0	-0.04	0.000
		100	0	1.39	1.451
	1	0	0	-0.02	0.000
		100	0	1.43	1.451
	2	0	0	-0.03	0.000
		100	0	1.43	1.451
chromel/alumel (calorimetric probe)	1	0	0	0.04	0.000
		100	0	4.16	4.095
copper/constantan (calorimetric probe)	1	0	0	0.00	0.000
		100	100	0.00	0.000
		100	0	4.27	4.277

*taken from: Omega Engineering, One Omega Drive, Box 4047, Stamford, CT, 06907, Temperature Measurement Handbook and Encyclopedia, (1985).

TABLE A-1: Thermocouple Calibrations

APPENDIX B

EXPERIMENTAL DATA

QUENCHER CONFIGURATION*	CURRENT (AMPERES)	ARC GAS FLOWRATE (L/MIN @ 22°C)	QUENCH GAS FLOWRATE (L/MIN @ 22°C)	AXIAL DISTANCE FROM ANODE TO PROBE TIP (MM)	RADIAL DISTANCE FROM CENTERLINE (MM)	PROBE COOLING WATER ROTAMETER READING	PROBE GAS SAMPLE ROTAMETER READING	"NO-FLOW" COOLING WATER TEMPERATURE RISE (°C)	"FLOW" COOLING WATER TEMPERATURE RISE (°C)	GAS SAMPLE OUTLET TEMPERATURE (°K)
1	150	45	25	38	0	74	17	1.72	1.79	307
1	150	106	25	38	0	76	17	1.72	1.81	308
1	200	45	25	38	0	76	17	1.76	1.83	308
1	200	75	25	38	0	76	17	2.05	2.13	310
1	200	106	25	38	0	76	17	2.08	2.17	310
1	250	45	25	38	15	76	17	2.12	2.17	308
1	250	45	25	38	0	76	17	2.02	2.11	309
1	250	75	25	38	15	76	17	1.92	1.97	309
1	250	75	25	38	0	76	17	2.11	2.21	309
1	250	106	25	38	15	76	17	1.70	1.76	308
1	250	106	25	38	0	76	17	2.22	2.32	310
2	150	45	25	31	0	66	17	1.41	1.53	301
2	150	75	25	31	0	66	17	1.98	2.09	303
2	150	106	25	31	0	66	17	2.01	2.14	304
2	200	45	25	31	15	67	17	1.72	1.78	301
2	200	45	25	31	0	67	16	2.55	2.65	303
2	200	75	25	31	15	67	17	1.66	1.73	301
2	200	75	25	31	0	67	17	2.60	2.73	306
2	200	106	25	31	15	66	17	1.67	1.74	302
2	200	106	25	31	0	66	17	2.08	2.21	306
2	250	45	25	31	15	66	17	1.64	1.70	301
2	250	45	25	31	0	66	17	2.42	2.55	303
2	250	75	25	31	15	74	16	1.88	1.93	307
2	250	75	25	31	0	74	17	2.79	2.92	308
2	250	106	25	31	15	74	17	1.93	2.00	304
2	250	106	25	31	0	74	17	3.06	3.20	304
2	150	45	90	30	0	74	17	1.43	1.52	305

* 1. Injection Ring #1
2. Injection Ring #2
3. Injection Ring #2 + Constant Diameter Cooled-Surface Module
4. Injection Ring #2 + Cooled Nozzle Module

TABLE B-1: Variables Associated with the Calorimetric Probe Calculations of Temperature

QUENCHER CONFIGURATION*	CURRENT (AMPERES)	ARC GAS FLOWRATE (L/MIN @ 22°C)	QUENCH GAS FLOWRATE (L/MIN @ 22°C)	AXIAL DISTANCE FROM ANODE TO PROBE TIP (MM)	RADIAL DISTANCE FROM CENTERLINE (MM)	PROBE COOLING WATER ROTAMETER READING	PROBE GAS SAMPLE ROTAMETER READING	"NO-FLAME" COOLING WATER TEMPERATURE RISE (°C)	"FLAME" COOLING WATER TEMPERATURE RISE (°C)	GAS SAMPLE OUTLET TEMPERATURE (°K)
2	150	75	90	30	0	74	17	1.52	1.62	302
2	150	106	90	30	0	74	17	1.72	1.84	308
2	200	45	90	29	15	74	17	1.49	1.55	308
2	200	45	90	29	0	74	17	1.76	1.86	307
2	200	75	90	29	15	74	17	1.72	1.78	308
2	200	75	90	29	0	74	17	2.12	2.23	307
2	200	106	90	29	15	76	17	1.65	1.71	307
2	200	106	90	29	0	76	17	2.26	2.36	309
2	250	45	90	29	15	74	17	1.51	1.58	310
2	250	45	90	29	0	74	17	1.93	2.04	308
2	250	75	90	29	15	74	17	1.63	1.70	307
2	250	75	90	29	0	74	17	2.51	2.64	311
3	150	45	25	32	0	69	16	1.51	1.58	308
3	150	75	25	32	0	69	16	1.73	1.81	308
3	150	106	25	32	0	69	16	1.88	1.96	309
3	200	45	25	32	0	69	16	1.79	1.86	306
3	200	75	25	32	0	69	16	1.94	2.02	311
3	200	106	25	32	0	69	16	2.20	2.29	309
3	250	45	25	32	0	69	16	1.95	2.02	308
3	250	75	25	32	0	69	16	2.36	2.44	309
3	250	106	25	32	0	69	17	2.46	2.57	306
3	150	45	90	32	0	68	17	1.62	1.70	305
3	150	75	90	32	0	68	17	1.76	1.84	305
3	150	106	90	32	0	68	17	1.65	1.74	303
3	200	45	90	32	0	68	17	1.75	1.83	310
3	200	75	90	32	0	68	17	2.00	2.09	309
3	200	106	90	32	0	68	17	1.92	2.02	309

* 1. Injection Ring #1
2. Injection Ring #2
3. Injection Ring #2 + Constant Diameter Cooled-Surface Module
4. Injection Ring #2 + Cooled Nozzle Module

TABLE B-1 (cont'd)

QUENCHER CONFIGURATION*	CURRENT (AMPERES)	ARC GAS FLOWRATE (L/MIN @ 22°C)	QUENCH GAS FLOWRATE (L/MIN @ 22°C)	AXIAL DISTANCE FROM ANODE TO PROBE TIP (MM)	RADIAL DISTANCE FROM CENTERLINE (MM)	PROBE COOLING WATER ROTAMETER READING	PROBE GAS SAMPLE ROTAMETER READING	"NO-FLOW" COOLING WATER TEMPERATURE RISE (°C)	"FLOW" COOLING WATER TEMPERATURE RISE (°C)	GAS SAMPLE OUTLET TEMPERATURE (°K)
3	250	45	90	32	0	68	17	2.63	2.73	313
3	250	106	90	32	0	68	17	2.24	2.35	306
4	150	45	25	62	0	63	17	2.02	2.11	308
4	150	75	25	62	0	63	17	2.61	2.73	309
4	150	106	25	62	0	64	17	2.68	2.81	308
4	200	45	25	66	0	64	17	2.48	2.58	307
4	200	75	25	66	0	63	17	3.12	3.22	310
4	200	106	25	66	0	64	17	3.34	3.47	312
4	250	45	25	66	0	64	17	3.35	3.46	311
4	250	75	25	66	0	64	17	3.76	3.88	310
4	150	45	90	61	0	64	17	2.02	2.11	306
4	150	75	90	61	0	64	17	2.60	2.71	306
4	150	106	90	61	0	64	17	2.81	2.93	306
4	200	45	90	66	0	64	17	2.75	2.85	308
4	200	75	90	66	0	64	17	2.63	2.74	310
4	200	106	90	66	0	64	17	3.12	3.24	307
4	250	45	90	66	0	64	17	3.40	3.52	307
4	250	75	90	66	0	64	17	3.49	3.61	308

* 1. Injection Ring #1
2. Injection Ring #2
3. Injection Ring #2 + Constant Diameter Cooled-Surface Module
4. Injection Ring #2 + Cooled Nozzle Module

TABLE B-1 (cont'd)

RADIAL DISTANCE FROM CENTERLINE (MM)	AXIAL DISTANCE FROM THE ANODE (MM)				
	38	52	76	114	151
45	457	521			538
30	540	643			592
15	2028	874			621
0	2933	1371	978	802	668

QUENCHER: Injection Ring #1
CURRENT: 150 Amperes
VOLTAGE: 65 Volts
ARC GAS FLOWRATE: 45 l/min @ 25°C
QUENCH GAS FLOWRATE: 25 l/min @ 25°C
TORCH COOLING WATER FLOWRATE: 79.5 l/min @ 12°C
TORCH COOLING WATER TEMPERATURE RISE: 0.8°C

RADIAL DISTANCE FROM CENTERLINE (MM)	AXIAL DISTANCE FROM THE ANODE (MM)				
	38	52	76	114	151
45	[illegible]	525			541
30	530	670			574
15	2086	869			632
0		1374	1095	830	680

QUENCHER: Injection Ring #1
CURRENT: 150 Amperes
VOLTAGE: 71 Volts
ARC GAS FLOWRATE: 75 l/min @ 25°C
QUENCH GAS FLOWRATE: 25 l/min @ 25°C
TORCH COOLING WATER FLOWRATE: 79.5 l/min @ 12°C
TORCH COOLING WATER TEMPERATURE RISE: 0.7°C

RADIAL DISTANCE FROM CENTERLINE (MM)	AXIAL DISTANCE FROM THE ANODE (MM)				
	38	52	76	114	151
45	495	559			551
30	562	685			609
15	2095	881			654
0	3772	1436	1088	881	695

QUENCHER: Injection Ring #1
CURRENT: 150 Amperes
VOLTAGE: 77 Volts
ARC GAS FLOWRATE: 106 l/min @ 25°C
QUENCH GAS FLOWRATE: 25 l/min @ 25°C
TORCH COOLING WATER FLOWRATE: 79.5 l/min @ 12°C
TORCH COOLING WATER TEMPERATURE RISE: 0.7°C

TABLE B-2: Calorimetrically Determined Temperatures, Thermocouple Temperatures and Values for the Operating Variables

RADIAL DISTANCE FROM CENTERLINE (MM)	AXIAL DISTANCE FROM THE ANODE (MM) 38	52	76	114	151
45	485	502			530
30	584	635			581
15	2061	906			635
0	3003	1332	943	829	682

QUENCHER: Injection Ring #1
CURRENT: 200 Amperes
VOLTAGE: 71 Volts
ARC GAS FLOWRATE: 45 1/min @ 25°C
QUENCH GAS FLOWRATE: 25 1/min @ 25°C
TORCH COOLING WATER FLOWRATE: 79.5 1/min @ 12°C
TORCH COOLING WATER TEMPERATURE RISE: 1.1°C

RADIAL DISTANCE FROM CENTERLINE (MM)	AXIAL DISTANCE FROM THE ANODE (MM) 38	52	76	114	151
45	492	535			563
30	614	620			618
15	2082	962			674
0	3389	1377	1051	865	720

QUENCHER: Injection Ring #1
CURRENT: 200 Amperes
VOLTAGE: 76 Volts
ARC GAS FLOWRATE: 75 1/min @ 25°C
QUENCH GAS FLOWRATE: 25 1/min @ 25°C
TORCH COOLING WATER FLOWRATE: 79.5 1/min @ 12°C
TORCH COOLING WATER TEMPERATURE RISE: 1.0°C

RADIAL DISTANCE FROM CENTERLINE (MM)	AXIAL DISTANCE FROM THE ANODE (MM) 38	52	76	114	151
45	529	588			564
30	655	714			621
15	2167	1002			687
0	3774	1461	1143	897	718

QUENCHER: Injection Ring #1
CURRENT: 200 Amperes
VOLTAGE: 83 Volts
ARC GAS FLOWRATE: 106 1/min @ 25°C
QUENCH GAS FLOWRATE: 25 1/min @ 25°C
TORCH COOLING WATER FLOWRATE: 79.5 1/min @ 12°C
TORCH COOLING WATER TEMPERATURE RISE: 1.1°C

TABLE B-2 (cont'd)

RADIAL DISTANCE FROM CENTERLINE (MM)	AXIAL DISTANCE FROM THE ANODE (MM) 38	52	76	114	151
45	497	533			575
30	620	657			640
15	2233	938			702
0	3773	1390	1040	901	714

QUENCHER: Injection Ring #1
CURRENT: 250 Amperes
VOLTAGE: 75 Volts
ARC GAS FLOWRATE: 45 l/min @ 25°C
QUENCH GAS FLOWRATE: 25 l/min @ 25°C
TORCH COOLING WATER FLOWRATE: 79.5 l/min @ 12°C
TORCH COOLING WATER TEMPERATURE RISE: 1.65°C

RADIAL DISTANCE FROM CENTERLINE (MM)	AXIAL DISTANCE FROM THE ANODE (MM) 38	52	76	114	151
45	547	572			603
30	688	760			650
15	2234	999			742
0	4158	1407	1188	940	761

QUENCHER: Injection Ring #1
CURRENT: 250 Amperes
VOLTAGE: 83 Volts
ARC GAS FLOWRATE: 75 l/min @ 25°C
QUENCH GAS FLOWRATE: 25 l/min @ 25°C
TORCH COOLING WATER FLOWRATE: 79.5 l/min @ 12°C
TORCH COOLING WATER TEMPERATURE RISE: 1.6°C

RADIAL DISTANCE FROM CENTERLINE (MM)	AXIAL DISTANCE FROM THE ANODE (MM) 38	52	76	114	151
45	592	633			609
30	687	824			686
15	2618	1080			736
0	4159	1568	1297	969	784

QUENCHER: Injection Ring #1
CURRENT: 250 Amperes
VOLTAGE: 88 Volts
ARC GAS FLOWRATE: 106 l/min @ 25°C
QUENCH GAS FLOWRATE: 25 l/min @ 25°C
TORCH COOLING WATER FLOWRATE: 79.5 l/min @ 12°C
TORCH COOLING WATER TEMPERATURE RISE: 1.6°C

TABLE B-2 (cont'd)

RADIAL DISTANCE FROM CENTERLINE (MM)	AXIAL DISTANCE FROM THE ANODE (MM)				
	31	50	74	112	149
45	445	486			522
30	496	622			589
15	2236	796			635
0	4294	1321	916	804	680

QUENCHER: Injection Ring #2
CURRENT: 150 Amperes
VOLTAGE: 66 Volts
ARC GAS FLOWRATE: 45 l/min @ 25°C
QUENCH GAS FLOWRATE: 25 l/min @ 25°C
TORCH COOLING WATER FLOWRATE: 84.8 l/min @ 12°C
TORCH COOLING WATER TEMPERATURE RISE: 0.4°C

RADIAL DISTANCE FROM CENTERLINE (MM)	AXIAL DISTANCE FROM THE ANODE (MM)				
	31	50	74	112	149
45	516	552			574
30	575	685			639
15	2347	853			656
0	3963	1387	970	817	697

QUENCHER: Injection Ring #2
CURRENT: 150 Amperes
VOLTAGE: 71 Volts
ARC GAS FLOWRATE: 75 l/min @ 25°C
QUENCH GAS FLOWRATE: 25 l/min @ 25°C
TORCH COOLING WATER FLOWRATE: 84.8 l/min @ 12°C
TORCH COOLING WATER TEMPERATURE RISE: 0.35°C

RADIAL DISTANCE FROM CENTERLINE (MM)	AXIAL DISTANCE FROM THE ANODE (MM)				
	31	50	74	112	149
45	556	583			616
30	677	741			670
15	2348	943			708
0	4630	1543	981	837	740

QUENCHER: Injection Ring #2
CURRENT: 150 Amperes
VOLTAGE: 75 Volts
ARC GAS FLOWRATE: 106 l/min @ 25°C
QUENCH GAS FLOWRATE: 25 l/min @ 25°C
TORCH COOLING WATER FLOWRATE: 84.8 l/min @ 12°C
TORCH COOLING WATER TEMPERATURE RISE: 0.4°C

TABLE B-2 (cont'd)

RADIAL DISTANCE FROM CENTERLINE (MM)	AXIAL DISTANCE FROM THE ANODE (MM) 31	50	74	112	149
45	492	545			521
30	518	687			623
15	2337	841			667
0	4120	1330	995	846	713

QUENCHER: Injection Ring #2
CURRENT: 200 Amperes
VOLTAGE: 69 Volts
ARC GAS FLOWRATE: 45 l/min @ 25°C
QUENCH GAS FLOWRATE: 25 l/min @ 25°C
TORCH COOLING WATER FLOWRATE: 84.8 l/min @ 12°C
TORCH COOLING WATER TEMPERATURE RISE: 0.6°C

RADIAL DISTANCE FROM CENTERLINE (MM)	AXIAL DISTANCE FROM THE ANODE (MM) 31	50	74	112	149
45	529	541			569
30	632	711			681
15	2676	921			697
0	4716	1468	1063	860	724

QUENCHER: Injection Ring #2
CURRENT: 200 Amperes
VOLTAGE: 76 Volts
ARC GAS FLOWRATE: 75 l/min @ 25°C
QUENCH GAS FLOWRATE: 25 l/min @ 25°C
TORCH COOLING WATER FLOWRATE: 84.8 l/min @ 12°C
TORCH COOLING WATER TEMPERATURE RISE: 0.6°C

RADIAL DISTANCE FROM CENTERLINE (MM)	AXIAL DISTANCE FROM THE ANODE (MM) 31	50	74	112	149
45	588	586			631
30	692	779			707
15	2631	1016			736
0	4632	1644	1109	887	764

QUENCHER: Injection Ring #2
CURRENT: 200 Amperes
VOLTAGE: 80 Volts
ARC GAS FLOWRATE: 106 l/min @ 25°C
QUENCH GAS FLOWRATE: 25 l/min @ 25°C
TORCH COOLING WATER FLOWRATE: 84.8 l/min @ 12°C
TORCH COOLING WATER TEMPERATURE RISE: 0.5°C

TABLE B-2 (cont'd)

RADIAL DISTANCE FROM CENTERLINE (MM)	AXIAL DISTANCE FROM THE ANODE (MM)				
	31	50	74	112	149
45	561	599			587
30	653	780			604
15	2297	1057			653
0	4629	1763	1148	939	683

QUENCHER: Injection Ring #2
CURRENT: 250 Amperes
VOLTAGE: 73 Volts
ARC GAS FLOWRATE: 45 l/min @ 25°C
QUENCH GAS FLOWRATE: 25 l/min @ 25°C
TORCH COOLING WATER FLOWRATE: 84.8 l/min @ 12°C
TORCH COOLING WATER TEMPERATURE RISE: 0.8°C

RADIAL DISTANCE FROM CENTERLINE (MM)	AXIAL DISTANCE FROM THE ANODE (MM)				
	31	50	74	112	149
45	565	603			591
30	657	756			635
15	2417	1090			674
0	5185	1749	1214	913	748

QUENCHER: Injection Ring #2
CURRENT: 250 Amperes
VOLTAGE: 79 Volts
ARC GAS FLOWRATE: 75 l/min @ 25°C
QUENCH GAS FLOWRATE: 25 l/min @ 25°C
TORCH COOLING WATER FLOWRATE: 84.8 l/min @ 12°C
TORCH COOLING WATER TEMPERATURE RISE: 0.7°C

RADIAL DISTANCE FROM CENTERLINE (MM)	AXIAL DISTANCE FROM THE ANODE (MM)				
	31	50	74	112	149
45	570	636			622
30	690	767			691
15	2930	1103			745
0	5556	1864	1250	918	786

QUENCHER: Injection Ring #2
CURRENT: 250 Amperes
VOLTAGE: 86 Volts
ARC GAS FLOWRATE: 106 l/min @ 25°C
QUENCH GAS FLOWRATE: 25 l/min @ 25°C
TORCH COOLING WATER FLOWRATE: 84.8 l/min @ 12°C
TORCH COOLING WATER TEMPERATURE RISE: 0.7°C

TABLE B-2 (cont'd)

RADIAL DISTANCE FROM CENTERLINE (MM)	AXIAL DISTANCE FROM THE ANODE (MM)				
	30	51	74	112	149
45	413	474			440
30	477	585			541
15	2076	772			590
0	3681	1265	776	667	611

QUENCHER: Injection Ring #2
CURRENT: 150 Amperes
VOLTAGE: 68 Volts
ARC GAS FLOWRATE: 45 l/min @ 25°C
QUENCH GAS FLOWRATE: 90 l/min @ 25°C
TORCH COOLING WATER FLOWRATE: 84.8 l/min @ 12°C
TORCH COOLING WATER TEMPERATURE RISE: 0.4°C

RADIAL DISTANCE FROM CENTERLINE (MM)	AXIAL DISTANCE FROM THE ANODE (MM)				
	30	51	74	112	149
45	461	526			507
30	569	653			606
15	2373	838			625
0	4054	1369	803	692	642

QUENCHER: Injection Ring #2
CURRENT: 150 Amperes
VOLTAGE: 73 Volts
ARC GAS FLOWRATE: 75 l/min @ 25°C
QUENCH GAS FLOWRATE: 90 l/min @ 25°C
TORCH COOLING WATER FLOWRATE: 84.8 l/min @ 12°C
TORCH COOLING WATER TEMPERATURE RISE: 0.4°C

RADIAL DISTANCE FROM CENTERLINE (MM)	AXIAL DISTANCE FROM THE ANODE (MM)				
	30	51	74	112	149
45	517	556			547
30	638	727			635
15	2415	905			650
0	4810	1458	870	761	682

QUENCHER: Injection Ring #2
CURRENT: 150 Amperes
VOLTAGE: 80 Volts
ARC GAS FLOWRATE: 106 l/min @ 25°C
QUENCH GAS FLOWRATE: 90 l/min @ 25°C
TORCH COOLING WATER FLOWRATE: 84.8 l/min @ 12°C
TORCH COOLING WATER TEMPERATURE RISE: 0.3°C

TABLE B-2 (cont'd)

RADIAL DISTANCE FROM CENTERLINE (MM)	AXIAL DISTANCE FROM THE ANODE (MM)				
	29	51	74	112	149
45	438	480			534
30	502	597			617
15	2559	788			659
0	4059	1267	775	709	669

QUENCHER: Injection Ring #2
CURRENT: 200 Amperes
VOLTAGE: 72 Volts
ARC GAS FLOWRATE: 45 l/min @ 25°C
QUENCH GAS FLOWRATE: 90 l/min @ 25°C
TORCH COOLING WATER FLOWRATE: 84.8 l/min @ 12°C
TORCH COOLING WATER TEMPERATURE RISE: 0.6°C

RADIAL DISTANCE FROM CENTERLINE (MM)	AXIAL DISTANCE FROM THE ANODE (MM)				
	29	51	74	112	149
45	471	498			586
30	594	657			674
15	2559	844			682
0	4434	1405	825	704	705

QUENCHER: Injection Ring #2
CURRENT: 200 Amperes
VOLTAGE: 78 Volts
ARC GAS FLOWRATE: 75 l/min @ 25°C
QUENCH GAS FLOWRATE: 90 l/min @ 25°C
TORCH COOLING WATER FLOWRATE: 84.8 l/min @ 12°C
TORCH COOLING WATER TEMPERATURE RISE: 0.6°C

RADIAL DISTANCE FROM CENTERLINE (MM)	AXIAL DISTANCE FROM THE ANODE (MM)				
	29	51	74	112	149
45	468	588			602
30	615	772			686
15	2617	1051			703
0	4158	1609	959	809	722

QUENCHER: Injection Ring #2
CURRENT: 200 Amperes
VOLTAGE: 83 Volts
ARC GAS FLOWRATE: 106 l/min @ 25°C
QUENCH GAS FLOWRATE: 90 l/min @ 25°C
TORCH COOLING WATER FLOWRATE: 84.8 l/min @ 12°C
TORCH COOLING WATER TEMPERATURE RISE: 0.55°C

TABLE B-2 (cont'd)

RADIAL DISTANCE FROM CENTERLINE (MM)	AXIAL DISTANCE FROM THE ANODE (MM)				
	29	51	74	112	149
45	549	584			571
30	642	714			624
15	2936	952			664
0	4435	1752	957	721	669

QUENCHER: Injection Ring #2
CURRENT: 250 Amperes
VOLTAGE: 78 Volts
ARC GAS FLOWRATE: 45 l/min @ 25°C
QUENCH GAS FLOWRATE: 90 l/min @ 25°C
TORCH COOLING WATER FLOWRATE: 84.8 l/min @ 12°C
TORCH COOLING WATER TEMPERATURE RISE: 0.6°C

RADIAL DISTANCE FROM CENTERLINE (MM)	AXIAL DISTANCE FROM THE ANODE (MM)				
	29	51	74	112	149
45	564	619			627
30	632	702			683
15	2933	1016			691
0	5188	1783	1053	864	722

QUENCHER: Injection Ring #2
CURRENT: 250 Amperes
VOLTAGE: 83 Volts
ARC GAS FLOWRATE: 75 l/min @ 25°C
QUENCH GAS FLOWRATE: 90 l/min @ 25°C
TORCH COOLING WATER FLOWRATE: 84.8 l/min @ 12°C
TORCH COOLING WATER TEMPERATURE RISE: 0.7°C

RADIAL DISTANCE FROM CENTERLINE (MM)	AXIAL DISTANCE FROM THE ANODE (MM)				
	29	51	74	112	149
45	571	680			649
30	662	763			708
15		1076			714
0		1806	1160	924	759

QUENCHER: Injection Ring #2
CURRENT: 250 Amperes
VOLTAGE: 88 Volts
ARC GAS FLOWRATE: 106 l/min @ 25°C
QUENCH GAS FLOWRATE: 90 l/min @ 25°C
TORCH COOLING WATER FLOWRATE: 84.8 l/min @ 12°C
TORCH COOLING WATER TEMPERATURE RISE: 0.7°C

TABLE B-2 (cont'd)

RADIAL DISTANCE FROM CENTERLINE (MM)	AXIAL DISTANCE FROM THE ANODE (MM) 46	68	90	114	151
45	472	529			530
30	585	683			586
15	1786	768			648
0	3082	1154	878	755	659

QUENCHER: Injection Ring #2 + Constant Diameter Cooled-Surface Module
CURRENT: 150 Amperes
VOLTAGE: 66 Volts
ARC GAS FLOWRATE: 45 l/min @ 25°C
QUENCH GAS FLOWRATE: 25 l/min @ 25°C
TORCH COOLING WATER FLOWRATE: 87.1 l/min @ 12°C
TORCH COOLING WATER TEMPERATURE RISE: 0.4°C

RADIAL DISTANCE FROM CENTERLINE (MM)	AXIAL DISTANCE FROM THE ANODE (MM) 46	68	90	114	151
45	490	560			557
30	599	715			618
15	1847	806			662
0	3479	1217	955	812	664

QUENCHER: Injection Ring #2 + Constant Diameter Cooled-Surface Module
CURRENT: 150 Amperes
VOLTAGE: 71 Volts
ARC GAS FLOWRATE: 75 l/min @ 25°C
QUENCH GAS FLOWRATE: 25 l/min @ 25°C
TORCH COOLING WATER FLOWRATE: 87.1 l/min @ 12°C
TORCH COOLING WATER TEMPERATURE RISE: 0.4°C

RADIAL DISTANCE FROM CENTERLINE (MM)	AXIAL DISTANCE FROM THE ANODE (MM) 46	68	90	114	151
45	534	596			574
30	619	722			657
15	1850	865			683
0	3480	1387	970	843	726

QUENCHER: Injection Ring #2 + Constant Diameter Cooled-Surface Module
CURRENT: 150 Amperes
VOLTAGE: 75 Volts
ARC GAS FLOWRATE: 106 l/min @ 25°C
QUENCH GAS FLOWRATE: 25 l/min @ 25°C
TORCH COOLING WATER FLOWRATE: 87.1 l/min @ 12°C
TORCH COOLING WATER TEMPERATURE RISE: 0.4°C

TABLE B-2 (cont'd)

RADIAL DISTANCE FROM CENTERLINE (MM)	AXIAL DISTANCE FROM THE ANODE (MM)				
	46	68	90	114	151
45	494	543			583
30	612	720			610
15	1811	834			669
0	3080	1263	976	797	725

QUENCHER: Injection Ring #2 + Constant Diameter Cooled-Surface Module
CURRENT: 200 Amperes
VOLTAGE: 69 Volts
ARC GAS FLOWRATE: 45 1/min @$^{\circ}$25 C
QUENCH GAS FLOWRATE: 25 1/min @ 25°C
TORCH COOLING WATER FLOWRATE: 87.1 1/min @ 12°C
TORCH COOLING WATER TEMPERATURE RISE: 0.6°C

RADIAL DISTANCE FROM CENTERLINE (MM)	AXIAL DISTANCE FROM THE ANODE (MM)				
	46	68	90	114	151
45	517	594			627
30	651	741			663
15	1854	823			738
0	3482	1355	1009	889	766

QUENCHER: Injection Ring #2 + Constant Diameter Cooled-Surface Module
CURRENT: 200 Amperes
VOLTAGE: 75 Volts
ARC GAS FLOWRATE: 75 1/min @ 25°C
QUENCH GAS FLOWRATE: 25 1/min @ 25°C
TORCH COOLING WATER FLOWRATE: 87.1 1/min @ 12°C
TORCH COOLING WATER TEMPERATURE RISE: 0.6°C

RADIAL DISTANCE FROM CENTERLINE (MM)	AXIAL DISTANCE FROM THE ANODE (MM)				
	46	68	90	114	151
45	542	638			625
30	659	794			687
15	1995	974			744
0	3876	1556	1086	919	777

QUENCHER: Injection Ring #2 + Constant Diameter Cooled-Surface Module
CURRENT: 200 Amperes
VOLTAGE: 79 Volts
ARC GAS FLOWRATE: 106 1/min @ 25°C
QUENCH GAS FLOWRATE: 25 1/min @ 25°C
TORCH COOLING WATER FLOWRATE: 87.1 1/min @ 12°C
TORCH COOLING WATER TEMPERATURE RISE: 0.6°C

TABLE B-2 (cont'd)

RADIAL DISTANCE FROM CENTERLINE (MM)	AXIAL DISTANCE FROM THE ANODE (MM) 46	68	90	114	151
45	525	566			564
30	600	781			608
15	1879	934			639
0	3082	1415	1075	971	687

QUENCHER: Injection Ring #2 + Constant Diameter
Cooled-Surface Module
CURRENT: 250 Amperes
VOLTAGE: 73 Volts
ARC GAS FLOWRATE: 45 l/min @ 25°C
QUENCH GAS FLOWRATE: 25 l/min @ 25°C
TORCH COOLING WATER FLOWRATE: 87.1 l/min @ 12°C
TORCH COOLING WATER TEMPERATURE RISE: 0.8°C

RADIAL DISTANCE FROM CENTERLINE (MM)	AXIAL DISTANCE FROM THE ANODE (MM) 46	68	90	114	151
45	576	597			600
30	646	814			676
15	1894	1013			759
0	3480	1553	1141	990	782

QUENCHER: Injection Ring #2 + Constant Diameter
Cooled-Surface Module
CURRENT: 250 Amperes
VOLTAGE: 80 Volts
ARC GAS FLOWRATE: 75 l/min @ 25°C
QUENCH GAS FLOWRATE: 25 l/min @ 25°C
TORCH COOLING WATER FLOWRATE: 87.1 l/min @ 12°C
TORCH COOLING WATER TEMPERATURE RISE: 0.75°C

RADIAL DISTANCE FROM CENTERLINE (MM)	AXIAL DISTANCE FROM THE ANODE (MM) 46	68	90	114	151
45	603	624			607
30	669	889			713
15	2031	1087			760
0	4181	1699	1282	1038	803

QUENCHER: Injection Ring #2 + Constant Diameter
Cooled-Surface Module
CURRENT: 250 Amperes
VOLTAGE: 84 Volts
ARC GAS FLOWRATE: 106 l/min @ 25°C
QUENCH GAS FLOWRATE: 25 l/min @ 25°C
TORCH COOLING WATER FLOWRATE: 87.1 l/min @ 12°C
TORCH COOLING WATER TEMPERATURE RISE: 0.8°C

TABLE B-2 (cont'd)

RADIAL DISTANCE FROM CENTERLINE (MM)	AXIAL DISTANCE FROM THE ANODE (MM)				
	46	68	90	114	151
45	441	502			516
30	551	676			561
15	1747	732			584
0	3071	1088	798	712	606

QUENCHER: Injection Ring #2 + Constant Diameter Cooled-Surface Module
CURRENT: 150 Amperes
VOLTAGE: 66 Volts
ARC GAS FLOWRATE: 45 l/min @ 25°C
QUENCH GAS FLOWRATE: 90 l/min @ 25°C
TORCH COOLING WATER FLOWRATE: 87.1 l/min @ 12°C
TORCH COOLING WATER TEMPERATURE RISE: 0.4°C

RADIAL DISTANCE FROM CENTERLINE (MM)	AXIAL DISTANCE FROM THE ANODE (MM)				
	46	68	90	114	151
45	462	570			526
30	554	649			570
15	1776	775			593
0	3071	1208	825	730	602

QUENCHER: Injection Ring #2 + Constant Diameter Cooled-Surface Module
CURRENT: 150 Amperes
VOLTAGE: 71 Volts
ARC GAS FLOWRATE: 75 l/min @ 25°C
QUENCH GAS FLOWRATE: 90 l/min @ 25°C
TORCH COOLING WATER FLOWRATE: 87.1 l/min @ 12°C
TORCH COOLING WATER TEMPERATURE RISE: 0.4°C

RADIAL DISTANCE FROM CENTERLINE (MM)	AXIAL DISTANCE FROM THE ANODE (MM)				
	46	68	90	114	151
45	528	562			569
30	595	673			601
15	1922	860			623
0	3415	1229	858	741	666

QUENCHER: Injection Ring #2 + Constant Diameter Cooled-Surface Module
CURRENT: 150 Amperes
VOLTAGE: 74 Volts
ARC GAS FLOWRATE: 106 l/min @ 25°C
QUENCH GAS FLOWRATE: 90 l/min @ 25°C
TORCH COOLING WATER FLOWRATE: 87.1 l/min @ 12°C
TORCH COOLING WATER TEMPERATURE RISE: 0.45°C

TABLE B-2 (cont'd)

RADIAL DISTANCE FROM CENTERLINE (MM)	AXIAL DISTANCE FROM THE ANODE (MM)				
	46	68	90	114	151
45	466	498			548
30	590	702			598
15	1824	829			641
0	3076	1228	887	770	690

QUENCHER: Injection Ring #2 + Constant Diameter
Cooled-Surface Module
CURRENT: 200 Amperes
VOLTAGE: 70 Volts
ARC GAS FLOWRATE: 45 l/min @ 25°C
QUENCH GAS FLOWRATE: 90 l/min @ 25°C
TORCH COOLING WATER FLOWRATE: 87.1 l/min @ 12°C
TORCH COOLING WATER TEMPERATURE RISE: 0.6°C

RADIAL DISTANCE FROM CENTERLINE (MM)	AXIAL DISTANCE FROM THE ANODE (MM)				
	46	68	90	114	151
45	490	567			556
30	596	708			620
15	1830	815			679
0	3421	1371	949	806	690

QUENCHER: Injection Ring #2 + Constant Diameter
Cooled-Surface Module
CURRENT: 200 Amperes
VOLTAGE: 74 Volts
ARC GAS FLOWRATE: 75 l/min @ 25°C
QUENCH GAS FLOWRATE: 90 l/min @ 25°C
TORCH COOLING WATER FLOWRATE: 87.1 l/min @ 12°C
TORCH COOLING WATER TEMPERATURE RISE: 0.6°C

RADIAL DISTANCE FROM CENTERLINE (MM)	AXIAL DISTANCE FROM THE ANODE (MM)				
	46	68	90	114	151
45	509	579			588
30	629	756			619
15	1963	943			686
0	3767	1497	1028	884	705

QUENCHER: Injection Ring #2 + Constant Diameter
Cooled-Surface Module
CURRENT: 200 Amperes
VOLTAGE: 79 Volts
ARC GAS FLOWRATE: 106 l/min @ 25°C
QUENCH GAS FLOWRATE: 90 l/min @ 25°C
TORCH COOLING WATER FLOWRATE: 87.1 l/min @ 12°C
TORCH COOLING WATER TEMPERATURE RISE: 0.6°C

TABLE B-2 (cont'd)

RADIAL DISTANCE FROM CENTERLINE (MM)	AXIAL DISTANCE FROM THE ANODE (MM)				
	46	68	90	114	151
45	495	541			516
30	627	744			612
15	1846	895			639
0	3771	1441	940	787	674

QUENCHER: Injection Ring #2 + Constant Diameter
Cooled-Surface Module
CURRENT: 250 Amperes
VOLTAGE: 75 Volts
ARC GAS FLOWRATE: 45 l/min @ 25°C
QUENCH GAS FLOWRATE: 90 l/min @ 25°C
TORCH COOLING WATER FLOWRATE: 87.1 l/min @ 12°C
TORCH COOLING WATER TEMPERATURE RISE: 0.8°C

RADIAL DISTANCE FROM CENTERLINE (MM)	AXIAL DISTANCE FROM THE ANODE (MM)				
	46	68	90	114	151
45	537	570			562
30	600	792			641
15	1904	968			689
0		1506	1020	916	704

QUENCHER: Injection Ring #2 + Constant Diameter
Cooled-Surface Module
CURRENT: 250 Amperes
VOLTAGE: 80 Volts
ARC GAS FLOWRATE: 75 l/min @ 25°C
QUENCH GAS FLOWRATE: 90 l/min @ 25°C
TORCH COOLING WATER FLOWRATE: 87.1 l/min @ 12°C
TORCH COOLING WATER TEMPERATURE RISE: 0.8°C

RADIAL DISTANCE FROM CENTERLINE (MM)	AXIAL DISTANCE FROM THE ANODE (MM)				
	46	68	90	114	151
45	587	603			612
30	657	814			696
15	1955	995			717
0	4110	1680	1184	992	742

QUENCHER: Injection Ring #2 + Constant Diameter
Cooled-Surface Module
CURRENT: 250 Amperes
VOLTAGE: 86 Volts
ARC GAS FLOWRATE: 106 l/min @ 25°C
QUENCH GAS FLOWRATE: 90 l/min @ 25°C
TORCH COOLING WATER FLOWRATE: 87.1 l/min @ 12°C
TORCH COOLING WATER TEMPERATURE RISE: 0.7°C

TABLE B-2 (cont'd)

RADIAL DISTANCE FROM CENTERLINE (MM)	AXIAL DISTANCE FROM THE ANODE (MM) 62	79	105	143	180
45	376	440			468
30	406	534			478
15	432	636			614
0	3126	1331	909	784	681

QUENCHER: Injection Ring #2 + Cooled Nozzle Module
CURRENT: 150 Amperes
VOLTAGE: 65 Volts
ARC GAS FLOWRATE: 45 l/min @ 25°C
QUENCH GAS FLOWRATE: 25 l/min @ 25°C
TORCH COOLING WATER FLOWRATE: 87.8 l/min @ 12°C
TORCH COOLING WATER TEMPERATURE RISE: 0.4°C

RADIAL DISTANCE FROM CENTERLINE (MM)	AXIAL DISTANCE FROM THE ANODE (MM) 62	79	105	143	180
45	404	469			502
30	410	561			548
15	443	686			635
0	4067	1425	968	825	701

QUENCHER: Injection Ring #2 + Cooled Nozzle Module
CURRENT: 150 Amperes
VOLTAGE: 71 Volts
ARC GAS FLOWRATE: 75 l/min @ 25°C
QUENCH GAS FLOWRATE: 25 l/min @ 25°C
TORCH COOLING WATER FLOWRATE: 87.8 l/min @ 12°C
TORCH COOLING WATER TEMPERATURE RISE: 0.4°C

RADIAL DISTANCE FROM CENTERLINE (MM)	AXIAL DISTANCE FROM THE ANODE (MM) 62	79	105	143	180
45	413	501			529
30	437	573			588
15	486	721			629
0	4464	1607	1079	854	714

QUENCHER: Injection Ring #2 + Cooled Nozzle Module
CURRENT: 150 Amperes
VOLTAGE: 75 Volts
ARC GAS FLOWRATE: 106 l/min @ 25°C
QUENCH GAS FLOWRATE: 25 l/min @ 25°C
TORCH COOLING WATER FLOWRATE: 87.8 l/min @ 12°C
TORCH COOLING WATER TEMPERATURE RISE: 0.4°C

TABLE B-2 (cont'd)

RADIAL DISTANCE FROM CENTERLINE (MM)	AXIAL DISTANCE FROM THE ANODE (MM)				
	66	79	105	143	180
45	399	448			504
30	428	584			552
15	465	700			662
0	3504	1350	993	818	716

QUENCHER: Injection Ring #2 + Cooled Nozzle Module
CURRENT: 200 Amperes
VOLTAGE: 70 Volts
ARC GAS FLOWRATE: 45 l/min @ 25°C
QUENCH GAS FLOWRATE: 25 l/min @ 25°C
TORCH COOLING WATER FLOWRATE: 87.8 l/min @ 12°C
TORCH COOLING WATER TEMPERATURE RISE: 0.6°C

RADIAL DISTANCE FROM CENTERLINE (MM)	AXIAL DISTANCE FROM THE ANODE (MM)				
	66	79	105	143	180
45	421	470			550
30	473	604			591
15	491	734			667
0	3442	1547	1010	865	733

QUENCHER: Injection Ring #2 + Cooled Nozzle Module
CURRENT: 200 Amperes
VOLTAGE: 77 Volts
ARC GAS FLOWRATE: 75 l/min @ 25°C
QUENCH GAS FLOWRATE: 25 l/min @ 25°C
TORCH COOLING WATER FLOWRATE: 87.8 l/min @ 12°C
TORCH COOLING WATER TEMPERATURE RISE: 0.6°C

RADIAL DISTANCE FROM CENTERLINE (MM)	AXIAL DISTANCE FROM THE ANODE (MM)				
	66	79	105	143	180
45	444	502			559
30	490	649			615
15	516	768			688
0	4468	1696	1136	907	752

QUENCHER: Injection Ring #2 + Cooled Nozzle Module
CURRENT: 200 Amperes
VOLTAGE: 83 Volts
ARC GAS FLOWRATE: 105 l/min @ 25°C
QUENCH GAS FLOWRATE: 25 l/min @ 25°C
TORCH COOLING WATER FLOWRATE: 87.8 l/min @ 12°C
TORCH COOLING WATER TEMPERATURE RISE: 0.5°C

TABLE B-2 (cont'd)

RADIAL DISTANCE FROM CENTERLINE (MM)	AXIAL DISTANCE FROM THE ANODE (MM)				
	66	79	105	143	180
45	433	487			496
30	478	625			583
15	531	807			635
0	3828	1367	1167	934	760

QUENCHER: Injection Ring #2 + Cooled Nozzle Module
CURRENT: 250 Amperes
VOLTAGE: 73 Volts
ARC GAS FLOWRATE: 45 l/min @ 25°C
QUENCH GAS FLOWRATE: 25 l/min @ 25°C
TORCH COOLING WATER FLOWRATE: 87.8 l/min @ 12°C
TORCH COOLING WATER TEMPERATURE RISE: 0.8°C

RADIAL DISTANCE FROM CENTERLINE (MM)	AXIAL DISTANCE FROM THE ANODE (MM)				
	66	79	105	143	180
45	449	515			520
30	504	686			591
15	592	854			663
0	4146	1546	1202	965	798

QUENCHER: Injection Ring #2 + Cooled Nozzle Module
CURRENT: 250 Amperes
VOLTAGE: 82 Volts
ARC GAS FLOWRATE: 75 l/min @ 25°C
QUENCH GAS FLOWRATE: 25 l/min @ 25°C
TORCH COOLING WATER FLOWRATE: 87.8 l/min @ 12°C
TORCH COOLING WATER TEMPERATURE RISE: 0.8°C

TABLE B-2 (cont'd)

	AXIAL DISTANCE FROM THE ANODE (MM)				
RADIAL DISTANCE FROM CENTERLINE (MM)	61	81	108	146	183
45	369	417			441
30	386	514			507
15	406	634			603
0	3183	1370	898	745	667

QUENCHER: Injection Ring #2 + Cooled Nozzle Module
CURRENT: 150 Amperes
VOLTAGE: 66 Volts
ARC GAS FLOWRATE: 45 l/min @ 25°C
QUENCH GAS FLOWRATE: 90 l/min @ 25°C
TORCH COOLING WATER FLOWRATE: 87.8 l/min @ 12°C
TORCH COOLING WATER TEMPERATURE RISE: 0.4°C

	AXIAL DISTANCE FROM THE ANODE (MM)				
RADIAL DISTANCE FROM CENTERLINE (MM)	61	81	108	146	183
45	384	441			461
30	401	558			520
15	456	665			619
0	3823	1396	973	808	691

QUENCHER: Injection Ring #2 + Cooled Nozzle Module
CURRENT: 150 Amperes
VOLTAGE: 72 Volts
ARC GAS FLOWRATE: 75 l/min @ 25°C
QUENCH GAS FLOWRATE: 90 l/min @ 25°C
TORCH COOLING WATER FLOWRATE: 87.8 l/min @ 12°C
TORCH COOLING WATER TEMPERATURE RISE: 0.4°C

	AXIAL DISTANCE FROM THE ANODE (MM)				
RADIAL DISTANCE FROM CENTERLINE (MM)	61	81	108	146	183
45	415	452			474
30	468	591			566
15	495	717			606
0	4142	1453	1144	858	703

QUENCHER: Injection Ring #2 + Cooled Nozzle Module
CURRENT: 150 Amperes
VOLTAGE: 76 Volts
ARC GAS FLOWRATE: 106 l/min @ 25°C
QUENCH GAS FLOWRATE: 90 l/min @ 25°C
TORCH COOLING WATER FLOWRATE: 87.8 l/min @ 12°C
TORCH COOLING WATER TEMPERATURE RISE: 0.4°C

TABLE B-2 (cont'd)

RADIAL DISTANCE FROM CENTERLINE (MM)	AXIAL DISTANCE FROM THE ANODE (MM) 66	81	108	146	183
45	380	430			487
30	405	565			533
15	445	671			641
0	3505	1335	953	794	706

QUENCHER: Injection Ring #2 + Cooled Nozzle Module
CURRENT: 200 Amperes
VOLTAGE: 70 Volts
ARC GAS FLOWRATE: 45 l/min @ 25°C
QUENCH GAS FLOWRATE: 90 l/min @ 25°C
TORCH COOLING WATER FLOWRATE: 87.8 l/min @ 12°C
TORCH COOLING WATER TEMPERATURE RISE: 0.6°C

RADIAL DISTANCE FROM CENTERLINE (MM)	AXIAL DISTANCE FROM THE ANODE (MM) 66	81	108	146	183
45	420	466			515
30	431	580			561
15	468	695			663
0	3827	1475	1002	848	719

QUENCHER: Injection Ring #2 + Cooled Nozzle Module
CURRENT: 200 Amperes
VOLTAGE: 77 Volts
ARC GAS FLOWRATE: 75 l/min @ 25°C
QUENCH GAS FLOWRATE: 90 l/min @ 25°C
TORCH COOLING WATER FLOWRATE: 87.8 l/min @ 12°C
TORCH COOLING WATER TEMPERATURE RISE: 0.55°C

RADIAL DISTANCE FROM CENTERLINE (MM)	AXIAL DISTANCE FROM THE ANODE (MM) 66	81	108	146	183
45	439	481			527
30	474	623			593
15	520	722			671
0	4143	1628	1141	869	744

QUENCHER: Injection Ring #2 + Cooled Nozzle Module
CURRENT: 200 Amperes
VOLTAGE: 84 Volts
ARC GAS FLOWRATE: 106 l/min @ 25°C
QUENCH GAS FLOWRATE: 90 l/min @ 25°C
TORCH COOLING WATER FLOWRATE: 87.8 l/min @ 12°C
TORCH COOLING WATER TEMPERATURE RISE: 0.6°C

TABLE B-2 (cont'd)

RADIAL DISTANCE FROM CENTERLINE (MM)	AXIAL DISTANCE FROM THE ANODE (MM) 66	81	108	146	183
45	428	477			491
30	469	600			554
15	495	799			643
0	4143	1564	1264	1025	768

QUENCHER: Injection Ring #2 + Cooled Nozzle Module
CURRENT: 250 Amperes
VOLTAGE: 75 Volts
ARC GAS FLOWRATE: 45 l/min @ 25°C
QUENCH GAS FLOWRATE: 90 l/min @ 25°C
TORCH COOLING WATER FLOWRATE: 87.8 l/min @ 12°C
TORCH COOLING WATER TEMPERATURE RISE: 0.7°C

RADIAL DISTANCE FROM CENTERLINE (MM)	AXIAL DISTANCE FROM THE ANODE (MM) 66	81	108	146	183
45	443	496			497
30	491	646			560
15	567	830			646
0	4144	1556	1302	1055	777

QUENCHER: Injection Ring #2 + Cooled Nozzle Module
CURRENT: 250 Amperes
VOLTAGE: 84 Volts
ARC GAS FLOWRATE: 75 l/min @ 25°C
QUENCH GAS FLOWRATE: 90 l/min @ 25°C
TORCH COOLING WATER FLOWRATE: 87.8 l/min @ 12°C
TORCH COOLING WATER TEMPERATURE RISE: 0.8°C

TABLE B-2 (cont'd)

Calorimetrically determined temperatures and thermocouple temperatures (both in °K) along with values for the operating variables are presented in Table B-2.

APPENDIX C

SAMPLE CALCULATIONS AND UNCERTAINTY ANALYSES

C-1 Calculation of and Uncertainty Analysis for the Calorimetric Probe Temperature

A sample calculation of the centerline temperature 9 mm from the exit of gas injection ring #2 is presented below for the following conditions:

$I = 150$ amperes

$Q_{\text{arc gas}} = 106.00$ L/min @ 25°C

$Q_{\text{quench gas}} = 25.00$ L/min @ 25°C

$w_{H_2O} = 102$ g/s

$w_{Ar} = 2.452 \times 10^{-2}$ g/s

$c_{p_{H_2O}} = 1.00$ cal/g°C

$c_{p_{Ar}} = 0.125$ cal/g°K

$\Delta T_{\text{flow}} = 2.14$°C

$\Delta T_{\text{no flow}} = 2.01$°C

$T_{\text{probe exit}} = 304$°K

Substitution of these values into equation 4-3 gives,

$$T_{\text{probe tip}} = \frac{(102)(1.00)(2.14 - 2.01)}{(2.452 \times 10^{-2})(0.125)} + 304$$

$$= 4630^{\circ}\text{K}$$

Given an expression of the form $w = f(x,y,z)$, the uncertainty in the dependent variable w may be expressed as:

$$\sigma_w = \left[\left(\frac{\partial w}{\partial x}\sigma_x\right)^2 + \left(\frac{\partial w}{\partial y}\sigma_y\right)^2 + \left(\frac{\partial w}{\partial z}\sigma_z\right)^2 \right]^{1/2} \qquad \text{(C-1)}$$

where x, y and z are experimental quantities and σ_x, σ_y and σ_z the corresponding uncertainties. For the case at hand,

$$\sigma_{T_{\text{probe tip}}} = \left[\left(\frac{\partial T_{\text{probe tip}}}{\partial w_{H_2O}} \sigma_{w_{H_2O}}\right)^2 + \left(\frac{\partial T_{\text{probe tip}}}{\partial w_{Ar}} \sigma_{w_{Ar}}\right)^2 + \right.$$

$$\left(\frac{\partial T_{\text{probe tip}}}{\partial \Delta T_{\text{flow}}} \sigma_{\Delta T_{\text{flow}}}\right)^2 + \left(\frac{\partial T_{\text{probe tip}}}{\partial \Delta T_{\text{no flow}}} \sigma_{\Delta T_{\text{no flow}}}\right)^2 +$$

$$\left. \left(\frac{\partial T_{\text{probe tip}}}{\partial T_{\text{probe exit}}} \sigma_{T_{\text{probe exit}}}\right)^2 \right]^{1/2} \qquad \text{(C-2)}$$

where

$$\frac{\partial T_{\text{probe tip}}}{\partial w_{H_2O}} = \frac{c_{p_{H_2O}} (\Delta T_{\text{flow}} - \Delta T_{\text{no flow}})}{(wc_p)_{Ar}} \qquad \text{(C-3)}$$

$$\frac{\partial T_{\text{probe tip}}}{\partial w_{Ar}} = \frac{-(wc_p)_{H_2O} (\Delta T_{\text{flow}} - \Delta T_{\text{no flow}})}{(w^2 c_p)_{Ar}} \qquad \text{(C-4)}$$

$$\frac{\partial T_{\text{probe tip}}}{\partial \Delta T_{\text{flow}}} = \frac{(wc_p)_{H_2O}}{(wc_p)_{Ar}} \qquad \text{(C-5)}$$

$$\frac{\partial T_{\text{probe tip}}}{\partial \Delta T_{\text{no flow}}} = \frac{-(wc_p)_{H_2O}}{(wc_p)_{Ar}} \qquad \text{(C-6)}$$

$$\frac{\partial T_{\text{probe tip}}}{\partial T_{\text{probe exit}}} = 1 \qquad \text{(C-7)}$$

and

$\sigma_{w_{H_2O}} = 1$ g/s ; $\sigma_{w_{Ar}} = 6.488 \times 10^{-4}$ g/s

$\sigma_{\Delta T_{\text{flow}}} = 0.03\,^{\circ}\text{C}$; $\sigma_{\Delta T_{\text{no flow}}} = 0.03\,^{\circ}\text{C}$

$$\sigma_{T_{\text{probe exit}}} = 0.1^{\circ}\text{C}$$

Substituting the numerical equivalents of equations C-3 to C-7 into C-2 yields:

$$\begin{aligned}
\sigma T_{\text{probe tip}} = \Bigg[& \left(\frac{(1.00)(2.14 - 2.01)}{(2.452 \times 10^{-2})(0.125)} (1) \right)^{2} + \\
& \left(\frac{-(102)(1.00)(2.14 - 2.01)}{(2.452 \times 10^{-2})^{2}(0.125)} (6.488 \times 10^{-4}) \right)^{2} + \\
& \left(\frac{(102)(1.00)}{(2.452 \times 10^{-2})(0.125)} (0.03) \right)^{2} + \\
& \left(\frac{-(102)(1.00)}{(2.452 \times 10^{-2})(0.125)} (0.03) \right)^{2} + ((1)(0.1))^{2} \Bigg]^{1/2}
\end{aligned}$$

$$= 1417^{\circ}\text{K}$$

Thus, this particular value of temperature could be expressed as 4630 ± 1417°K. Individual uncertainties used in the calculations were based upon the precision attainable by each particular instrument.

C-2 Calculation of and Uncertainty Analysis for Average Quenching Rate

A sample calculation of the average quenching rate afforded by gas injection ring #2 is presented for the conditions specified below:

$I = 150$ amperes $\qquad \sigma_I = 10$ amperes

$V_1 = 77$ volts $\qquad \sigma_{V_1} = 3$ volts

$V_2 = 80$ volts $\qquad \sigma_{V_2} = 3$ volts

$w_1^o = 1323.5$ g/s $\qquad \sigma_{w_1^o} = 6.3$ g/s

$w_2^o = 1411.8$ g/s $\qquad \sigma_{w_2^o} = 6.3$ g/s

$(\Delta T_1)_{H_2O} = 0.75\,^\circ C$ $\qquad \sigma_{\Delta T_1} = 0.05\,^\circ C$

$(\Delta T_2)_{H_2O} = 0.3\,^\circ C$ $\qquad \sigma_{\Delta T_2} = 0.05\,^\circ C$

$w^o_{\substack{arc\\gas}} = 2.89$ g/s $\qquad \sigma_{w^o_{\substack{arc\\gas}}} = 0.02$ g/s

$w^o_{\substack{quench\\gas}} = 2.45$ g/s $\qquad \sigma_{w^o_{\substack{quench\\gas}}} = 0.01$ g/s

$(c_{p_1})_{gas} = 0.124$ cal/g°K

$(c_{p_2})_{gas} = 0.125$ cal/g°K

$c_{p_{H_2O}} = 1.00$ cal/g°C

$\rho^o_{gas} = 1.6349 \times 10^{-6}$ g/mm^3

$T^o = 298\,^\circ K$

$A_1 = 507$ mm^2

$A_2 = 507$ mm^2

$\Delta x = 22$ mm

1 calorie = 4.184 Joules

Substituting the appropriate quantities into equation 4-7 gives:

$$\frac{\Delta\bar{T}}{\Delta t} = \frac{1}{(2)(22)(1.6349 \times 10^{-6})(298)} \times$$

$$\left[\left(\frac{(150)(77)-(4.184)(1323.5)(1.00)(0.75)}{(4.184)(2.89)(0.124)} + 298\right) - \left(\frac{(150)(80)-(4.184)(1411.8)(1.00)(0.3)}{(4.184)(2.89 + 2.45)(0.125)} + 298\right)\right] \times$$

$$\left[\left(\frac{2.89}{507}\right)\left(\frac{(150)(77) - (4.184)(1323.5)(1.00)(0.75)}{(4.184)(2.89)(0.124)} + 298\right) + \left(\frac{2.89 + 2.45}{507}\right)\left(\frac{(150)(80) - (4.184)(1411.8)(1.00)(0.3)}{(4.184)(2.89 + 2.45)(0.125)} + 298\right)\right]$$

$$= 4.25 \times 10^{6}\,{}^{\circ}K/s$$

Combining the individual uncertainties into an expression for the overall uncertainty analogous to equation C-1 yields:

$$\sigma_{\frac{\Delta\bar{T}}{\Delta t}} = \left[\left(\frac{\partial\frac{\Delta\bar{T}}{\Delta t}}{\partial I}\,\sigma_I\right)^2 + \left(\frac{\partial\frac{\Delta\bar{T}}{\Delta t}}{\partial V_1}\,\sigma_{V_1}\right)^2 + \left(\frac{\partial\frac{\Delta\bar{T}}{\Delta t}}{\partial V_2}\,\sigma_{V_2}\right)^2 + \left(\frac{\partial\frac{\Delta\bar{T}}{\Delta t}}{\partial w_1}\,\sigma_{w_1}\right)^2 + \right.$$
$$\left(\frac{\partial\frac{\Delta\bar{T}}{\Delta t}}{\partial w_2}\,\sigma_{w_2}\right)^2 + \left(\frac{\partial\frac{\Delta\bar{T}}{\Delta t}}{\partial \Delta T_1}\,\sigma_{\Delta T_1}\right)^2 + \left(\frac{\partial\frac{\Delta\bar{T}}{\Delta t}}{\partial \Delta T_2}\,\sigma_{\Delta T_2}\right)^2 + \left(\frac{\partial\frac{\Delta\bar{T}}{\Delta t}}{\partial w_{\substack{\text{arc}\\ \text{gas}}}}\,\sigma_{w_{\substack{\text{arc}\\ \text{gas}}}}\right)^2 +$$
$$\left.\left(\frac{\partial\frac{\Delta\bar{T}}{\Delta t}}{\partial w_{\substack{\text{quench}\\ \text{gas}}}}\,\sigma_{w_{\substack{\text{quench}\\ \text{gas}}}}\right)^2\right]^{1/2} \qquad \text{(C-8)}$$

where

$$\frac{\partial\frac{\Delta\bar{T}}{\Delta t}}{\partial I} = \frac{1}{2\Delta x \rho^{o}_{\text{gas}}}\left(\frac{2IV_1^2 - 2V_1(w_1 c_p \Delta T_1)_{H_2O}}{T^{o} A_1 w_{\substack{\text{arc}\\ \text{gas}}} (c_{p_1})^2_{\text{gas}}} + \frac{2V_1}{A_1 (c_{p_1})_{\text{gas}}} + \right.$$

$$\frac{2IV_1V_2 - V_1(w_2c_p\Delta T_2)_{H_2O} - V_2(w_1c_p\Delta T_1)_{H_2O}}{T^oA_2w_{\substack{arc\\gas}}(c_{p_1}c_{p_2})_{gas}} + \frac{V_1(w_{\substack{arc\\gas}}+w_{\substack{quench\\gas}})}{A_2w_{\substack{arc\\gas}}(c_{p_1})_{gas}} +$$

$$\frac{V_2}{A_2(c_{p_2})_{gas}} + \frac{-2IV_1V_2 + V_2(w_1c_p\Delta T_1)_{H_2O} + V_1(w_2c_p\Delta T_2)_{H_2O}}{T^oA_1(c_{p_1}c_{p_2})_{gas}(w_{\substack{arc\\gas}} + w_{\substack{quench\\gas}})} -$$

$$\frac{w_{\substack{arc\\gas}}V_2}{A_1(w_{\substack{arc\\gas}} + w_{\substack{quench\\gas}})(c_{p_2})_{gas}} - \frac{V_1}{A_1(c_{p_1})_{gas}} +$$

$$\left.\frac{-2IV_2^2 + 2V_2(w_2c_p\Delta T_2)_{H_2O}}{T^oA_2(w_{\substack{arc\\gas}} + w_{\substack{quench\\gas}})(c_{p_2})^2_{gas}} - \frac{2V_2}{A_2(c_{p_2})_{gas}}\right) \qquad (C\text{-}9)$$

$$\frac{\partial\frac{\Delta\bar{T}}{\Delta t}}{\partial V_1} = \frac{1}{2\Delta x\rho^o_{gas}(c_{p_1})_{gas}}\left(\frac{2I^2V_1 - 2I(w_1c_p\Delta T_1)_{H_2O}}{T^oA_1w_{\substack{arc\\gas}}(c_{p_1\,gas})} + \frac{2I}{A_1} +\right.$$

$$\frac{I^2V_2 - I(w_2c_p\Delta T_2)_{H_2O}}{T^oA_2w_{\substack{arc\\gas}}(c_{p_2})_{gas}} + \frac{(w_{\substack{arc\\gas}} + w_{\substack{quench\\gas}})I}{A_2w_{\substack{arc\\gas}}} +$$

$$\frac{-I^2V_2 + I(w_2c_p\Delta T_2)_{H_2O}}{T^O A_1 (c_{p_2})_{gas} (w_{\substack{arc\\gas}} + w_{\substack{quench\\gas}})} - \frac{I}{A_1}\Bigg) \tag{C-10}$$

$$\frac{\partial \frac{\Delta \bar{T}}{\Delta t}}{\partial V_2} = \frac{1}{2\Delta x \rho^O_{gas} (c_{p_2})_{gas}} \Bigg(\frac{I^2V_1 - I(w_1c_p\Delta T_1)_{H_2O}}{T^O A_2 w_{\substack{arc\\gas}} (c_{p_1})_{gas}} + \frac{I}{A_2} +$$

$$\frac{-I^2V_1 + I(w_1c_p\Delta T_1)_{H_2O}}{T^O A_1 (c_{p_1})_{gas} (w_{\substack{arc\\gas}} + w_{\substack{quench\\gas}})} - \frac{w_{\substack{arc\\gas}} I}{A_1 (w_{\substack{arc\\gas}} + w_{\substack{quench\\gas}})} +$$

$$\frac{-2I^2V_2 + 2I(w_2c_p\Delta T_2)_{H_2O}}{T^O A_2 (w_{\substack{arc\\gas}} + w_{\substack{quench\\gas}}) (c_{p_2})_{gas}} - \frac{2I}{A_2}\Bigg) \tag{C-11}$$

$$\frac{\partial \frac{\Delta \bar{T}}{\Delta t}}{\partial w_1} = \frac{1}{2\Delta x \rho^O_{gas} (c_{p_1})_{gas}} \Bigg(\frac{-2IV_1(c_p\Delta T_1)_{H_2O} + 2(w_1c_p^2\Delta T_1^2)_{H_2O}}{T^O A_1 w_{\substack{arc\\gas}} (c_{p_1})_{gas}} -$$

$$\frac{2(c_p\Delta T_1)_{H_2O}}{A_1} + \frac{-IV_2(c_p\Delta T_1)_{H_2O} + (w_2c_p^2\Delta T_1\Delta T_2)_{H_2O}}{T^O A_2 w_{\substack{arc\\gas}} (c_{p_2})_{gas}} -$$

$$\frac{(c_p\Delta T_1)_{H_2O}(w_{\substack{arc\\gas}} + w_{\substack{quench\\gas}})}{A_2 w_{\substack{arc\\gas}}} + \frac{IV_2(c_p\Delta T_1)_{H_2O}}{T^o A_1 (c_{p_2})_{gas}(w_{\substack{arc\\gas}} + w_{\substack{quench\\gas}})} -$$

$$\frac{(w_2 c_p^2 \Delta T_1 \Delta T_2)_{H_2O}}{T^o A_1 (c_{p_2})_{gas}(w_{\substack{arc\\gas}} + w_{\substack{quench\\gas}})} + \left.\frac{(c_p\Delta T_1)_{H_2O}}{A_1}\right) \qquad \text{(C-12)}$$

$$\frac{\partial \frac{\Delta \overline{T}}{\Delta t}}{\partial w_2} = \frac{1}{2\Delta x \rho^o_{gas}(c_{p_2})_{gas}} \left(\frac{-IV_1(c_p\Delta T_2)_{H_2O} + (w_1 c_p^2 \Delta T_1 \Delta T_2)_{H_2O}}{T^o A_2 w_{\substack{arc\\gas}}(c_{p_1})_{gas}} - \right.$$

$$\frac{(c_p\Delta T_2)_{H_2O}}{A_2} + \frac{IV_1(c_p\Delta T_2)_{H_2O} - (w_1 c_p^2 \Delta T_1 \Delta T_2)_{H_2O}}{T^o A_1 (c_{p_1})_{gas}(w_{\substack{arc\\gas}} + w_{\substack{quench\\gas}})} +$$

$$\frac{w_{\substack{arc\\gas}}(c_p\Delta T_2)_{H_2O}}{A_1(w_{\substack{arc\\gas}} + w_{\substack{quench\\gas}})} + \frac{2IV_2(c_p\Delta T_2)_{H_2O} - 2(w_2 c_p^2 \Delta T_2^2)_{H_2O}}{T^o A_2 (c_{p_2})_{gas}(w_{\substack{arc\\gas}} + w_{\substack{quench\\gas}})} +$$

$$\left.\frac{2(c_p\Delta T_2)_{H_2O}}{A_2}\right) \qquad \text{(C-13)}$$

$$\frac{\partial \frac{\Delta \bar{T}}{\Delta t}}{\partial \Delta T_1} = \frac{1}{2\Delta x \rho^o_{gas}(c_{p_1})_{gas}} \Bigg(\frac{-2IV_1(w_1c_p)_{H_2O} + 2(w_1^2c_p^2\Delta T_1)_{H_2O}}{T^oA_1w_{\substack{arc\\gas}}(c_{p_1})_{gas}} -$$

$$\frac{2(w_1c_p)_{H_2O}}{A_1} + \frac{-IV_2(w_1c_p)_{H_2O} + (w_1w_2c_p^2\Delta T_2)_{H_2O}}{T^oA_2w_{\substack{arc\\gas}}(c_{p_2})_{gas}} -$$

$$\frac{(w_1c_p)_{H_2O}(w_{\substack{arc\\gas}} + w_{\substack{quench\\gas}})}{A_2w_{\substack{arc\\gas}}} + \frac{IV_2(w_1c_p)_{H_2O} - (w_1w_2c_p^2\Delta T_2)_{H_2O}}{T^oA_1(c_{p_2})_{gas}(w_{\substack{arc\\gas}}+w_{\substack{quench\\gas}})} +$$

$$\frac{(w_1c_p)_{H_2O}}{A_1}\Bigg) \qquad \text{(C-14)}$$

$$\frac{\partial \frac{\Delta \bar{T}}{\Delta t}}{\partial \Delta T_2} = \frac{1}{2\Delta x \rho^o_{gas}(c_{p_2})_{gas}} \Bigg(\frac{-IV_1(w_2c_p)_{H_2O} + (w_1w_2c_p^2\Delta T_1)_{H_2O}}{T^oA_2w_{\substack{arc\\gas}}(c_{p_1})_{gas}} -$$

$$\frac{(w_2c_p)_{H_2O}}{A_2} + \frac{IV_1(w_2c_p)_{H_2O} - (w_1w_2c_p^2\Delta T_1)_{H_2O}}{T^oA_1(c_{p_1})_{gas}(w_{\substack{arc\\gas}} + w_{\substack{quench\\gas}})} +$$

$$\frac{w_{\substack{\text{arc}\\\text{gas}}}(w_2c_p)_{H_2O}}{A_1(w_{\substack{\text{arc}\\\text{gas}}} + w_{\substack{\text{quench}\\\text{gas}}})} + \frac{2IV_2(w_2c_p)_{H_2O} - 2(w_2^2c_p^2\Delta T_2)_{H_2O}}{T^oA_2(c_{p_2})_{\text{gas}}(w_{\substack{\text{arc}\\\text{gas}}} + w_{\substack{\text{quench}\\\text{gas}}})} +$$

$$\left.\frac{2(w_2c_p)_{H_2O}}{A_2}\right) \qquad \text{(C-15)}$$

$$\frac{\partial\frac{\Delta\bar{T}}{\Delta t}}{\partial w_{\substack{\text{arc}\\\text{gas}}}} = \frac{1}{2\Delta x\rho^o_{\text{gas}}}\left(\frac{-I^2V_1^2 + 2IV_1(w_1c_p\Delta T_1)_{H_2O} - (w_1^2c_p^2\Delta T_1^2)_{H_2O}}{T^oA_1w^2_{\substack{\text{arc}\\\text{gas}}}(c_{p_1})^2_{\text{gas}}} +\right.$$

$$\frac{-I^2V_1V_2 + IV_1(w_2c_p\Delta T_2)_{H_2O} + IV_2(w_1c_p\Delta T_1)_{H_2O}}{T^oA_2w^2_{\substack{\text{arc}\\\text{gas}}}(c_{p_1}c_{p_2})_{\text{gas}}} -$$

$$\frac{(w_1w_2c_p^2\Delta T_1\Delta T_2)_{H_2O}}{T^oA_2w^2_{\substack{\text{arc}\\\text{gas}}}(c_{p_1}c_{p_2})_{\text{gas}}} - \frac{w_{\substack{\text{quench}\\\text{gas}}}IV_1}{A_2w^2_{\substack{\text{arc}\\\text{gas}}}(c_{p_1})_{\text{gas}}} + \frac{w_{\substack{\text{quench}\\\text{gas}}}(w_1c_p\Delta T_1)_{H_2O}}{A_2w^2_{\substack{\text{arc}\\\text{gas}}}(c_{p_1})_{\text{gas}}} +$$

$$\frac{I^2V_1V_2 - IV_2(w_1c_p\Delta T_1)_{H_2O} - IV_1(w_2c_p\Delta T_2)_{H_2O}}{T^oA_1(c_{p_1}c_{p_2})_{\text{gas}}(w_{\substack{\text{arc}\\\text{gas}}} + w_{\substack{\text{quench}\\\text{gas}}})^2} +$$

$$\frac{(w_1 w_2 c_p^2 \Delta T_1 \Delta T_2)_{H_2O}}{T^o A_1 (c_{p_1} c_{p_2})_{gas} (w_{\substack{arc\\gas}} + w_{\substack{quench\\gas}})^2} -$$

$$\frac{w_{\substack{quench\\gas}} IV_2}{A_1 (c_{p_2})_{gas} (w_{\substack{arc\\gas}} + w_{\substack{quench\\gas}})^2} + \frac{w_{\substack{quench\\gas}} (w_2 c_p \Delta T_2)_{H_2O}}{A_1 (c_{p_2})_{gas} (w_{\substack{arc\\gas}} + w_{\substack{quench\\gas}})^2} +$$

$$\left. \frac{I^2 V_2^2 - 2IV_2 (w_2 c_p \Delta T_2)_{H_2O} + (w_2^2 c_p^2 \Delta T_2^2)_{H_2O}}{T^o A_2 (c_{p_2})^2_{gas} (w_{\substack{arc\\gas}} + w_{\substack{quench\\gas}})^2} \right) \qquad \text{(C-16)}$$

$$\frac{\partial \frac{\Delta \bar{T}}{\Delta t}}{\partial w_{\substack{quench\\gas}}} = \frac{1}{2 \Delta x \rho^o_{gas}} \left(\frac{IV_1 - (w_1 c_p \Delta T_1)_{H_2O}}{A_2 w_{\substack{arc\\gas}} (c_{p_1})_{gas}} + \right.$$

$$\frac{I^2 V_1 V_2 - IV_2 (w_1 c_p \Delta T_1)_{H_2O} - IV_1 (w_2 c_p \Delta T_2)_{H_2O}}{T^o A_1 (c_{p_1} c_{p_2})_{gas} (w_{\substack{arc\\gas}} + w_{\substack{quench\\gas}})^2} +$$

$$\frac{(w_1 w_2 c_p^2 \Delta T_1 \Delta T_2)_{H_2O}}{T^o A_1 (c_{p_1} c_{p_2})_{gas} (w_{\substack{arc\\gas}} + w_{\substack{quench\\gas}})^2} +$$

$$\frac{w_{\substack{arc\\gas}} I V_2 - w_{\substack{arc\\gas}} (w_2 c_p \Delta T_2)_{H_2O}}{A_1 (c_{p_2})_{gas} (w_{\substack{arc\\gas}} + w_{\substack{quench\\gas}})^2} +$$

$$\left.\frac{I^2 V_2^2 - 2IV_2 (w_2 c_p \Delta T_2)_{H_2O} + (w_2 c_p \Delta T_2)^2_{H_2O}}{T^o A_2 (c_{p_2})^2_{gas} (w_{\substack{arc\\gas}} + w_{\substack{quench\\gas}})^2}\right) \qquad \text{(C-17)}$$

Substituting the numerical equivalents of equations C-9 to C-17 into C-8 gives:

$$\sigma_{\frac{\Delta \bar{T}}{\Delta t}} = 1.79 \times 10^{5} \, {}^{o}K/s$$

Thus, the average quenching rate could be expressed as $4.25 \times 10^6 \pm 1.79 \times 10^5 \, {}^{o}K/s$. Individual uncertainties were, again, approximated by the precision of the particular instrument.

DISTRIBUTION

Dr. D. Mills	Director of Research
Prof. M. Boulos	Universite de Sherbrooke Chemical Engineering Dept Sherbrooke, Quebec J1K 2R1
Prof. W. Gauvin	McGill University Chemical Engineering Dept 845 Sherbrooke St. W. Montreal, Quebec H3A 2T5
Mr. R.J. Duff	Ministry of Energy Fuels Research, Energy Programs & Technology Division 56 Wellesley St. W. Toronto, Ontario M7A 2B7
Mr. G.W. Carter	Resorption Canada Ltd 2465 Stevenage Drive Ottawa, Ontario K1G 3W2
Mr. H.E. Douglas (3)	Canadian Electrical Association Suite 500, 1 Westmount Square Montreal, Quebec H3Z 2P9
Dr. P. Mayer	Metallurgical Research
Dr. N. Anyas-Weiss	Electrical Research
Dr. F.Y. Chu	Electrical Research
Mr. J.T. Strack	Electrical Research
Dr. M.R. Booth	Acting Manager, Chemical Research
Mr. D.J.R. Dodd	Chemical Research
Mr. O.T. Melo	Chemical Research
Dr. V.P. Singh	Chemical Research
Dr. C.J. Simpson	Divisional Projects
Dr. M. Alvarez-Cuenca	Empresa Nacional de Electricidad, S.A. Principe de Vergara, 187 28002 Madrid, Spain
Mr. G.P. Kushla	Hatch Associates 21 St. Clair Ave. E. Toronto, Ontario M4T 1L9

Public Reference Centre
Editorial Section (2)
Office Copies (2)
Extra Copies (3)